IDENTIFICATION OF SUBSTRATES AND PATHWAYS REGULATED BY WNK1

APPROVED BY SUPERVISORY COMMITTEE

Melanie H. Cobb, Ph.D.

Leon Avery, Ph.D.

Joseph Albanesi, Ph.D.

Cai Li, Ph.D.

Dedicated to My Family

IDENTIFICATION OF SUBSTRATES AND PATHWAYS REGULATED BY WNK1

By

Byung-Hoon Lee

DISSERTATION

Presented to the Faculty of the Graduate School of Biomedical Sciences

The University of Texas Southwestern Medical Center at Dallas

In Partial Fulfillment of the Requirements

For the degree of

DOCTOR OF PHILOSOPHY

The University of Texas Southwestern Medical Center at Dallas

Dallas, Texas

December, 2004

Copyright

by

Byung-Hoon Lee 2004

All Rights Reserved

Acknowledgments

First of all, I feel deeply grateful to my mentor, Melanie Cobb, for all her advice, encouragement, and patience during my Ph.D. I have always been amazed by her phenomenal thinking about science and great passion for pursuing it. I am really happy to have had her in my life, and hopefully she feels the same about me. I wish I can see myself becoming a good scientist in the future from what I have learned from her. I would also like to thank all my research committee, Joe Albanesi, Leon Avery, and Cai Li, for all their helpful advice and warm encouragement. I really doubt I could have accomplished my Ph.D. without their keen suggestions.

I sincerely thank people in the Cobb laboratory for making my life here really memorable. My special thanks go to the WNK project team and people in Antarctica (L5.128). I like to thank Bing, Lisa, Xiaoshan, and Charles for their “WNKredible” ideas, and I certainly feel proud of our teamwork. And I would like to express my love to the former and present Antarctica folks, Mali, Fred, Wei, Gray, Anthony, and others. I thank tem for our special friendships.

Last of all, I deeply thank my family for their love and support. They mean everything to me. And I am aware that what they wish from me is to be a good scientist with a good character. I also want to express my gratitude to my Korean friends in my mother country and here.

IDENTIFICATION OF SUBSTRATES AND PATHWAYS REGULATED BY WNK1

Publication No. _____

Byung-Hoon Lee, Ph.D.

The University of Texas Southwestern Medical Center at Dallas, 2004

Supervising Professor: Melanie H. Cobb, Ph.D.

Abstract: WNK (With No lysine (K)), a serine/threonine protein kinase, is a unique molecule not belonging to any other canonical protein kinase family including mitogen-activated protein (MAP) kinases. The name of the WNK protein kinase family reflects the fact that a catalytic lysine lies in a position different in WNKs from that in all other protein kinases. The urgency of a mechanistic examination of the WNK family protein kinase was heightened by the discovery that mutations in at least two of the four human WNKs, WNK1 and 4, caused a heritable form of

hypertension. My study focused on unveiling WNK1 substrates and interactors for a better understanding of the molecular pathways served by WNK kinases. Yeast two-hybrid screening was performed to identify the binding partners of WNK1 and yielded genuine interactors including synaptotagmin (Syt) isoforms, Smad2, and dynein light chain (LC8/PIN). WNK1, not WNK4, selectively binds to and phosphorylates Syt2 within its calcium binding C2 domains. Calcium strongly enhanced their binding in vitro. Essential Ca^{2+}-binding residues in the Syt2 C2 domains were critical for formation of a WNK1-Syt2 complex and for Syt2 phosphorylation. WNK1 displayed specificity among Syt isoforms and mutational analysis implicated a hydrophobic residue on the WNK1 kinase domain surface as essential for the high affinity WNK1-Syt2 interaction and phosphorylation. Endogenous WNK1 and Syt2 coimmunoprecipitated and colocalized on a subset of secretory granules in the INS-1 cell line, a pancreatic beta cell model system. Importantly, phosphorylation by WNK1 increased the amount of Ca^{2+} required for Syt2 binding to phospholipid vesicles; mutation of Thr202, a WNK1 phosphorylation site identified from mass spectrometric analysis, partially prevented this change. These findings provide a biochemical scenario that could lead to the retention or insertion of proteins in the plasma membrane. WNK1 may serve as a molecular switch for vesicle trafficking and other membrane events that regulate ion balance. The interaction with and phosphorylation of other molecules by WNK1 were also investigated here.

Table of Contents

Title	i
Dedication	ii
Title page	iii
Copyright	iv
Acknowledgments	v
Abstract	vi-vii
Table of Contents	viii-xii
Publications presented in this dissertation	xiii
List of Figures and Tables	xiv-xvi
List of Abbreviations	xvii-xviii

Chapter 1: General Overview

I. Signal transduction through protein kinases 1-9

A. Protein kinases

B. Catalog of the eukaryotic protein kinase superfamily

C. Structural organization of protein kinases

II. Regulation of protein kinase signaling 9-16

A. Regulation of kinase activity from a structural view

B. Regulation by post-translational modification

C. Scaffolding, protein interaction modules, and temporospatial regulation

III. Protein kinases, disease, and clinical implications 17-18

Chapter 2: WNK (with no lysine (K))

I. WNKs from a biochemical view 19-27

A. Discovery of the WNK family protein kinases

B. The kinase domain and other functional modules of WNK

C. Biochemical studies of WNKs

D. Structure of WNK1

II. WNKs and hypertension 27-38

A. Overview of the molecular basis of hypertension

B. WNKs and pseudohypoaldosteronism type II (PHAII)

C. Localization and expression pattern of WNKs

D. WNK1 knockout mouse model

E. Description of research in thesis

Chapter 3: WNK1 interacts with Synaptotagmin 2 (Syt2)

I. Abstract 39-40

II. Introduction 40-43

A. Synaptotagmins (Syts)

B. Localization and post-translational regulation of Syt

III. Materials and methods 43-49

IV. Results 49-75

A. Summary of yeast two-hybrid screening

B. The kinase domain of WNK1 interacts with Syts

C. WNK1 and Syt2 exist as a native complex in a subset of subcellular compartments

D. WNK1 displays specificity among Syt isoforms

E. WNK1 interacts with Syt2 through essential Ca^{2+}-binding residues in the C2 domains

F. WNK1 contains a selective Syt binding pocket

G. WNK1 phosphorylates Syt2 on its C2 domains

H. Phosphorylation by WNK1 changes the Ca^{2+} requirement for Syt2 binding to phospholipid vesicles

V. Discussion 75-83

Chapter 4: WNK1 Interacts with Smad2 and Dynein Light Chain

I. Abstract 84-85

II. Introduction 85-95

A. TGF-β signaling and Smads

B. Regulation of Smad signaling

C. LC8/PIN (dynein light chain)

III. Materials and methods 95-98

IV. Results 98-114

A. The kinase domains of WNK1 and 4 interact with Smad2

B. Both WNK1 and WNK4 phosphorylate Smad2

C. WNK1 did not affect the activity or stability of Smad2 in cells under currently defined conditions

D. WNK1 binds to and phosphorylates LC8/PIN

E. Mutation of Ala622 to Asp abolished WNK1 binding to LC8/PIN

F. LC8/PIN may attenuate the autoinhibition of WNK1

Discussion 114-123

A. WNK and Smad2

B. WNK and LC8/PIN

Chapter 5: WNK1 and Other Observations

I. Abstract 124-125

II. Material and methods 125-126

III. Results and discussion 126-144

A. Analysis in *C. elegans*

B. Analysis by gel filtration

C. Analysis by pairwise two-hybrid

D. Analysis of hypertension-causing mutations

Future Directions 145-148

References 149-163

Vita 164

Publications presented in this dissertation

Xu BE, Min X, Stippec S, **Lee BH**, Goldsmith EJ, and Cobb MH. (2002) Regulation of WNK1 by an autoinhibitory domain and autophosphorylation. **J. Biol. Chem.** 277, 48456-48462.

Xu BE, Stippec S, Lenertz L, **Lee BH**, Zhang W, Lee YK, and Cobb MH. (2004) WNK1 activates ERK5 by an MEKK2/3-dependent mechanism. **J. Biol. Chem.** 279, 7826-7831.

Min X, **Lee BH**, Cobb MH, and Goldsmith EJ. (2004) Crystal structure of the kinase domain of WNK1, a kinase that causes a hereditary form of hypertension. **Structure** 12, 1303-1311.

Lee BH, Min X, Heise CJ, Xu BE, Chen S, Shu H, Luby-Phelps K, Goldsmith EJ, and Cobb MH. (2004) WNK1 phosphorylates synaptotagmin 2 and modulates its membrane binding. **Mol. Cell** 15, 741-751

List of Figures and Tables

Figure 1-1 Integrated circuit in signaling pathway

Figure 1-2 Molecular networks regulating hypoxia-responsive elements

Figure 1-3 Dendogram of 491 eukaryotic protein kinase domains from 478 genes

Figure 1-4 Structure of the active form of cAMP-dependent protein kinase (PKA)

Figure 2-1 WNK1 contains a unique catalytic lysine

Figure 2-2 Schematic representation of pattern and profile analyses of WNK primary sequences

Figure 2-3 Summary of biochemical studies of WNKs

Figure 2-4 Crystal structure of the inactive form of the kinase domain of WNK1

Figure 2-5 Diagram of the nephron and its components

Figure 2-6 Schematic representation of hypertension-causing mutations in WNKs

Figure 2-7 Published reports linking WNKs and channel/transporters, and their respective models

Figure 3-1 Identification of Syt2 as a WNK1-interacting protein

Figure 3-2 Co-immunoprecipitation of overexpressed Syt2 and WNK1

Figure 3-3 Mapping of the regions of Syt2 that bind to WNK1

Figure 3-4 Interaction of endogenous Syt2 and WNK1

Figure 3-5 Subcellular localization of insulin, WNK1, and Syt2 in INS-1 cells

Figure 3-6 Specificity of the WNK1-Syt interaction

Figure 3-7 The role of Ca^{2+} in the specificity of the WNK1-Syt2 interaction

Figure 3-8 Molecular modeling of WNK4 based on WNK1 structure and mutagenesis analysis of surface residues with different charges between WNK1 and WNK4

Figure 3-9 Phosphorylation of Syt2 by WNK1

Figure 3-10 Effect of phosphorylation on the interaction of Syt2 with phospholipid vesicles

Figure 4-1 Schematic representation of TGF-β signaling pathway

Figure 4-2 The Smad family and their domains

Figure 4-3 The dynein motor complex and structural organization of the LC8 dimer

Figure 4-4 Mapping of the regions in Smad2 that bind to WNK1 and WNK4

Figure 4-5 Phosphorylation of Smad2 by WNK1 and WNK4

Figure 4-6 The selective phosphorylation of C-terminal serine residues on Smad2 by WNK1 relative to WNK4

Figure 4-7 Effects of WNK1 on endogenous Smad2 protein level

Figure 4-8 No change in Smad2 nuclear translocation caused by WNK1

Figure 4-9 WNK1 interacts with LC8/PIN

Figure 4-10 WNK1 phosphorylates LC8/PIN

Figure 4-11 LC8/PIN binding to WNK1 and mutants

Figure 4-12 Attenuation of the autoinhibitory effects of WNK1 by LC8/PIN

Figure 5-1 Expression of WNK1 in *C. elegans*

Figure 5-2 WNK1 does not exist as a monomer

Figure 5-3 One representative silver-stained gel of the WNK1-associated proteins

Figure 5-4 Schematic representation of the self assembly of WNK1 proteins

Figure 5-5 Current models concerning intermolecular and intramolecular interactions of WNK1

Figure 5-6 WNK1 Q637E displayed decreased activity

Table 3-1 Summary of properties of Syt isoforms

Table 3-2 Summary of the results of yeast two-hybrid screens with WNK1

Table 5-1 Pairwise yeast two-hybrid interactions between WNK1 and WNK4 and between WNK4 and WNK4

Table 5-2 Pairwise yeast two-hybrid interactions between WNK1 and WNK1

Table 5-3 Pairwise yeast two-hybrid interactions between WNK1 and the WNK1 N-terminal region (residues 1-222)

Table 5-4 Pairwise yeast two-hybrid interactions between WNK1 or 4 and hypertension-causing mutants in WNK1

List of Abbreviations

CaMKII	Ca^{2+}/calmodulin-dependent protein kinase II
CCD	cortical collecting duct
CKII	casein kinase II
DCT	distal convoluted tubule
ENaC	epithelial sodium channel
ERK	extracellular signal-regulated kinase
GPCR	G-protein-coupled receptor
JIP	JNK inhibiting/interacting protein
LC8/PIN	8 KDa dynein light chain/protein inhibitor of nitric oxide synthase
MAPK	mitogen-activated protein kinase
MAP2K	MAP kinase kinase (MEK)
MAP3K	MAP2K kinase (MEKK)
MAP4K	MAP3K kinase
MH	Mad homology domain
NCC	Na-Cl cotransporter (SLC12A3)
NEDD4-2	neural precursor cell expressed, developmentally down-regulated 4-2
NKCC	Na-K-2Cl cotransporter (SLC12A1 and 2)
OSR1	oxidative stress-responsive 1
PAK	p21-activated protein kinase

PHAII	pseudohypoaldosteronism type II
PI3K	phosphatidylinositol 3-kinase
PKA	cAMP-dependent protein kinase (protein kinase A)
PKC	Ca^{2+}-dependent protein kinase (protein kinase C)
RNAi	RNA interference
ROMK	Kir1.1 subtype of inward rectifier K^+ channel
RTK	receptor tyrosine kinases
SAPK/JNK	stress-activated protein kinase/c-Jun NH_2-terminal kinase
SARA	Smad anchor for receptor activation
SH3	src homology 3
Syt	synaptotagmin
TGF-β	transforming growth factor β
TβR	transforming growth factor β receptor
WNK	with no lysine (K) kinase

Chapter 1: General Overview

I. Signal transduction through protein kinases

A. Protein kinases

Since the discovery of the first protein kinase, phosphorylase kinase, in glycogen metabolism by Krebs and Fischer, compelling evidence has shown that protein phosphorylation is an integral event in biological systems that regulate every aspect of cellular fate (Krebs and Fisher, 1956). It is believed that at least one-third of all eukaryotic proteins contain covalently linked phosphate groups (Zolnierowicz and Bollen, 2000). The completion of genomic sequencing projects has revealed that eukaryotic protein kinases occupy from 1.5% to 2.5% of the total genes from yeast to humans, placing kinases among the largest families of genes in eukaryotes (Manning et al., 2002).

Protein kinases mediate a plethora of cellular events; by post-translationally modifying the activity of substrates, they control numerous cellular processes, including development, transcription, metabolism, proliferation, differentiation, and apoptosis. Dysregulation of and genetic alterations in protein kinases often cause disease or developmental defects. Therefore, the discovery of pharmacological agents to modulate specific protein kinases and phosphatases is a priority in disease therapy (Hunter, 2000).

Signaling through protein kinases bears similarity to the wiring of electronic circuitry. A mitogen-activated protein kinases (MAPK) cascade, for example, represents a phosphorelay system for transmitting extracellular information to coordinate cellular

responses by achieving amplification of the original short-lived signaling events. This cascade is wired through diverse cross-connections with other pathways. For instance, several agonists of G-protein-coupled receptors (GPCRs) can activate receptor tyrosine kinases (RTKs) and the extracellular signal-regulated kinase (ERK) pathway; this is referred to as transactivation (Wetzker and Bohmer, 2003). These cross-connections enable the same core signaling machinery to elicit multiple cell biological effects. In fact, global screening has just begun to elucidate how nodes from isolated cascades, which were identified by traditional genetic and biochemical approaches, have been interwoven together to integrate individual pathways to achieve specific outcomes (Figure 1-1) (Hanahan and Weinberg, 2000). Accumulation of large scale systematic analyses and post-genomic knowledge of signal transducers, protein-protein interaction modules, spatiotemporal regulation, and kinetics motivates attempts to build up a resource of predictive signaling networks and algorithms in silico. These efforts have already yielded predictions of the networks of the cell cycle regulation, hypoxia responses, and cellular responses to DNA double-strand breaks (Figure 1-2) (Kohn, 1999; Kohn et al., 2004; http://discover.nci.nih.gov/mim).

B. Catalog of the eukaryotic protein kinase superfamily

The catalytic domains of protein kinases are highly conserved with a remarkable degree of sequence identity among over 500 known mammalian enzymes. The kinase domains that define this group of enzymes contain 12 conserved subdomains and display conserved structural motifs within a common three dimensional fold, as revealed by

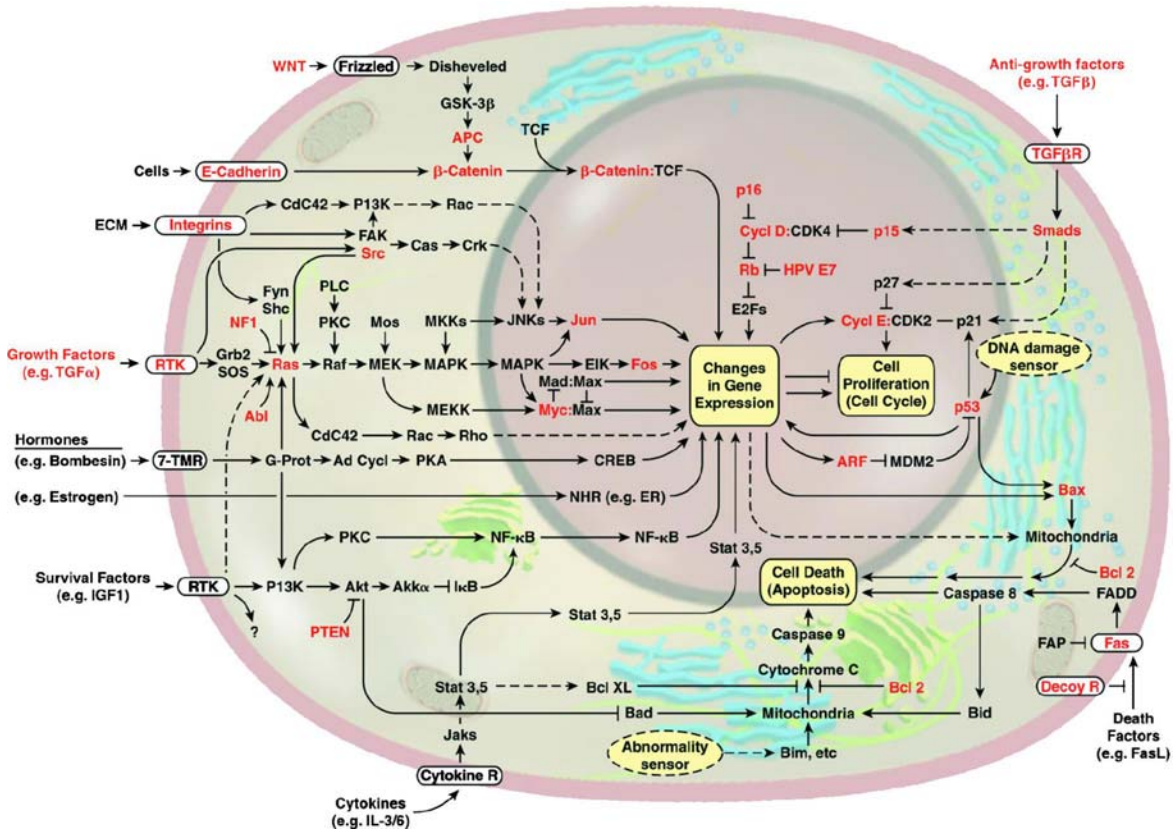

Hanahan and Weinberg, 2000

Figure 1-1. Integrated circuit in signaling pathway
Signaling networks bear resemblance to electronic integrated circuits, where transistors are replaced by proteins, such as kinases and phosphatases, and the electrons by phosphates and lipids. For example, the Raf-Ras-MAP kinase cascade experiences diverse cross-connections with other signaling pathways.

A

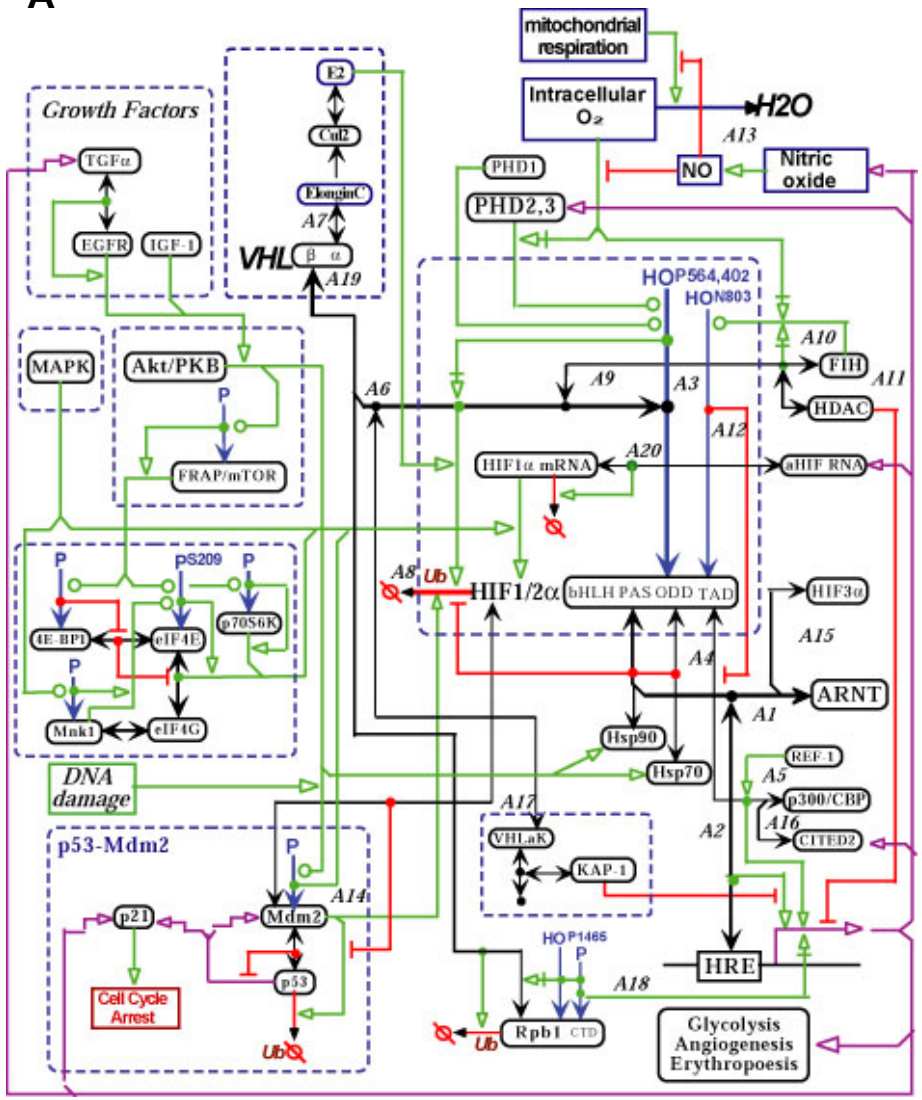

B

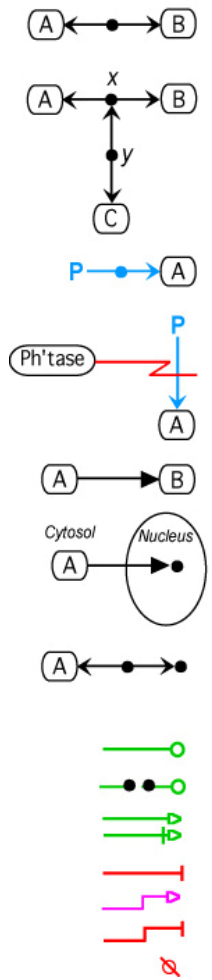

Proteins **A** and **B** can bind to each other.
The 'node' placed on the line represents the **A:B** complex.

Representation of multimolecolar complexes: x is **A:B**; y is **(A:B):C**. This notation is extensible to any number of components in a complex.

Covalent modification of protein **A**. The single-arrowed line indicates that **A** can exist in a phosphorylated state. The node represents the phosphorylated species.

Cleavage of a covalent bond: dephosphorylation of **A** by a phosphatase.

Stoichiometric conversion of **A** into **B**.

Transport of **A** from cytosol to nucleus. The filled circle represents **A** after it has been transported into the nucleus (an isolated node functions like a ditto mark).

Formation of a homodimer. Filled circle on the right represents another copy of **A**. The filled circle on the binding line represents the homodimer **A:A**.

Enzymatic stimulation of a reaction.

Enzymatic stimulation of a reaction in *trans*.

General symbol for stimulation of a process.
A bar behind the arrow head signifies necessity.

General symbol for inhibition.

Shorthand symbol for transcriptional activation.

Shorthand symbol for transcriptional inhibition.

Degradation products.

Kohn et al.2004

Figure 1-2. Molecular networks regulating hypoxia-responsive elements
A. This molecular interaction map describes the regulatory network that governs hypoxia-induced transcriptional switches (Kohn et al., 2004; http://discover.nci.nih.gov/mim). B. Definition of symbols.

crystallization of numerous members of the family. Hanks et al developed a classification system founded on a catalytic domain phylogeny, which arranges these enzymes in groups of subfamilies that have related functions. The major branches include AGC, CaMK, CMGC, PTK, and other protein kinase families (Hanks et al., 1988; Hanks and Hunter, 1995). The AGC group contains second-messenger regulated protein kinases, such as cAMP-dependent protein kinase (PKA), Ca^{2+}-dependent protein kinase (PKC), cGMP-dependent protein kinase (PKG), and Akt, etc. The CaMK group encompasses the calcium/calmodulin-dependent protein kinases and their relatives. The CMGC group includes cyclin-dependent protein kinases (CDKs), MAP kinases, glycogen synthase kinase 3 (GSK3), and casein kinase II (CKII). The PTK group covers conventional protein-tyrosine kinases. Lastly protein kinases not falling into the major groups aforementioned belong to a miscellaneous or other protein kinase subfamily.

The completion of the eukaryotic genome project expanded our knowledge of the protein kinase catalog by taking advantage of public and proprietary databases. The most recent classification of the human protein kinase complement or kinome has expanded the human protein kinase categories with four new groups (Manning et al., 2002); sterile (STE), tyrosine kinase-like (TKL), receptor guanylate kinase (RGC), and casein kinase 1 (CK1) (Figure 1-3). STE consists of MAP kinase kinase (MAP2K), MAP2K kinase (MAP3K), and MAP3K kinase (MAP4K) protein kinases – yeast Ste7p, Ste11p, and Ste20p orthologs, respectively. TKL includes the kinase families that bear resemblance to both tyrosine and serine/threonine kinases. RGC is composed of tyrosine kinase-like protein kinases, notably lacking functional kinase activity. The CK1 group contains CK1, tau tubulin kinase (TTBK),

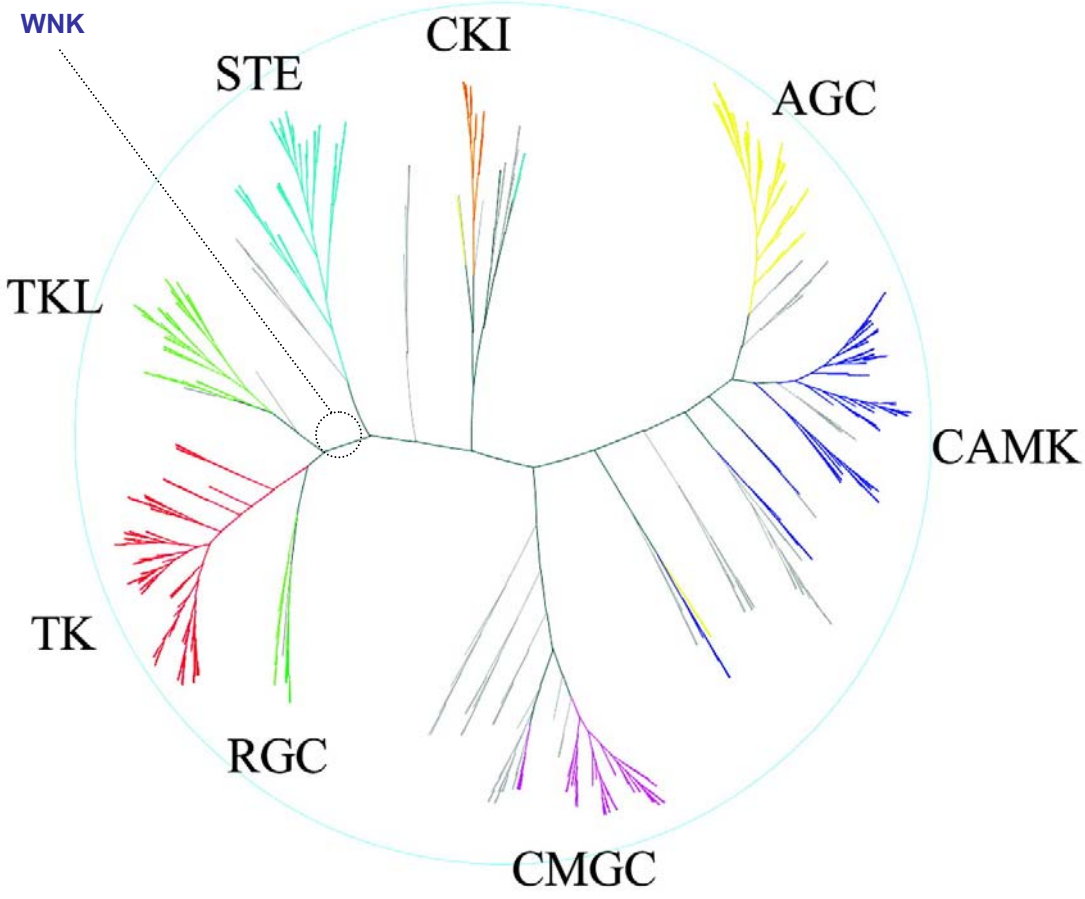

Figure 1-3. Dendogram of 491 eukaryotic protein kinase domains from 478 genes
Major groups are described in the text. For genomic trees, see www.kinase.com/human/kinome/ (Manning et al., 2002).

and vaccinia-related kinase (VRK) subfamilies. Interestingly, about 10% of the categorized protein kinase domains are unlikely to retain catalytic activity. These inactive kinases may have noncatalytic functions as scaffold proteins or regulators of the active domains. However, the prediction that a protein lacks kinase activity requires experimental validation. For instance, WNK (with no lysine (K)) family protein kinases, once believed to be kinase deficient (KDP), contain the catalytic lysine in an atypical position and therefore appear to use a modified catalytic mechanism (Xu et al, 2000). WNK is an example indicating that simple deduction from the primary sequence information may belie the real function.

C. Structural organization of protein kinases

The ternary structure of the first protein kinase was first visualized by X-ray crystallography of PKA (Knighton et al., 1991). Currently, there are more than 40 protein kinase structures deposited in the database in either active or inactive states. Protein kinase domains can be viewed as occupying one of two extreme conformational states: active (on) or inactive (off). In the active state, they adopt strikingly similar conformations, whereas the off states reveal remarkable diversity that allows distinct regulatory mechanisms (Nolen et al., 2004).

The protein kinase domain consists of two domains (also called lobes). The smaller N-terminal domain is composed of a five-stranded β-sheet and one α helix (helix αC). The larger C-terminal domain contains primarily α helices. ATP binds in the interior cleft of the active site which is formed at the interface of the two domains. Protein or peptide substrates bind on the exterior near the front of the nucleotide binding pocket. The highly

conserved catalytic lysine in β3 strand (Lys72 in PKA) functions to anchor and orient ATP through interactions with the α- and β- phosphates of the nucleotide for the phosphotransfer reaction. This lysine gains its stability from an ionic interaction with a glutamate residue (Glu91 in PKA) in the αC helix. The glycine-rich loop with the consensus sequence GXGXXG in β2 strand provides the necessary flexibility and the glycine residues in this motif make contact with all three parts of ATP. The activation loop that lies in the vicinity of the active site cleft provides a platform for the substrate and makes several contacts with residues from both the N-and C-terminal domains. Another absolutely conserved aspartic acid residue (Asp184 in PKA) at the N-terminus of the activation loop (the magnesium binding loop), a constituent of the conserved DFG/DLG motif, stabilizes the ATP molecule by binding to the divalent cation. The catalytic reaction also involves three residues (Asp166, Lys168, and Asn171 in PKA) in the catalytic loop, a highly conserved loop lying at the base of the active site. The hydrophobic residue in the P+1 pocket, originally referred to in the PKA structure, is important for determining the substrate specificity by contacting the residue following the phosphorylation site (P+1) in the substrate (Figure 1-4) (Zheng et al., 1993; Bossemeyer et al., 1993).

II. Regulation of protein kinase signaling

Conventional regulatory mechanisms include secondary messenger-mediated regulation, allosteric mechanisms, effector (regulator or inhibitor) binding, feedback mechanisms, spatiotemporal regulation, post-translational modifications, and certainly many more.

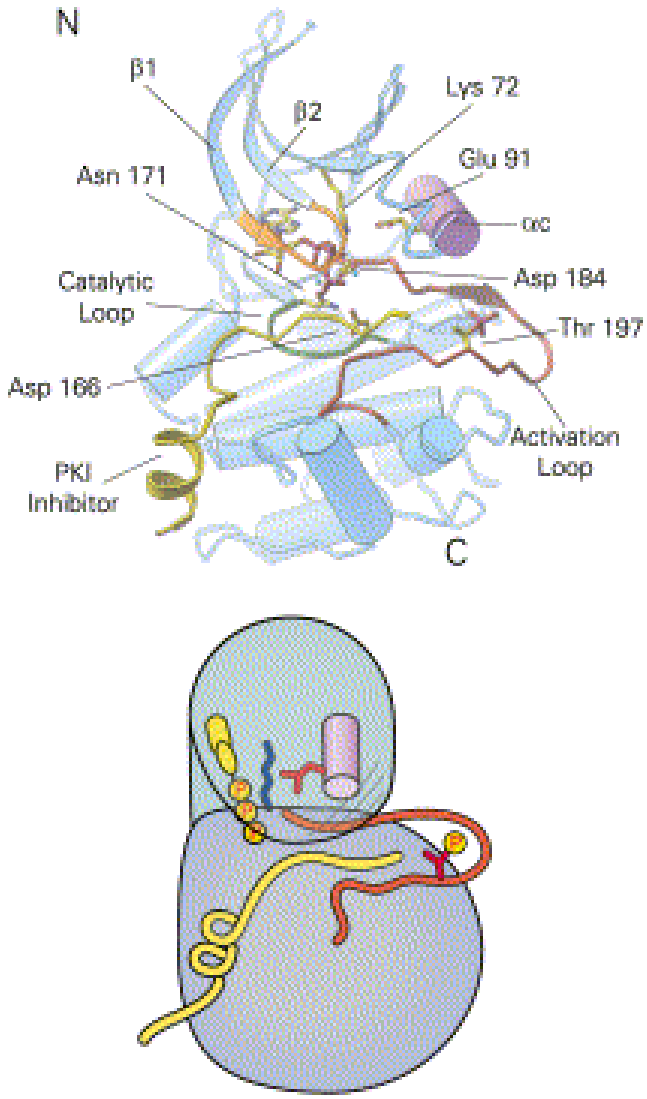

Figure 1-4. Structure of the active form of cAMP-dependent protein kinase (PKA)

The crystal structures of the active form of PKA revealed key structural elements within the kinase domain are colored as follows: activation loop, red; αC helix, purple; P loop, orange; and catalytic loop, green (Top). The structure has been simplified to clearly represent the active site and critical structural components for the regulation of kinase activity (Bottom). Figure was from Huse and Kuriyan, 2002.

A. Regulation of kinase activity from a structural view

As described earlier, protein kinases undergo conformational changes as they are in on and off states, and these changes are under tight regulation. A handful of kinase structures clearly provide the insights into the mechanism of regulation.

Primarily, the correct positioning and proper conformation of the activation segment are pivotal for catalytic activity (Johnson et al., 1996). And this activation loop seems to be structurally coupled with αC helix, accompanying the conformational changes when kinases switch between inactive and active states. Among examples, 1) phosphorylation of the activation loop of the MAP kinase ERK2 creates the interactions that extend to and orient properly αC helix, promoting the closure of the N- and C-terminal subdomains so that the kinase becomes active. This functional change also creates the homodimerization interface. 2) Activation of the Src family tyrosine kinase proves the significance of the coupling between the activation segment and αC helix as well, yet with somewhat different mechanisms. An inactive conformation of Src kinase can be stabilized by intramolecular interactions through its Src homology 2 (SH2) and SH3 domains. Once the intramolecular interactions are disrupted by ligands of SH2 and SH3 domains, this disengagement triggers conformational changes in the active site and allows αC helix to move into an active conformation. 3) The structures of the calcium-regulated myosin light chain kinase subfamily and the p21-activated protein kinase (PAK) add more examples of generally similar mechanism of regulation. These kinases reveal a conserved mode of autoinhibition. In PAK, for instance, the N-terminal inhibitory domain contains a pseudosubstrate

sequence. By binding to the C-terminal domain of the kinase and sliding the pseudosubstrate portion into the active site cleft, the autoinhibitory domain traps the activation loop and pushes αC helix away from the catalytic core. Studies suggested that the binding of the small G protein within the inhibitory domain would dissociate both the inhibitory domain and the pseudosubstrate segment, liberating the kinase to allow the stimulatory phosphorylation on its activation loop (Huse and Kuriyan, 2002).

N- and C-terminal anchor points in the extended activation loop are important in considering activation and inactivation mechanisms. It was suggested that subtle changes in the activation loop may disturb the anchor points and this perturbation can be amplified into the major changes leading to kinase inactivity (Nolen et al., 2004).

Aside from regulation of kinase activity, association of substrates with protein kinases through docking sites distant from the active site are also important regulatory mechanisms for protein kinases (Tanoue et al., 2001). A structural study showed that p38 MAP kinase binds docking motifs of the substrates, such as MEF2A, and this interaction induces the proper conformational change and structural coupling of the activation loop for kinase activity (Chang et al., 2002).

B. Regulation by post-translational modification

Protein kinases can be regulated by stimulatory and inhibitory phosphorylation and also by autophosphorylation. Dual phosphorylation on the activation loop is required to activate MAP kinases (Cobb and Goldsmith, 1995). The activities of CDK and Src kinase are controlled by both stimulatory and inhibitory phosphorylation events (Krupa et al,. 2004).

Autophosphorylation can be determined by substrate specificity of the kinase and the environment surrounding the activation segment (Johnson et al., 1996), although underlying mechanisms are not fully understood. For instance, the activity of Ca^{2+}/calmodulin-dependent protein kinase II (CaMKII) can be modulated by autophosphorylation on multiple sites, which generates an active form of the kinase or blocks the Ca^{2+}/calmodulin binding (Colbran, 2004).

Dephosphorylation by phosphatases is certainly the most straightforward among the regulatory mechanisms. However, rather than being simply reversal machinery to counter the actions of protein kinases, phosphatases must be regulated on their own as well perhaps by even more complex mechanism, especially considering that there are many fewer phosphatase catalytic subunits than kinase catalytic subunits (Alonso et al., 2004).

Signaling can be negatively regulated by ubiquitin-mediated protein modification. Downregulation of RTKs by endocytosis and degradation is an example to show that the duration of signaling is critical for the cellular response (Sanjay et al., 2001). Additionally, the plant homeodomain (PHD) of MEKK1 acts as an E3 ubiquitin ligase and downregulates ERK1/2. SUMO proteins also appear to covalently modify the protein kinases (Lu et al., 2002). In *Dictyostelium*, for instance, a MAP2K protein MEK1 is sumoylated or ubiquitinated in response to signaling and these modifications appear to regulate the function and localization of MEK1 (Sobko et al., 2002). However, the understanding of these modifications is not yet well established.

Other types of post-translational modifications are also likely to regulate protein

kinase activities by affecting stability, subcellular localization, and kinetics of the enzymes. The modifications may include acetylation and methylation, glycosylation, myristoylation and palmytoylation, farnesylation, hydroxylation, nitrosylation, and sulfonylation. While we now mostly resort to protein mass spectrometry for the assessment of post-translational modifications, many of the types are still beyond within detection. Therefore, new types of modifications may turn out to be as significant as phosphorylation.

C. Scaffolding, protein interaction modules, and temporospatial regulation

Signaling specificity and efficiency can be greatly enhanced as signal transducers act in particular places at any specific time, suggesting that signaling components should be highly organized in specific cellular compartments to competently transduce the signals upon responding to stimuli.

The concept of scaffolding proteins in MAP kinase modules first emerged in works done with budding yeast (Kranz et al., 1994; Marcus et al., 1994). Since then the types and significance of scaffolding have been discussed in detail (Karandikar and Cobb, 1999; Morrison and Davis, 2003). In yeast, Ste11p (mammalian MEKK or MAP3K level) functions in both mating and high osmolarity responsive pathways. Studies suggested that signaling specificity can be achieved by selective association of the MAP kinase modules with scaffold proteins, Ste5p (mating pathway) and Pbs2p (also the MAP2K in the osmolarity pathway). JIP (JNK inhibiting/interacting protein) protein family and KSR (kinase suppressor of Ras) were identified to as possible functional scaffolds in mammalian MAP kinase cascades. Scaffolding may increase the fidelity and specificity of signaling by

localizing MAP kinase modules and also by insulating the specific cascade from irrelevant stimuli. Somewhat different but functionally related are so called adaptor or anchor proteins, such as A-kinase anchoring proteins (AKAPs) and Smad anchor for receptor activation (SARA). They localize their target proteins (PKA and Smad, respectively) to particular subcellular compartments for specific signaling events.

Caveolae, lipid rafts, that are known to be present in many cells, contain a variety of signaling molecules and membrane transporters. These higher order of macromolecular structures are flask-shaped invaginatons of the plasma membrane that were first detected around 50 years ago on the surface of endothelial cells. Association of numerous signaling molecules with these microdomains point out their role in compartmentalization and regulation of specific signaling cascades (Anderson, 1998; Conner and Schmid, 2003). Among discrete membrane signaling domains are focal adhesions, where integrins bind to extracellular matrix proteins and to cytoskeletal structures. This association mediates integrin signaling through phosphorylation events (Bershadsky et al., 2003).

Trafficking of receptors and signal transducers to the right place at the right time is critical for specificity and efficiency of signaling. Indeed, signaling proteins may be directionally transported in a semi-solid state fashion - by vesicular transport and motor proteins. JIP family proteins, scaffolds for stress-activated protein kinase/c-Jun NH_2-terminal kinase (SAPK/JNK) modules, also interact with the tetratricopeptide repeat domain (TPR) of kinesin light chain (Bowman et al., 2000; Verhey et al., 2001; Ito et al., 1999; Kelkar et al., 2000). This interaction with a motor protein may explain the accumulation of JIP proteins in growth cones of developing neurons. This observation emphasizes that

signaling molecules are dynamically redistributed within subcellular compartments that may allow the targeting of substrates for the spatial regulation.

Seminal work by the Pawson's group and others identified SH2 and phosphotyrosine binding (PTB) domains that mediate signaling specificity from tyrosine kinases through noncatalytic domains by protein-protein interaction modules (Pawson, 1995). Further studies uncovered numerous modular domains that recognize diverse molecules. These include SH3, WW, FHA, SAM, LIM, PH, EH, EVH1, GYF, DD, DED, MH2, PBD, and PDZ domains. Among these discoveries, the pleckstrin homology (PH) domain recognizes specific phospholipids and occasionally protein molecules. Phosphoserine/threonine binding domains (e.g. 14-3-3; MH2 domain of Smad proteins) have also been identified, which suggests that signaling specificities of Ser/Thr protein kinases are regulated through protein-protein interactions analogous to those identified in tyrosine kinase signaling (Yaffe and Cantley, 1999). These modular protein interactions are now regarded as a general means of propagating a signal. The recent catalog of the human protein kinase complement (kinome) revealed previously unknown but conserved regions which may be folding (Manning et al., 2002).

One of the challenges to study signaling is how the cellular systems determine the exact timing of the initiation and termination of signaling and also how the speed of the process is accelerated or sustained. These dynamic properties of signaling events have begun to be elucidated through the study of real-time movements of signaling molecules in living cells (Sakai et al., 1997; Oancea and Meyer, 1998). Notably, a recent work used small sized quantum dots (QDs) as fluorescent probes to study the dynamics of individual

glycine receptors over time in living cells (Dahan et al., 2003).

III. Protein kinases, disease, and clinical implications

A myriad of diseases, including cancer, diabetes, inflammation, and other systemic disorders, are related to mutations and dysregulation of protein kinases and their regulators. The first connection between a protein kinase and disease came with the discovery by the Erikson's and Bishop's groups that the oncogene, v-Src, is actually a protein kinase (Collett and Erikson, 1978; Levinson et al., 1978). More than 18 protein tyrosine kinases (PTKs) are now implicated as potent oncoproteins, when mutated or structurally altered. Ser/Thr protein kinases are also suspects in many genetic diseases. Raf was the first Ser/Thr kinase implicated in cancer (Mark and Rapp, 1984). The gene mutated in Coffin-Lowry syndrome (CLS), an X-linked mental retardation, encodes RSK2, a Ser/Thr protein kinase (Trivier et al., 1996), and a number of mutations in the transforming growth factor β receptor I and II (TβRI and TβRII) were observed in different types of carcinomas (de Caestecker et al., 2000). Additionally, two WNK family members have been associated with a heritable form of monogenic hypertension known as pseudohypoaldosteronism type II (PHAII) (Wilson et al., 2001). Recent analysis of the human kinome linked kinase chromosomal regions with known disease loci. The linkage data indicated that 164 kinases map to the region often found in human neoplasms and 80 kinases map to candidate loci of other human diseases (Manning et al., 2002).

Protein kinases are now the second largest group of drug targets after G-protein-coupled receptors (GPCRs) (Cohen, 2002; Noble et al., 2004). Fasudil (Rho-kinase

inhibitor), Gleevec (ABL kinase inhibitor), rapamycin (mTOR inhibitor), Herceptin (ErbB2 or HER2 receptor inhibitor), and many more are in the clinic or undergoing clinical trials. Certainly, structural information has illuminated the mechanism of inhibition and aided the development of highly specific protein kinase and phosphatase inhibitors. Structure-based optimization of drug targets has revealed some currently followed principles. Noteworthy among these, inactive forms of kinases appear to be more attractive for drug design, because, in active states, kinases display greater similarities in conformation. In addition, in several cases drugs, most of which are ATP competitors, compete more favorably with ATP for the nucleotide binding site. Nevertheless, there are a few successful inhibitors that bind to the active form of their target kinases, including Tarceva (tyrosine kinase inhibitor) and UCN-01 (Chk1 or PDK1 inhibitor). In addition to that, informed with the structure of the Herceptin-bound HER2 complex, the design of drugs for targeting noncatalytic – or less conserved –- domains that inhibit a particular kinase, but not others, appears to be rational for ensuring required specificity. The higher demand of mechanistic understanding of drug actions on kinases became doubly acute from the use of substance, like anthrax toxin for bioterrorism, which selectively inactivates MAP2K family of protein kinases (Duesbery et al., 1998)

Chapter 2: WNK (with no lysine (K))

I. WNKs from a biochemical view

A. Discovery of the WNK family protein kinases

Our lab originally isolated the first two members of the WNK protein kinase subgroup from a rat brain cDNA library (Xu et al., 2000). Four WNK family members are present in the human genome, whereas only one WNK ortholog is present in worm and fly, suggesting evolutionary duplications for functional diversities. No WNKs are present in unicellular organisms. Interestingly, plants have 8 or more WNK homologs, which indicates that plants have found additional uses of WNK genes that have yet to be determined (Verissimo and Jordan, 2001).

WNKs display very weak similarities with any known protein kinases within their kinase domains, clearly not falling into any of the currently defined subgroups (see Figure 1-3). Still distant but the closest sequence homology, however, is observed with Ste20p-like (MAP4K) protein kinases, suggesting that in part WNK may play a role as a MAP4K kinase. The yeast Ste20p, the prototypical MAP4K kinase, was first identified in screens for genes that function downstream of heterotrimeric G protein $\beta\gamma$ subunits but upstream of MAP kinase modules. The human genome contains more than thirty Ste20p-related kinases, and these are further divided into PAK and germinal center kinase (GCK) subfamilies (Xu et al., 2000).

B. The kinase domain and other functional modules of WNK

WNK family protein kinases gained primary attention due to their unique active site organization. The catalytic domains of protein kinases reveal remarkable sequence identity and conserved catalytic and structural residues within a common three dimensional fold (Knighton et al., 1991). One of the most highly conserved residues is a lysine in β3 strand (kinase subdomain II). This invariant lysine anchors and orients ATP through interactions with its phosphate groups to facilitate phosphoryl transfer. Replacement of this lysine by any other amino acid greatly reduces protein kinase activity. In WNK1, this residue was replaced by cysteine, but WNK1 still displayed catalytic activity (Figure 2-1A). Subsequent mutagenesis analysis showed that the catalytic lysine is contributed from β2 strand (kinase subdomain I), replacing the third glycine in the conserved GXGXXG motif (Figure 2-1B). Initial molecular modeling of the WNK1 kinase domain based on the backbone of ordinary protein kinase structures strongly suggested that this repositioned lysine may be as competent as a canonical catalytic lysine by properly snaking into the active site (Figure 2-1C). This unique positioning of the catalytic lysine is conserved among WNK isoforms across species, ranging from worms and plants to vertebrates, underscoring the functional relevance of this novel position and also a modified catalytic mechanism (Xu et al., 2000; Min et al., 2004). In fact, residue swapping experiments strongly supported the significance of the unique position of the catalytic lysine; a WNK1 mutant that has the normal catalytic lysine arrangement exhibits no kinase activity, but ERK2 mutants that adopt the WNK catalytic lysine placement still retained kinase activity (Xu et al., 2002).

The four human WNK family members possess more than 85% sequence identity

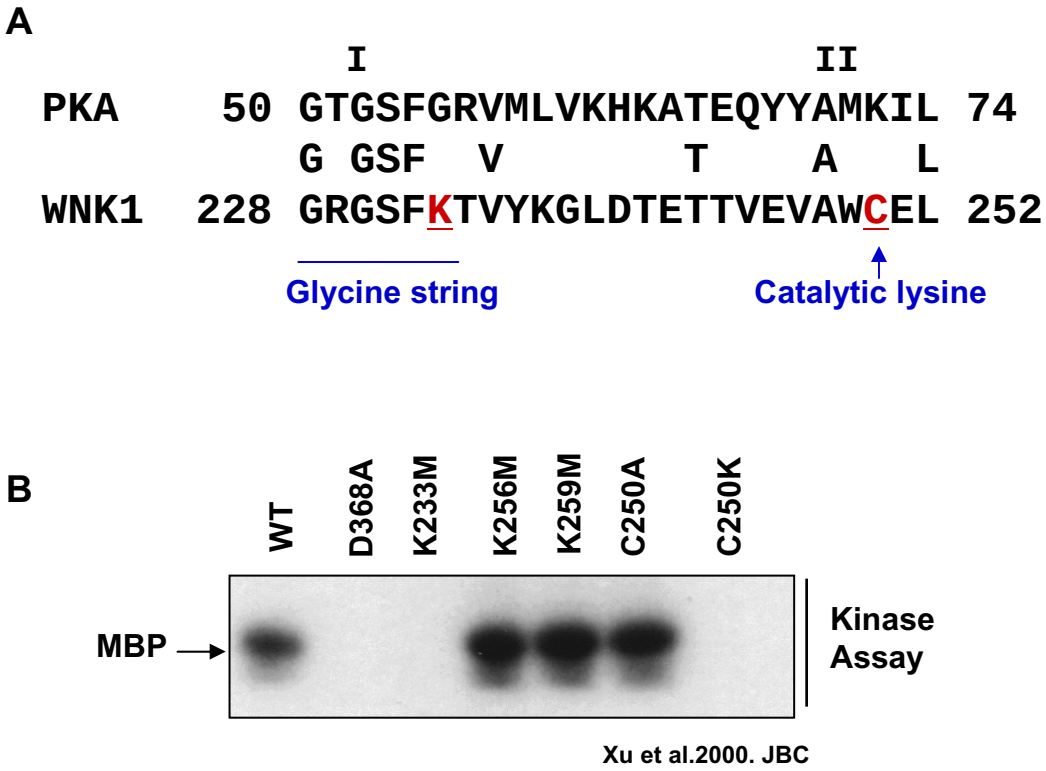

Figure 2-1. WNK1 contains a unique catalytic lysine
Structure/function analyses revealed that K233 serves as an atypical catalytic lysine for WNK1. See the text for the details.

within their N- terminal kinase domains. Such as PAS repeat and polyadenylate binding domains are predicted by sequence analysis but with nearly marginal scores. Otherwise, there are few identifiable domains in WNKs outside the kinase core. Nevertheless, the full length rat WNK1, of 2126 amino acids, contains potential protein interaction modules and motifs including proline-rich sequences with many PXXP SH3 binding motifs, coiled-coiled domains, and glutamine-rich regions (Figure 2-2) (Xu et al., 2000). In addition to that, protein sequence alignment of orthologous or paralogous kinase pairs among WNKs showed some local sequence conservation; for example, amino acid sequence comparison between human WNK1 and WNK4 identified an internal homology domain with around 50% sequence identity (Wilson et al., 2001), and pairwise sequence alignment of human and mouse WNK2 and WNK3 orthologs revealed a number of previously unknown highly conserved regions (Caenepeel et al., 2004). These previously undescribed conserved domains may possibly behave as functional modules. On the contrary, a completely unpredicted autoinhibitory domain in WNK1 of around 50 residues, proximally located to the C-terminus of kinase domain, was uncovered by biochemical studies. This domain suppressed WNK1 kinase activity both in cis and in trans, and also appears to act in trans among WNK isoforms, probably due to sequence conservation within this region (Xu et al., 2002; Wang et al., 2004).

C. Biochemical studies of WNKs

As noted above, at least one regulatory mechanism for WNK is by autoinhibition. In fact, many protein kinases, such as PAK1, PKA, and twitchin, show a conserved mode of

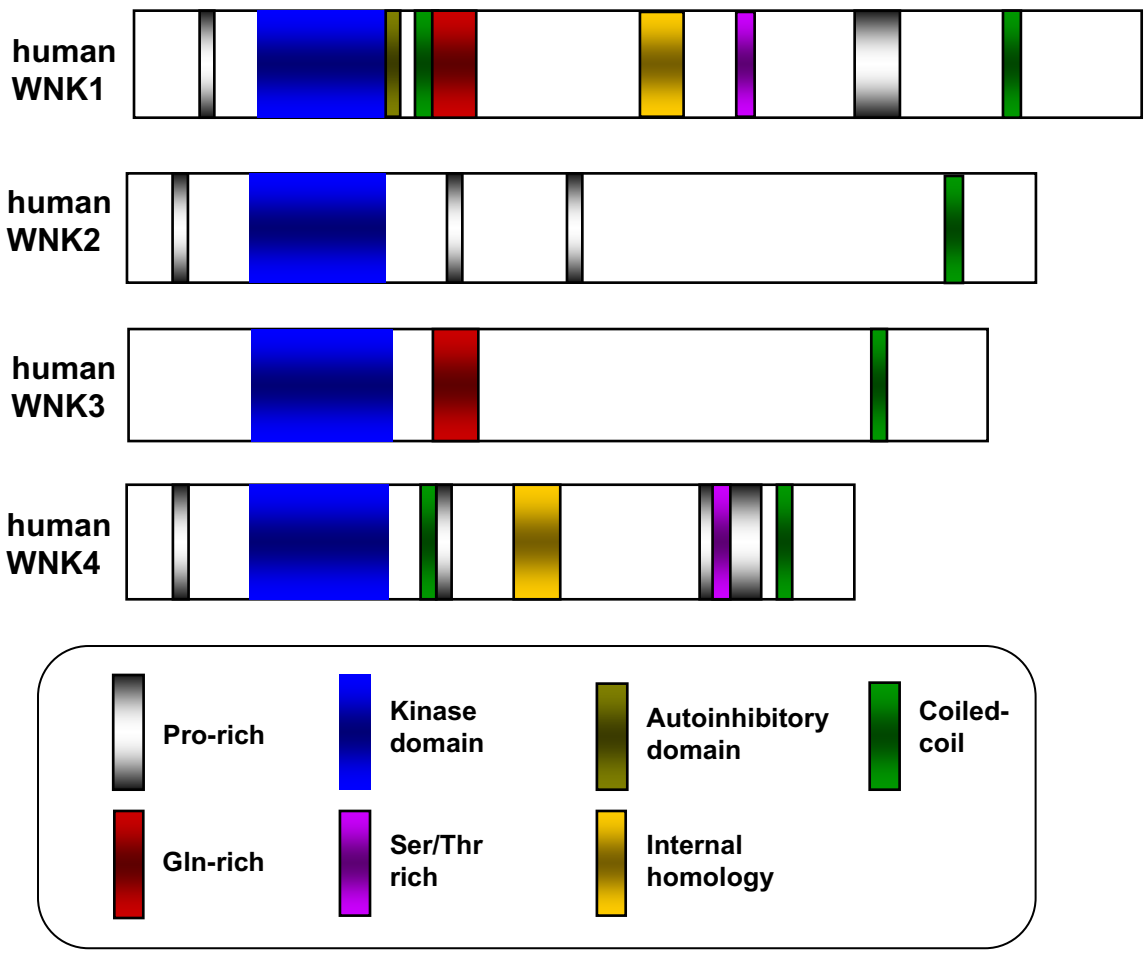

Figure 2-2. Schematic representation of pattern and profile analyses of WNK primary sequences

WNKs consist of multiple potential protein interaction modules and motifs. Sequences were retrieved from Entrez in NCBI (hWNK1: NM_018979, hWNK2: NM_006648, hWNK3: NM_020922, hWNK4: NM_032387) and were analyzed by Coils (http://www.ch.embnet.org/software/COILS_form.html) and motif scan (http://myhits.isb-sib.ch/cgi-bin/motif_scan) programs. An autoinhibitory domain was deduced from a structure/function study done with rat WNK1 (Xu et al., 2002).

autoinhibition, in which an autoinhibitory region outside the catalytic domain suppresses kinase activity until activating signals relieve it from an inhibitory state. Rat WNK1 contains an autoinhibitory domain located C-terminal to the kinase domain (residues 490-555), and a short segment, including two key hydrophobic residues, within this domain showed high sequence similarity among WNK isoforms (Figure 2-3) (Xu et al., 2002).

Among stimuli tested, only high osmolarity reproducibly activated endogenous WNK1 (Figure 2-3). In a separate study, *C. elegans* injected with DNA encoding ceWNK-GFP showed GFP localized to the H-shaped excretory cell and hypodermal cells, which will be discussed again in a later chapter. These data suggest that WNK1 may be involved in osmosensing or ion-balance adaptation pathways (Xu et al., 2000; B.-H. Lee and M. Cobb, unpublished data).

Like many protein kinases, WNK1 is autophosphorylated on Ser residues. Two Ser residues on the activation loop were identified as autophosphorylation sites in rat WNK1 from mass spectrometry, and phosphorylation of one of the two residues (Ser382) appears to be essential for WNK1 activity (Xu et al., 2002).

The notion that WNK1 is a distant Ste20p-related protein and therefore may act as a MAP4K motivated us to test the functional relation between WNK1 and MAP kinase pathways. While initial tests with WNK1 fragment containing the autoinhibitory domain suggested that WNK had little impact on MAPK pathways such as ERK2, JNK1, p38, and ERK5, the removal of the autoinhibitory domain led to the discovery that WNK1 activates ERK5. Kinase inactive MEKK3 blocked the ability of WNK1 to enhance ERK5 activity, and WNK1 phosphorylated and coimmunoprecipitated with MEKK2 and MEKK3, which is

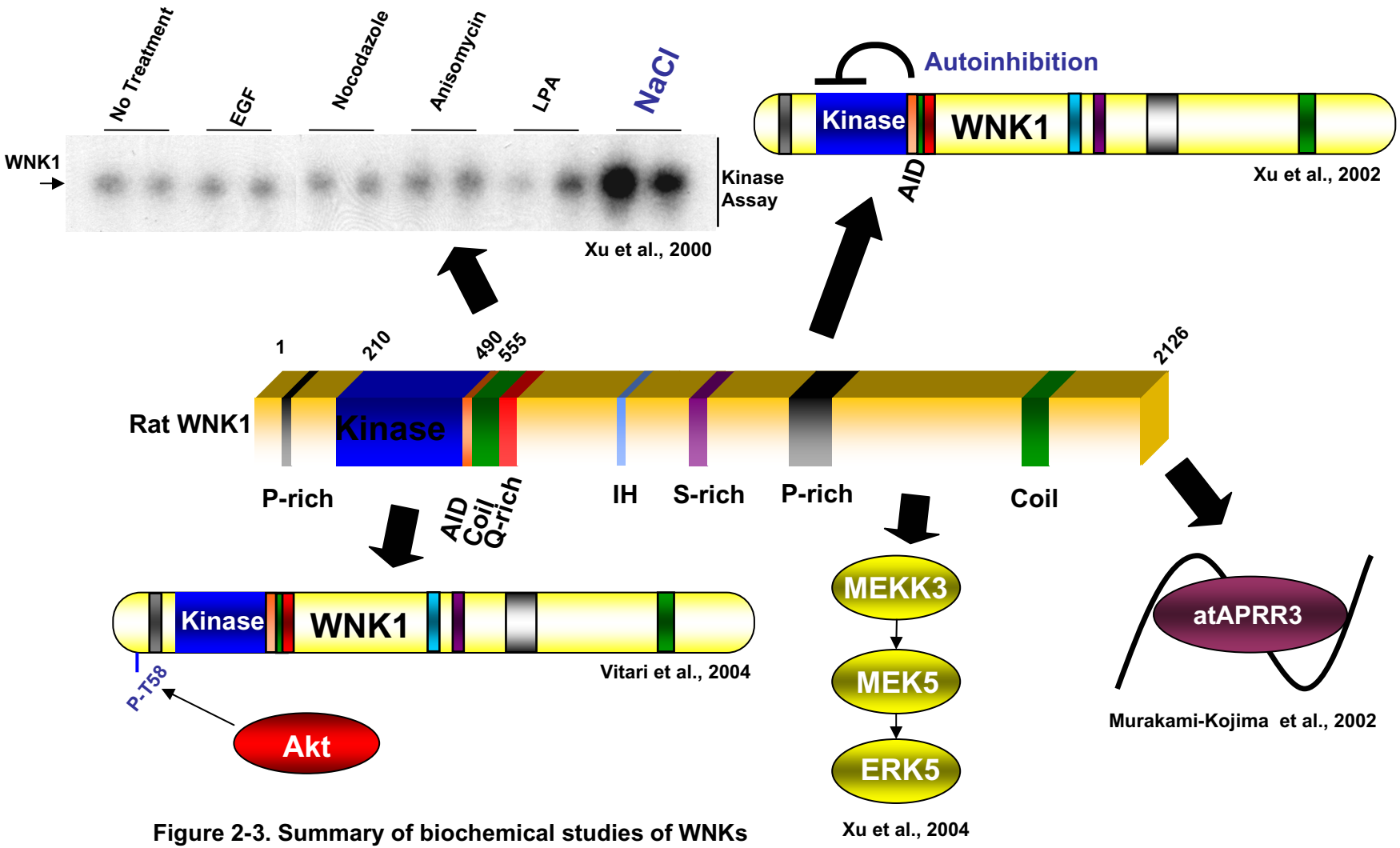

Figure 2-3. Summary of biochemical studies of WNKs
See the text for the details

consistent with the idea that at least one WNK1 function is as a MAP4K kinase (Figure 2-3) (Xu et al., 2004).

WNK isoforms contain multiple putative modification sites which can be predicted by motif scanning (http://scansite.mit.edu). These speculative sites include PKA, Akt, PKC alpha/beta/gamma/delta/zeta, CK1 and 2, and GSK3 phosphorylation motifs. Recently Alessi's group reported that at least one of these potential modifications occurs in cells. They showed that Akt efficiently phosphorylates WNK1 at an N-terminal threonine site (Thr60 in human WNK1) (Figure 2-3). Since this phosphorylation did not change either WNK1 kinase activity or localization, the functional consequences of Akt phosphorylation of WNK1 were not clear (Vitari et al., 2004).

In *Arabidopsis thaliana*, more than twice the number of WNKs are present. Mizuno and coworkers isolated a plant WNK homolog by yeast two-hybrid screening with APRR3 as bait. APRR3 is regulated via circadian rhythms in plants (Figure 2-3). They also showed that APRR3 is a substrate of WNK1, and intriguingly, certain subsets of plant WNK isoforms oscillated transcriptionally under the control of circadian rhythms (Murakami-Kojima et al., 2002; Nakamichi et al., 2002).

WNK1 was also identified from yeast two-hybrid screening with a transcription factor, E2F3, although there are no further biochemical and functional insights into this interaction (Giangrande et al., 2003). In addition to that, partial cDNA clones of WNK1 and WNK2 were isolated from malignant prostate tissues and pancreatic cancer cells, respectively. However, their roles in tumorigenesis, if any, are not known yet (Moore et al., 2000; Ito et al., 2001).

D. Structure of WNK1

The crystal structure of the WNK1 kinase domain was solved at 1.8 Å resolution in a low activity conformation (Figure 2-4). The catalytic lysine (Lys233) was contributed from β2 strand rather than β3 strand and still properly oriented into the active site as previously expected from earlier mutagenesis. The activation loop displayed a unique well-folded inactive conformation, and some noticeable modifications within the active site and the activation loop strongly suggest a unique catalytic mechanism. Otherwise, the overall topology of WNK1 represented a typical inactive state of a kinase domain (Min et al., 2004).

II. WNKs and hypertension

A. Overview of the molecular basis of hypertension

Elevated blood pressure, hypertension, is thought to affect almost one in four adults worldwide, and is a significant risk factor for public health due to higher chance of heart attacks, strokes, and renal disease. Human genetic studies have currently identified mutations in at least 8 genes for hypertension and 9 genes for hypotension which conform to Mendelian rules (Lifton et al., 2001). The molecular understanding of known Mendelian hypertension disorders suggests that higher blood pressure can be attributed to a final common pathway, that is, the regulation of renal sodium reabsorption. The nephron is anatomically composed of the proximal tubule (PT), thick ascending limb of Henle (TAL), distal convoluted tubule (DCT), and cortical collecting duct (CCD). While the distal part of

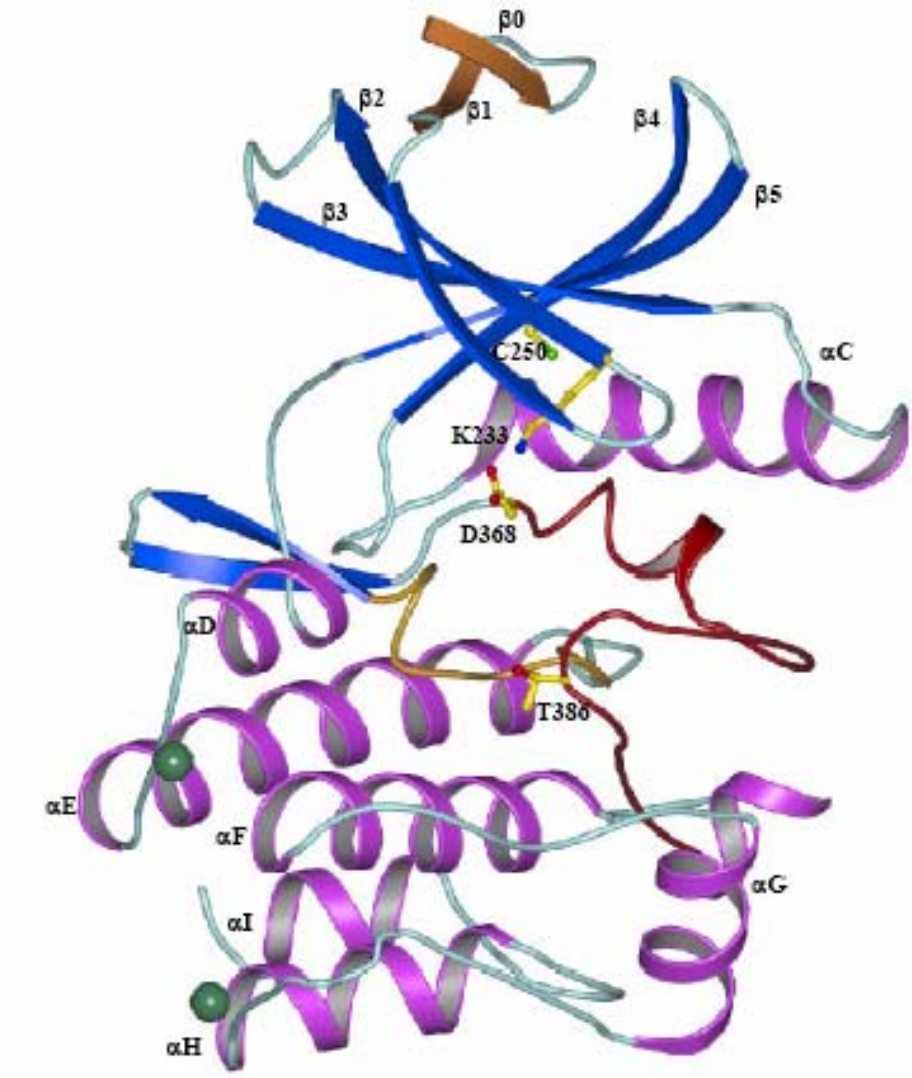

Figure 2-4. Crystal structure of the inactive form of the kinase domain of WNK1

Ribbon diagram of WNK1 structure. The activation loop is red and the catalytic loop is yellow, respectively. Some of the key residues are represented in the ball-and-stick model (Min et al., 2004).

kidney accounts for only less than 10% of filtered salt reabsorption, this is the place where the net salt balance is tightly regulated. The pathophysiological link between salt and blood pressure is predictable from the relationship between salt and vascular volume homeostasis (Figure 2-5) (Karet, 2002).

Among many disorders, Gitelman's syndrome led to the finding that this disorder is caused by loss-of-function mutations in the thiazide-sensitive Na-Cl cotransporter (NCC, also called solute carrier family 12 member 3, SLC12A3). NCC is an electroneutral ion transporter present on the DCT and mediates sodium and chloride reabsorption. Patients with this disorder typically show renal salt wasting and consequently reduced blood pressure. The fact that this syndrome also accompanies hypomagnesemia (low serum Mg^{2+}) and hypocalciuria (low urinary Ca^{2+} excretion) indicates that NCC functionally couples to the homeostasis of these divalent ions by unappreciated mechanisms. Mutations of the inward-rectifier potassium channel, ROMK, found in Bartter's syndrome also cause salt wasting. Two more genes, the Na-K-2Cl cotransporters (NKCCs, SLC12A1 and 2) and basolateral chloride channel (CLCNKB), are functionally related to ROMK activity, and loss-of-function mutations of the two genes also contribute to different subtypes of Bartter's syndrome. For example, in Bartter's syndrome type II, impaired ROMK activity causes rapid depletion of fluid K^+ levels and a subsequent decrease of salt reabsorption by NKCC2 (SLC12A1) resulting in severe salt wasting and hyperkalemia (high serum K^+) (Lifton et al., 2001; Karet, 2002). Liddle's syndrome is one of the well known monogenic disorders caused by mutations in the collecting duct epithelial sodium channel (ENaC), and this autosomal dominant disorder is characterized by early onset hypertension

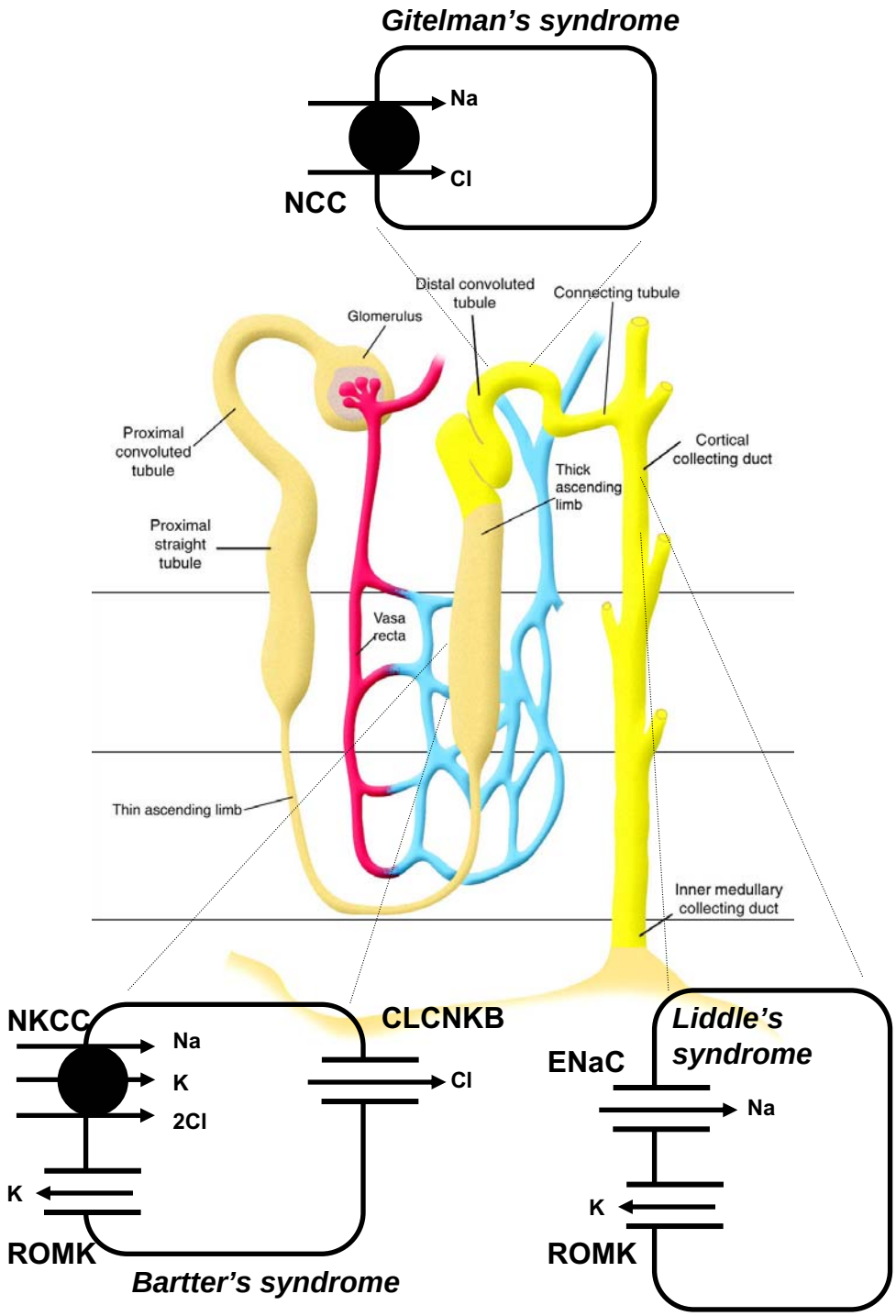

Figure 2-5. Diagram of the nephron and its components
Representative channels and transporters in the distal part of nephron are depicted and renal salt-handling disorders are designated for corresponding channels/transporters. See the text for the details. Figure is modified from Rossier, 2003

and hypokalemia. Evidence suggested that the mutations result in enhanced ENaC activity, mostly due to the increased concentration of this channel on the cell surface. Further studies demonstrated that at least one mechanism for increased number of the channels can be the prolonged half-life of ENaC mutants because these mutation sites belong to the interaction motif of ENaC with NEDD4-2, a ubiquitin ligase. Therefore, these mutations are likely to disturb membrane clearance of ENaC by the ubiqutination machinery (Staub et al., 1996).

Although transcellular transport has been relatively well studied for its role in ion homeostasis through specific membrane transporters and channels, the paracellular pathway also appears to contribute significantly to the overall characteristics of epithelial transport. The tight junction at the paracellular barrier, where proteins such as claudin and occludin are enriched and form a protein complex, is not only a boundary but also displays solute selectivity. Mutations in claudin family members of proteins show specific defects in ion homeostasis. In particular, paracellular chloride permeability may be important for regulating Na^+ and K^+ balance in the distal part of nephron, because around 70% of Cl^- reabsorption through the paracellular pathway occurs in this region of the nephron (Tsukita et al., 2001; Kahle et al., 2004b). However, the underlying mechanisms for the regulation of paracellular permeability are not well understood.

B. WNKs and pseudohypoaldosteronism type II (PHAII)

In 2001, a significant finding by Lifton's group revealed that a familial form of hypertension disease can be caused by mutations in at least two of the four human WNKs.

Genetic screening of families with PHAII identified large intronic deletions in the first intron of WNK1, which increased its transcript levels up to 5-fold in the affected individuals, leading to monogenic hypertension. In contrast, mutations in WNK4 were in the coding sequence C-terminal to the kinase domain. Three missense mutations were clustered in a short highly conserved region near a coiled-coil region right after the autoinhibitory domain and one missense mutation was localized C-terminal to another coiled-coil segment near the end of the protein (Figure 2-6) (Wilson et al., 2001).

PHAII, also referred to as Gordon's syndrome, is a rare autosomal dominant disorder characterized by elevated renal salt reabsorption, hyperkalemia (low renal K^+ excretion), and hyperchloremia (high serum Cl^-), with a concomitant fall in serum bicarbonate level. This hyperkalemic hypertension is a clinical mirror image of Gitelman's syndrome in many ways; e.g. the hypotension, hypokalemia, and hypocalciuria in Gitelman's syndrome (Kahle et al., 2004c). From the observation of this reversal relationship along with the thiazide sensitivity in PHAII patients, the possible functional linking between WNK and NCC has been tested. Reconstitution studies in *Xenopus* oocytes showed that WNK4 negatively regulates the thiazide-sensitive NCC by reducing its expression on the membrane surface, and that one of the mutations associated with hypertension significantly ameliorated these inhibitory effects (Figure 2-7A). Interestingly, WNK1 was reported to inhibit the negative regulatory activity of WNK4 on ion transport, without changing the membrane expression of NCC on its own (Figure 2-7B) (Wilson et al., 2003; Yang et al., 2003). These observations fit in renal hypertension model of PHAII, but cannot explain the hyperkalemia of the disorder. A recent study suggested an answer for

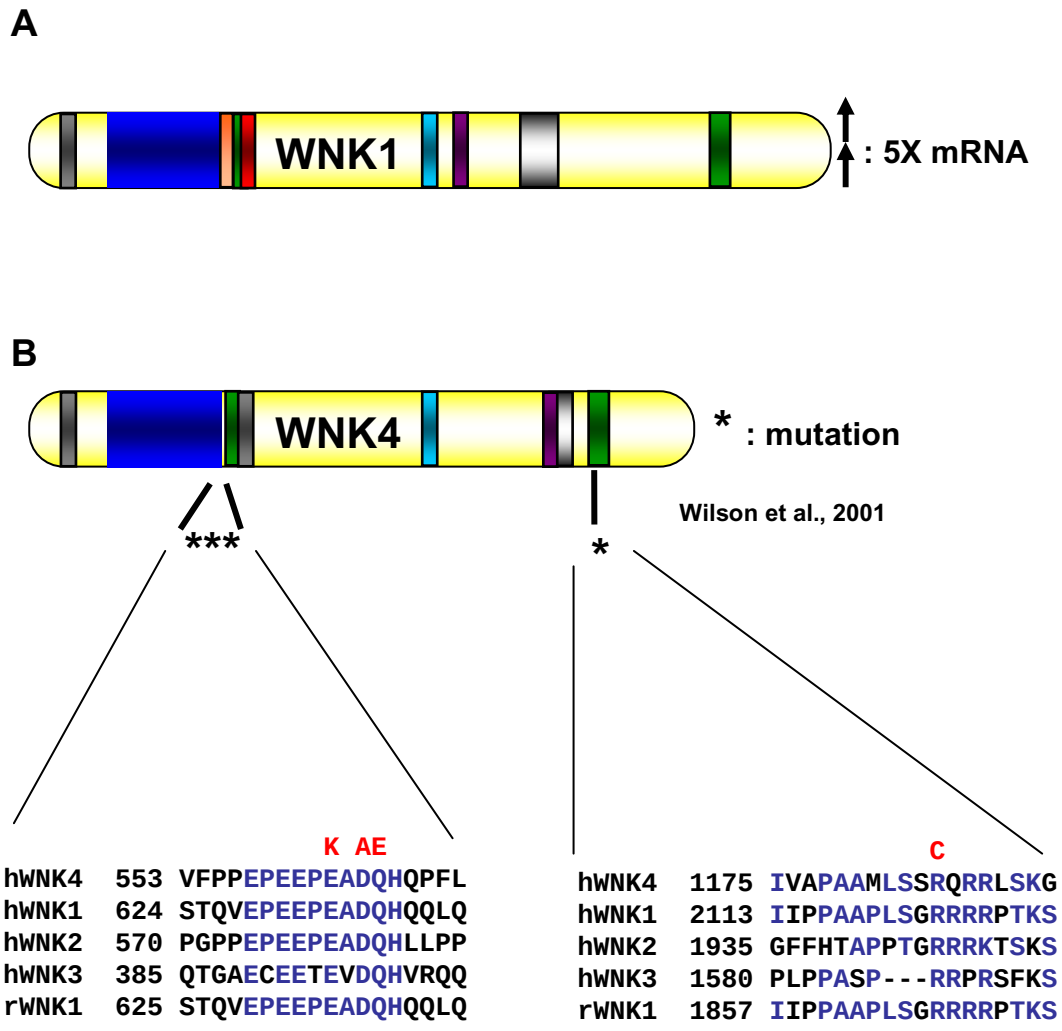

Figure 2-6. Schematic representation of hypertension-causing mutations in WNKs

A. Overexpression of WNK1 transcripts was found in PHAII patients. B. The sequences of WNKs in a conserved region containing the missense mutations found in WNK4 were aligned and mutations associated with WNK4-induced hypertension are shown on top (in red).

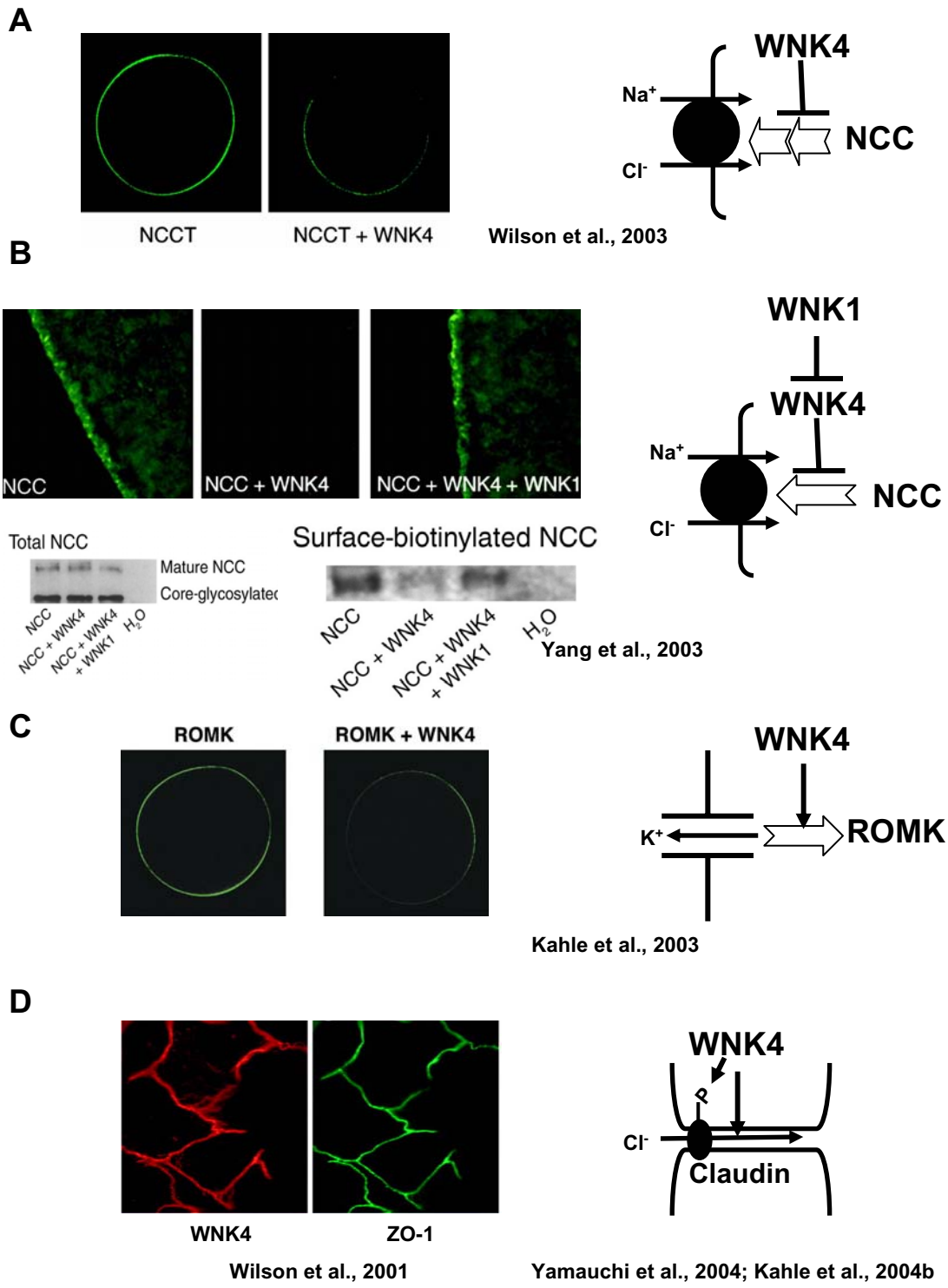

Figure 2-7. Published reports linking WNKs and channel/transporters, and their respective models

Hypertension-causing mutations further increase or decrease the activity of WNK4 depending upon its molecular targets. See the text for the details.

the question by showing that WNK4 also inhibits ROMK activity by endocytosis, and that the hypertension causing mutation can enhance WNK4 inhibitory effects (Figure 2-7C). This finding is rather intriguing because the same mutation relieved WNK4 inhibitory effects on NCC. More curiously, ROMK inhibition was not dependent on WNK4 kinase activity, which is not the case with the effects on NCC (Kahle et al., 2003). In the same context, the similar physiological approach was adopted to address the hyperchloremia phenotype in PHAII patients, because PHAII is chloride-dependent and WNK4 was exclusively observed in the tight junctions in the CCD. WNK4 PHAII mutants significantly increased transepithelial paracellular chloride permeability and also strongly phosphorylated claudin proteins, which are known to be involved in the regulation of ion permeability at tight junctions (Figure 2-7D) (Yamauchi et al., 2004; Kahle et al., 2004b). WNK4 also appears to inhibit the Na-K-2Cl (NKCC) and the Cl^-/base exchanger (CFEX), implying multiple targets in diverse epithelia (Kahle et al., 2004a).

C. Localization and expression pattern of WNKs

WNK1 is mostly cytoplasmic, and early Northern and Western analysis suggested that WNK1 is widely distributed in tissues and cell lines, suggesting its universal roles in many organs (Xu et al., 2000). The poor correlation of WNK1 protein amounts with its transcript levels, such as in brain where mRNA is low but protein expression is very high, probably indicating significant post-transcriptional regulation of WNK1 expression. By contrast, WNK4 is more restricted in expression, predominantly occurring in kidney. Both WNK1 and WNK4 localized to DCT and CCD in kidney. While WNK4 was exclusively

present in intercellular junctions and colocalized with the tight junction protein, ZO-1, in DCT, it showed both cytoplasmic and intercellular junction expression in CCD (Wilson et al., 2001). Subsequent immunofluorescence studies consistently confirmed that WNK1 expression is ubiquitous, but additionally, the protein is also abundantly localized in the cytoplasm or at the membrane in polarized epithelial tissues including hepatic biliary ducts, pancreatic ducts, epididymis, colonic crypts, sweat ducts and gallbladder. WNK4 expression was also seen in some extrarenal tissues, especially the epithelia significant for Cl^- flux (Kahle et al., 2004a; Choate et al., 2003).

WNK1 is regulated post-transcriptionally and exists as multiple splice forms, notably in kidney where a form lacking N-terminal residues and significant portion of the kinase domain has been detected. This kidney-specific alternatively spliced form was originally identified in an automated genome-wide analysis in the human transcriptome by Lee's group (Xu et al., 2002). Subsequently two other groups performed WNK1 promoter assays, and confirmed that there are multiple splice variants for WNK1 expressed in a tissue-specific manner and especially, in kidney, a kinase-defective form of WNK1 transcript predominates (O'Reilly et al., 2003; Delaloy et al., 2003).

D. WNK1 knockout mouse model

Lexicon Genetics generated WNK1 null mice as proof-of-principle of their gene-trapping technology (Zambrowicz et al., 2003). The WNK1 gene-trap mouse showed lowered blood pressure in the heterozygous state, consistent with the idea that WNK1 overexpression leads to hypertension. What is striking here is the haploinsufficiency and

dosage sensitivity of WNK1 in blood pressure control. The fact that the WNK1 hypomorphic phenotype could not be compensated by other WNK isoforms probably suggests that WNKs (at least WNK1 and WNK4) have unique roles for blood pressure control at multiple different points or they may act epistatically within a pathway. WNK1 inhibition of WNK4 on NCC and our unpublished data showing WNK1 phosphorylation of WNK4 partly support this idea.

Perhaps even a more surprising phenotype came from WNK1-deficient homozygous mice, because they did not survive past E13. This phenotype strongly suggests that WNK1 plays an essential role during mouse development, which may be independent of its proposed role in hypertension. However, there are still concerns in that this gene-trapping insertion may affect neighboring genes or there may be background mutations outside the WNK1 locus. Detailed descriptions that can exclude those possibilities are absent from their paper and other information about the WNK1 null phenotypes other than lethality is lacking.

E. Description of research in thesis

The following questions or aims are raised based on the previous findings. First, in spite of the proposed roles for WNK1 in hypertension, there are few insights as to the mechanism used by WNK1 for ion homeostasis. Furthermore, the ubiquitous pattern of WNK1 expression (including extrarenal tissues) and embryonic lethality of WNK1 null mice strongly suggest that there should be more general roles of WNK1 in organisms. Blood pressure regulation may be just one part of the job that WNK1 does. Second, WNK1

substrates and binding partners have not been identified. Third, related to the second question, the molecular pathways in which WNK1 is involved have been little characterized. Based on these questions, I have been identifying WNK1 substrates and interactors, eventually in order to build up knowledge of WNK signaling networks and comprehend its cellular functions.

Chapter 1 has covered general overview and my ideas about protein kinase signaling.

Chapter 2 has presented the relevant backgrounds about WNK1. This section also includes some of the data that I contributed, but that are not well fit into the storylines for later chapters.

Chapter 3 mainly discusses WNK1 and its interactor, synaptotagmin 2 (Syt2).

Chapter 4 describes other interactors of WNK1 – smad2 and LC8/PIN.

Chapter 5 is about some other observations and preliminary data that I made.

Future direction follows after the chapters above.

Chapter 3: WNK1 interacts with Synaptotagmin 2 (Syt2)

I. Abstract

To identify WNK1 targets, I performed yeast two-hybrid screens of a neonatal mouse brain cDNA library with WNK1 fragments. Three different kinase baits commonly identified the synaptotagmin (Syt) family of proteins as WNK1 interactors. The WNK1-Syt2 interaction was confirmed by in vitro binding assays and endogenous co-immunoprecipitation, and the two proteins were found co-localized on a subset of secretory vesicles by immunofluorescence and sedimentation. The region of Syt2 that binds to the WNK1 kinase domain was mapped to its Ca^{2+}-binding C2 domains. WNK1 displayed highly selective binding to subsets of Syt isoforms, especially to Ca^{2+}-responsive Syts, relative to WNK4, suggesting that Syt binding may predominantly be WNK1 specific. Furthermore, Ca^{2+} strongly increased their binding in vitro and mutations of essential Ca^{2+}-coordinating residues disrupted the WNK1-Syt2 complex formation. WNK1 also phosphorylated Syt2. Mass spectrometric analysis revealed that phosphorylation sites are distributed within the C2 domains. Additionally, Syt2 mutants lacking Ca^{2+}-binding residues were significantly less phosphorylated by WNK1, demonstrating the importance of Ca^{2+}-binding properties for both binding and phosphorylation. ^{32}P-labeling experiments and immunoblotting with a phospho-specific antibody (P-Thr202) further confirmed WNK1 phosphorylation of Syt2 under physiological conditions. Finally, phosphorylation by WNK1 enhanced the amount of Ca^{2+} required for Syt2 binding to phospholipid vesicles and mutation of Thr202 partially prevented this phosphorylation-driven change. Taken together, these findings strongly

suggest that phosphorylation of Syt by WNK1 is a mechanism to regulate Ca^{2+}-sensing and the subsequent Ca^{2+}-dependent membrane events mediated by Syt C2 domains. These findings may provide a biochemical mechanism that could regulate the insertion or clearance of membrane proteins on the cell surface. Perturbation of this regulatory pathway may disturb electrolyte homeostasis.

II. Introduction

A. Synaptotagmins (Syts)

Syts comprise a large family of proteins that are thought to regulate membrane trafficking and fusion in various cell types. This protein family is characterized by a short N-terminus, a single transmembrane region, and two C2 domains (C2A and C2B) (see Figure 3-1B). Syt1, the best studied, is a strong candidate for the Ca^{2+} sensor that regulates both exocytosis and endocytosis in neurons and neuroendocrine cells. Genetic studies with flies and mice established that the lack of synaptotagmin 1 results in a specific defect in the fast synchronous phase of synaptic vesicle fusion. Its C2 domains confer Ca^{2+}-dependent phospholipid binding to Syt1 resulting in catalysis of the membrane fusion process. These domains also mediate protein-protein interactions with SNARE proteins, forming a Ca^{2+}-stimulated fusion complex. Structural studies indicated that Syt1 binds five Ca^{2+} ions, three to C2A and two to C2B, through conserved negatively charged amino acids. Mutations of these critical Ca^{2+}-binding residues in either C2A or C2B domains significantly impair Ca^{2+}-dependent binding to phospholipids and effector molecules (Südhof, 2002; Tucker and

Chapman, 2002).

B. Localization and post-translational regulation of Syt

Recent genomic analyses indicate that at least 16 Syts are present in mammalian genomes (Craxton M, 2004). Südhof's group categorized 13 vertebrate Syts in 6 classes based on their characteristics (Table 3.1) (Südhof, 2002). To date, substantial understanding has been achieved concerning Syt1, but little is known about the functions of the other Syt isoforms. Syt2 is assumed to have the same function as Syt1 due to its sequence similarity. Syt1 and 2 showed complementary patterns of expression in brain. Syt4 and 11 have an evolutionarily conserved substitution of Asp to Ser in one of Ca^{2+}-binding sites in their C2A domains and consequently lose their Ca^{2+}-dependent binding to phospholipids. Very little is known about Syt8, 12, and 13 which belong to the atypical Syt class. They appear to be Ca^{2+}-insensitive due to their lack of consensus Ca^{2+}-binding sites. Syt1 is generally thought to be a synaptic vesicle protein, but some Syts are also localized to the active zone and the plasma membrane, suggesting cooperative actions during the membrane fusion process. Non-neuronal isoforms of Syts also exist in many types of cells as well as endocrine cells. Thus Syts may act as widespread regulatory proteins that not only confer Ca^{2+}-responsive synaptic vesicle fusion but also control other analogous membrane events.

Not much is known about the regulation of Syts by post-translational modification. The evidences have shown that Ca^{2+}/calmodulin-dependent protein kinase II (CaMKII), casein kinase II (CKII), and protein kinase C (PKC) were able to phosphorylate Syt1

Isoforms	Features
Class 1, Syts 1 and 2	The most abundant vesicular Ca^{2+} sensors, *N*-glycosylated N-termini
Class 2, Syt 7	>12 splice forms, active zone Ca^{2+} sensors
Class 3, Syts 3, 5, 6, and 10	Disulfide bonds at N-termini, plasma membrane Ca^{2+} sensors
Class 4, Syts 4 and 11	**D → S substitution in C2A domains**
Class 5, Syt 9	Also named Syt V, in brain and nonneuronal cells
Class 6, Syts 8, 12, and 13	**No consensus Ca^{2+}-binding sites**

Table 3-1. Summary of properties of Syt isoforms
Table is modified from Südhof, 2002.

(Popoli, 1993; Davletov et al., 1993; Hilfiker et al., 1999). Phosphorylation sites for all three kinases were identified within the linker between the transmembrane region and the C2 domains; this linker is poorly conserved among isoforms and species. Therefore, little physiological meaning was assigned to these modifications. Syts also contain glycosylation and palmitoylation sites. These sugar and fatty acid modifications are reported to be important for proper targeting and trafficking for Syts (Han et al., 2004; Kang et al., 2004).

III. Materials and methods

Yeast two-hybrid screen

Yeast two-hybrid screens were performed with a neonatal mouse brain cDNA library (gift from M. Henkemeyer) in yeast strain L40 with baits composed of lexA fused to the WNK1 kinase domain (151-494, 217-494, or 217-494 K233M) (Vojtek and Hollenberg, 1995). Yeast were plated on complete synthetic medium (CSM) or drop-out (DO) medium lacking Trp, Leu, and His, containing 1-10 mM 3-aminotriazole (Sigma). From 3 x 10^7 yeast transformants screened, twenty three colonies were recovered whose insert interactions were confirmed by reintroducing isolated prey plasmids into bait-containing host strains. LexA-lamin was used as a negative control. The expression of baits was confirmed by Western blotting of lysates with either an anti-WNK1 antibody (Q256 (Xu et al., 2000)) or an anti-lexA antibody (Clontech). For pairwise interaction tests in yeast, the L40 strain was cotransformed with bait and prey plasmids using Frozen EZ-Yeast Transformation II (Zymo Research) and plated on CSM lacking Leu and Trp. Interactions were tested by streaking

co-transformants on CSM lacking Leu, Trp, and His. Results were confirmed with β-galactosidase assays. Yeast lysates were prepared as described (http://www.protocol-online.org/prot/Model_Organisms/Yeast/Protein/).

Subcloning and mutagenesis

Two-hybrid vectors were generated by PCR with pBluescript-WNK1 as template (Xu et al., 2000) and introduced into pVJL11. The full length-coding region of WNK4 was amplified from rat testis cDNA (gift of W. Chen) by PCR. To construct the WNK4 kinase domain bait, WNK4 (158-444) was cut from pGEM-T Easy-WNK4 (158-444) and ligated into pVJL11. Rat Syt cDNAs in pCMV5 (gift from T. Südhof) were used as templates to generate prey constructs containing the cytoplasmic portion of each isoform in the pGADGH vector.

pGEX-KG-WNK1 (1-639) was as described (Xu et al., 2002). pGEX-KG-Syt2 (81-422) and pGEX-KG-Syt2 (141-422) were constructed by PCR-based subcloning using pCMV5-Syt2 as template. pHis$_6$Parallel-WNK1 (198-491) was as described (Xu et al., 2002) and pHis$_6$Parallel-WNK1 (193-483) was created similarly. His$_6$-Syt2 (81-422) was created by digesting pGEX-KG-Syt2 (81-422) with EcoRI and HindIII and ligating into pRSETA (Invitrogen). His$_6$-Syt2 (141-422) was generated by PCR from pCMV5-Syt2 and cloned into pHis$_6$-Parallel.

Mammalian expression vectors encoding 3xFlag-Syt2 (1-422), (81-422), and (141-422) were created by PCR amplification and subcloning into p3xFlag-CMV7.1 (Sigma). pCMV5-Myc-Syt2 full length, WNK1 (159-555), WNK1 (180-555), and WNK1 (216-491) were made similarly.

Site-directed mutagenesis was done with the QuikChange kit (Stratagene) according to the manufacturer's instructions. All constructs and mutants were confirmed by sequencing.

Expression of recombinant proteins and protein kinase assays

GST-Syt2, His_6-Syt2 (141-422), and WNK1 were expressed in *E. coli* BL21 (DE3) cells as described (Shao et al., 1997; Xu et al., 2000). Tags were cleaved in some cases. Protein concentrations were determined with an Emax microplate reader (Molecular Devices) and confirmed by comparing to serial concentrations of bovine serum albumin on a Coomassie blue-stained gel.

Kinase assays were performed in 30 μl of kinase buffer (20 mM Hepes, pH 7.6, 10 μM ATP, 10 mM $MgCl_2$, 10 mM β-glycerophosphate, 1 mM dithiothreitol, and 1 mM benzamidine) containing 10 μCi of [γ-^{32}P]ATP. WNK1 and Syt2 were added at final concentrations of 1 μM and 0.7 μM, respectively. Reactions were terminated by the addition of 5x SDS sample buffer and heating for 2 min.

Identification of phosphorylation sites

For determination of phosphorylation sites, 0.7 μM Syt2 (141-422) was incubated with 2.5 μM WNK1 (193-483) plus 4 mM ATP at 30 ^{o}C for up to 12 hr. Syt2 was resolved by SDS-PAGE and stained with colloidal Coomassie blue (Invitrogen).

Phosphorylation sites were identified by precursor ion scanning and nanoelectrospray tandem mass spectrometry (MS/MS). The colloidal blue stained bands were excised and digested with trypsin as described (http://www.signaling-gateway.org/reports/v1/DA0008/DA0008.pdf). Dried digests were dissolved in 5% formic

acid and loaded onto a pulled capillary filled with POROS R2 resin. After washing 3x with 5% formic acid, the peptides were eluted into a nanoelectrospray needle with 1-2 μl of nanoelectrospray sample solution for precursor ion scanning in negative ion mode or MS/MS in positive ion mode.

Mass spectrometry analyses were performed on a QSTAR Pulsar-i quadrupole time-of-flight tandem mass spectrometer (Applied Biosystems/MDS Sciex, Toronto, Canada) equipped with a nanoelectrospray ion source (MDS Proteomics, Odense, Denmark). For precursor ion scanning experiments, the instrument was set in negative ion mode, with the quadrupole q2 pulsing function turned on, to detect the PO^{3-} fragment ion at m/z 79. The optimum collision energies were determined for each experiment by gradually increasing the voltage of Q0 in steps corresponding to one twentieth of the m/z value of the precursor ion. After data acquisition by precursor ion scanning, the instrument was switched to positive ion mode, and the phosphopeptide sequence and sites of phosphorylation were identified by MS/MS. In the MS/MS scan mode, precursor ions were selected in quadrupole Q1 and fragmented in the collision cell (q2), using argon as the collision gas.

Cell culture, immunoblotting, and immunoprecipitation

HEK293 or COS7L cells were maintained in Dulbecco's modified eagle medium (DMEM) containing 10% fetal bovine serum (FBS), and were transfected at 50–80% confluence in 60-mm dishes using Fugene (Roche). After 36 hr, lysates were prepared by pipetting up and down through a 23 gauge needle in 0.5 ml of lysis buffer (50 mM Hepes, pH 7.5, 150 mM NaCl, 10% glycerol, 100 mM NaF, 0.2 mM Na-orthovanadate, 0.5% NP-40,

1.5 mM $MgCl_2$, 1 mM EGTA, 1 mM dithiothreitol, 1 μg/ml leupeptin, 10 mM benzamidine, 1 μg/ml pepstatin A, 10.5 μg/ml aprotinin, and 1 mM phenylmethylsulfonyl fluoride). 20 μg of lysate protein was used for immunoblotting. For co-immunoprecipitation, 0.2 ml of lysate was incubated with 2 μg of anti-Flag M2 antibody (Sigma), 1 μg of anti-Myc antibody (National Cell Culture Center), or 2 μl of anti-WNK1 antiserum Q256 (Xu et al., 2000) along with 30 μl of protein A-sepharose CL-4B beads (Amersham Pharmacia) for 2 hr at 4 ^{o}C. Syt2 was immunoprecipitated as described (Shin et al., 2003). The immunoprecipitates were washed 4x with 20 mM Tris, pH 7.5, 150 mM NaCl, and 7.5 mM $MgCl_2$ and associated proteins were analyzed by immunoblotting. The anti-phosphoT202 Syt2 rabbit antibody was generated by PhosphoSolutions (www.PhosphoSolutions.com; Denver, CO) using the synthetic peptide, KYETKVHRK**pT**LNPAFNE. Antibody specificity was confirmed by immunoblotting His_6-Syt2 (81-422) WT or T202A phosphorylated by WNK1.

In vitro pulldown assays

Equimolar amounts (0.05 nmol) of GST or GST-WNK1 (1-639) were immobilized on 20 μl of glutathione-agarose beads in 0.5 ml of PBS (137 mM NaCl, 2.7 mM KCl, 4.3 mM Na_2HPO_4, and 1.47 mM KH_2PO_4, pH 7.4) containing 0.1 mg/ml bovine serum albumin. After washing 3x with PBS, 0.03 nmol of His_6-Syt2 (141-422) was incubated with the beads for 1 hr at 4 ^{o}C. Beads were pelleted and washed 3x with 50 mM Tris, pH 7.4, 0.3 M NaCl, and 0.1% Triton X-100. Associated proteins were analyzed by immunoblotting with an anti-His_6 mouse monoclonal antibody (Clontech). The nitrocellulose membrane was stripped and reprobed with an anti-GST (Z-5; sc-459) rabbit polyclonal antibody (Santa Cruz). All binding experiments were repeated a minimum of three times.

To test the effects of Ca^{2+} on WNK1-Syt2 binding, the free Ca^{2+} concentration was adjusted with Ca^{2+}-EGTA based on calculations from WINMAXC (http://www.stanford.edu/~cpatton/winmaxc2.html). Concentrations were confirmed using a Ca^{2+}-electrode.

Phospholipid binding assays

Phosphatidylcholine (PC) and phosphatidylserine (PS) (Avanti Polar Lipids) were dissolved in chloroform at 25 mg/ml and 10 mg/ml, respectively. Sucrose-loaded liposomes were prepared in 50 mM Hepes, pH 6.8, 100 mM NaCl, 4 mM EGTA, and 0.5 M sucrose as described (Fernandez et al., 2001). 0.1 nmol purified GST-Syt2 or His_6-Syt2 was incubated with 0.2 μmol of heavy liposomes in solutions at various concentrations of free Ca^{2+}. The samples were sedimented, washed, and analyzed by electrophoresis and Coomassie blue staining. Samples lacking phospholipids were analyzed to eliminate contributions from protein aggregation. 0.2 nmol Syt2 was phosphorylated with 1 nmol WNK1 kinase domain or active p38 for 3-9 hr at 30 ^{o}C in the presence of 4 mM ATP. Reaction mixtures were centrifuged to remove protein precipitates prior to the liposome binding assay.

Localization of proteins in INS-1 cells by Immunofluorescence and sedimentation

For immunocytochemistry, INS-1 cells were grown on coverslips at 8 X 10^4 cells/35 mm well. Coverslips were rinsed 3X with PBS, fixed in 3.7% formaldehyde, and permeabilized with 0.2% Triton X-100. For costaining of WNK1 and Syt2, 1 μg each of Q256 and U6129 was labeled with Zenon rabbit IgG labeling reagents (Molecular Probes). Primary antibodies were incubated for 1 hr at 1:200 (Q256) and 1:500 (U6129). FITC-conjugated anti-insulin antibody (Molecular Probes) was used at 1:400. Images were

obtained using a Leica TCS SP1 confocal microscope. Alexa 488 was excited with the 488 line of an argon laser. Alexa 568 and 594 were excited with the 568 nm line of a Krypton laser. The two color channels were acquired sequentially to minimize cross-talk. Images were filtered in Photoshop 7.0 to remove speckle noise; intensity levels were adjusted so that the signal stretched from 0 to 255; and finally, the images were unsharp masked before merging the two color channels into an RGB image.

For sedimentation analysis, 4 x 10^7 INS-1 cells were lysed by 20 passes through a Balch cell cracker (EMBL, Heidelberg, Germany) in 0.32 M sucrose, 4 mM HEPES pH 7.4 and protease inhibitors. The lysate was layered on a 10 ml 0.4-2.0 M continuous sucrose gradient and centrifuged for 20 hr at 4 ^{o}C and 110,000 x g. Fractions (0.5 ml) were collected from the bottom with a Beckman Fraction Recovery System. Aliquots were analyzed by immunoblotting as above.

Phosphate labeling

Transfected 293 or COS7L cells were incubated with phosphate-free medium containing 0.22 mCi/ml [^{32}P]phosphate (MP Biomedicals) for 3 hr. Lysates were then subjected to immunoprecipitation with anti-Flag antibody. Proteins were resolved by electrophoresis and visualized by autoradiography

IV. Results

A. Summary of yeast two-hybrid screening

I generated a number of baits covering the entire coding region of WNK1 to identify

as many as possible of the molecules - including substrates - which bind to WNK1. Each of the baits was first tested for its expression by immunoblotting with the anti-lexA antibody or the anti-WNK1 antibody (Q256), because it has been suggested that the chance of success in screening can be increased as much as 6-fold when the bait is expressed at detectable levels (http://www.fccc.edu/research/labs/golemis/InteractionTrapInWork.html). Except the bait derived from the WNK1 C-terminus (residues 2031-2126), all of the WNK1 baits were clearly detected by immunoblotting (data not shown). As a second step, autoactivation by baits was tested by growth selection or color reporter (β-galactosidase) assays. A few of the baits showed weak autoactivation, but in all cases, autoactivation was suppressed by adding 1 to 10 mM 3-aminotriazole. Next, I performed yeast two-hybrid screening in the presence of up to 10 mM 3-aminotriazole based on the results above. To cover the genomic complexity of the library (more than 10^6 transformants), some of baits were screened repeatedly until achieving maximal transformation efficiency under given conditions. The outcome of screening is summarized in Table 3-2.

B. The kinase domain of WNK1 interacts with Syts

To identity WNK1 substrates by yeast two-hybrid screening, three different baits each containing the kinase domain (WNK1 217-494, 217-494 K233M (kinase-dead), and 151-494) were used. The use of multiple baits provides one means of substantiating interactions found with any individual bait. Approximately 3 x 10^7 transformants were screened with these baits and twenty three inserts were isolated that showed reproducible binding to the WNK1 kinase domain baits, but not to lamin. Syt2 was encoded in six of the

Baits (arbitrarily named)	Amino acids	Characteristics	Results
1 – 555	1 – 555	Original cDNA isolated	**SGK, Munc18** ***(by J. English)***
1 – 800	1-800	-	**-**
1-1200	1-1200	-	**-**
K-1	151-494	Kinase domain	**Syt2**
K-2	217-494	Kinase domain	**Syt2**
1C	481-660	The region covering autoinhibitory domain, coiled-coil and hypertension-causing amino acid changes	**PIN/LC8**
2C	1811-1910	The region covering coiled-coil and a hypertension-causing amino acid change	**E2 (ubc4/5 family)**
IH	815-932	Internal homology region between WNK1 and WN4	**-**
KD	217-494	Kinase dead of K-2	**Syt3, Syt9, Smad2, 3XC2 protein ...**
C-t	2031-2126	C-terminal tail	**-**

Table 3-2. Summary of the results of yeast two-hybrid screens with WNK1
The residue numbers, characteristics, and interactions identified with the baits are described. WNK1 (1-555) was used for screening by J. English and yielded SGK1 and Munc18 as candidates. Other baits not represented here are still being used for screening.

inserts and was identified with every bait; Syt3 and 9 were encoded in inserts identified three and four times, respectively (Figure 3-1A). Because Syt2 was identified most frequently, my studies were primarily focused on Syt2. As additional controls, neither ERK2 nor other pieces of WNK1 interacted with Syt2 (data not shown); Syt2 was not found as an interactor in screens of this cDNA library with unrelated baits ((Cowan and Henkemeyer, 2001); M. Raman and M. Cobb, unpublished data), nor are Syts in the list of common false positives at "Interaction Trap At Work" (http://www.fccc.edu/research/labs/golemis/InteractionTrapInWork.html). Other positive interactors included Smad2 and a protein containing three tandem C2 domains, which will be discussed in detail later.

We further established the interaction between WNK1 and Syt2 using an in vitro pull down assay with recombinant proteins and by co-immunoprecipitation. The C2 domain of Syt2 (residues 141-422) and WNK1 (1-639) were expressed in bacteria and purified via their respective tags. GST-WNK1 (1-639) was immobilized on glutathione-agarose and incubated with His_6-Syt2 (141-422) proteins. Immunoblotting with an anti-His_6 antibody showed that Syt2 directly bound to GST-WNK1 (1-639) (Figure 3-1C). Myc-WNK1 fragments (residues 160-555 and 180-555) were expressed in 293 cells along with Flag-Syt2 fragments (residues 81-422 and 141-422). These proteins co-immunoprecipitated using antibodies to either Myc or Flag tags (Figure 3-2A). Endogenous full length WNK1 also co-immunoprecipitated with overexpressed Syt2 (Figure 3-2B).

Sy2 and Syt1 are 88% identical in the cytoplasmic region; these two proteins are thought to function similarly but in different locations due to their complementary expression

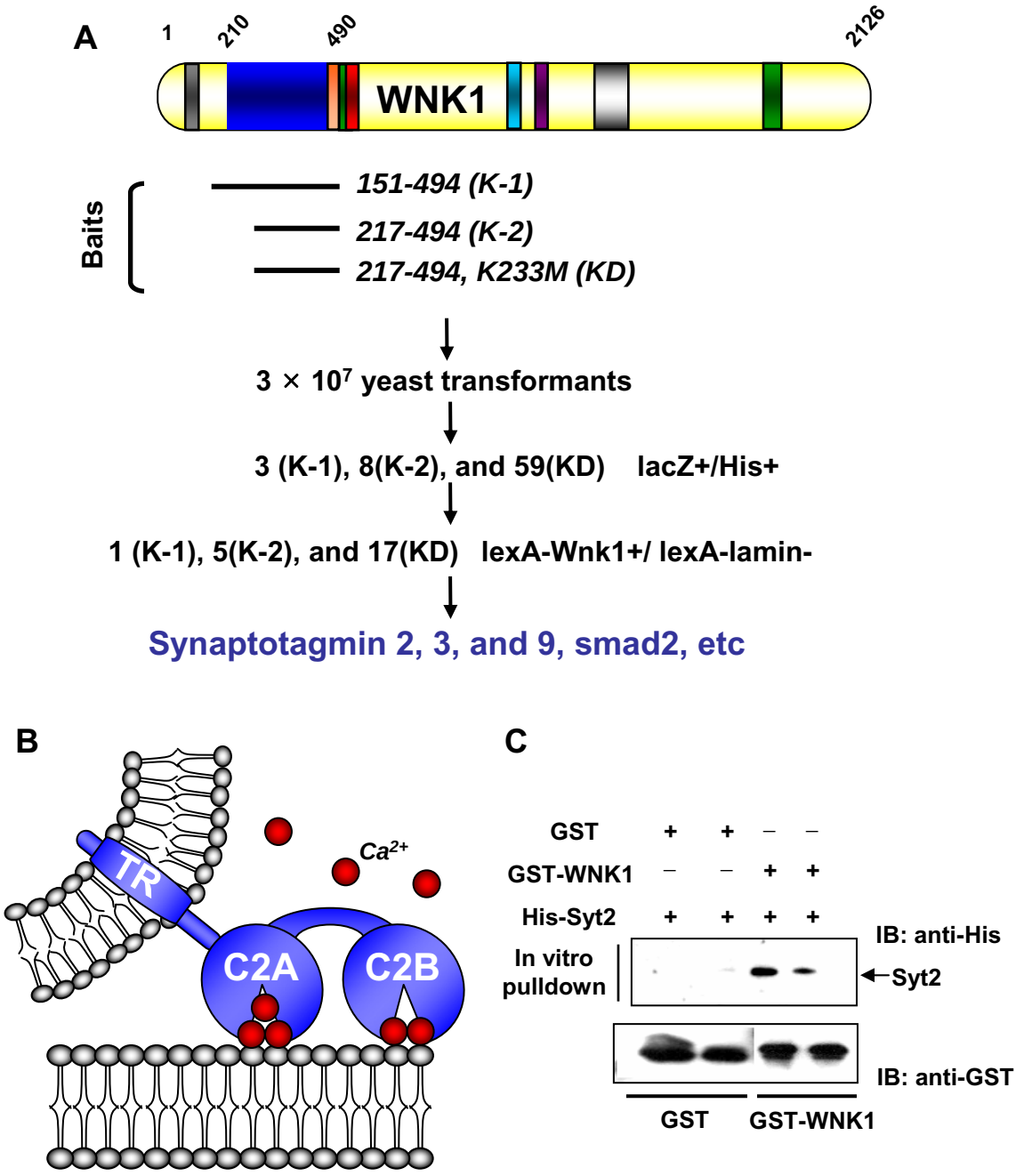

Figure 3-1. Identification of Syt2 as a WNK1-interacting protein
A. Rat WNK1 (top) and WNK1 baits containing the kinase domain (middle). The kinase domain is in black and two coiled-coil regions (coil) are shaded. The inserts containing Syts are indicated (bottom). KD (kinase-dead) refers to a bait containing K233M. B. Schematic representation of Syt protein. C.GST or GST-WNK1 (1-639) (0.05 nmol) were immobilized on glutathione-agarose beads and incubated in duplicate with 0.03 nmol of His_6-Syt2 C2 (residues 141-422). The associated Syt2 proteins were resolved by SDS-PAGE and detected by immunoblotting with an anti-His_6 antibody (top). The stripped membrane was reprobed with an anti-GST antibody (bottom).

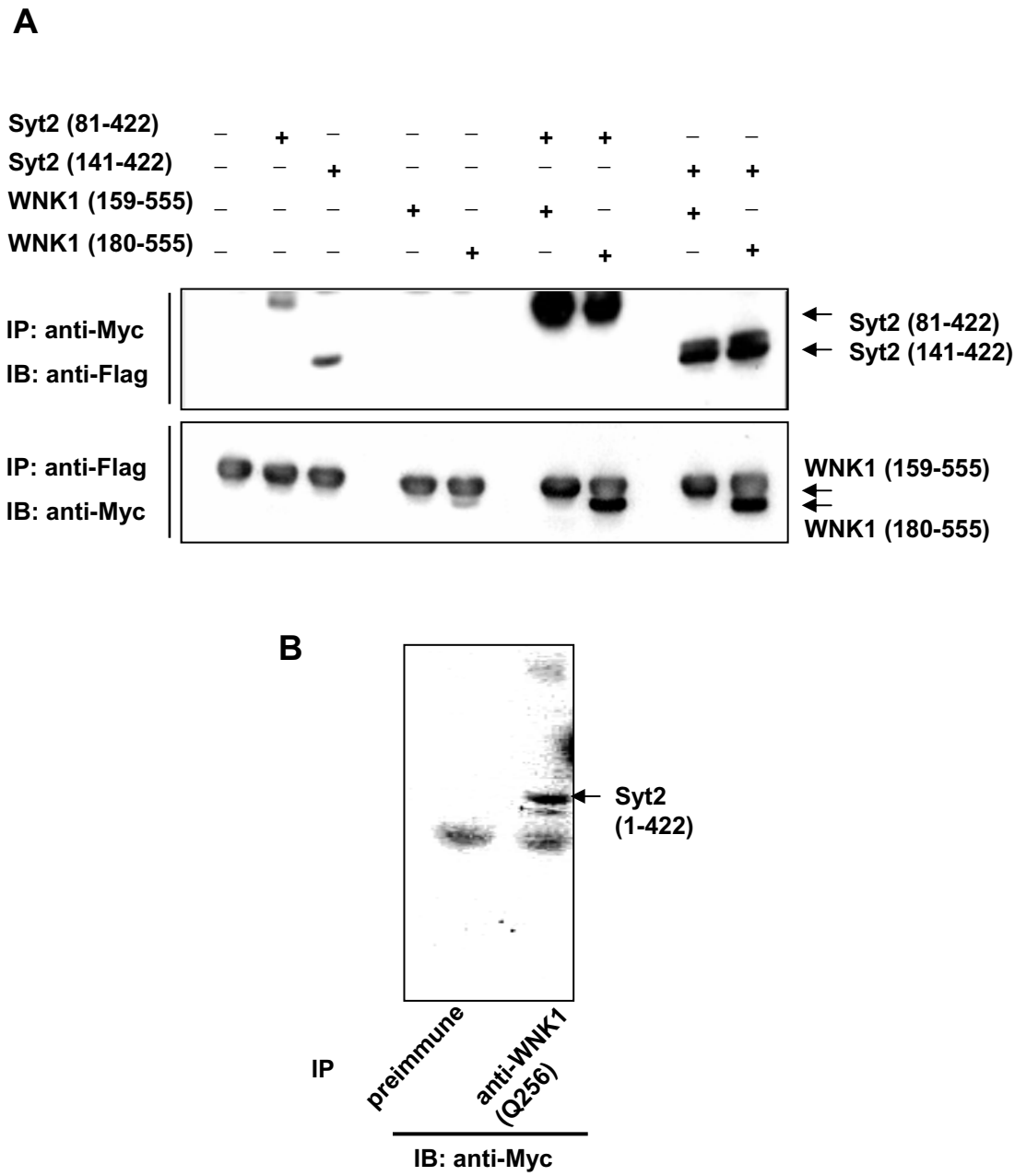

Figure 3-2. Co-immunoprecipitation of overexpressed Syt2 and WNK1
A. Cells were transfected with plasmids encoding Myc-WNK1 (159-555, 180-555) and Flag-Syt2 C2 fragments (81-422, 141-422). Myc-WNK1 was immunoprecipitated and associated proteins were immunoblotted with anti-Flag (top panel). Flag-Syt2 was immunoprecipitated and associated proteins were immunoblotted with anti-Myc (bottom panel). B. WNK1 was immunoprecipitated with antiserum Q256 from 293 cells transfected with Myc-Syt2 (1-422). The precipitates were resolved on gels and immunoblotted with anti-Myc.

patterns in brain (Geppert et al., 1991). Each of the original Syt2 inserts identified by two-hybrid screening encoded the entire cytoplasmic region containing both C2A and C2B domains. To map the region of Syt2 that binds to the WNK1 kinase domain, I performed directed two-hybrid with the WNK1 kinase domain and various regions of Syt2. Both intact C2A and C2B domains independently interacted with WNK1 (Figure 3-3). Interestingly, WNK1 binding to the C2B domain was only detected by including 20 amino acids from the C-terminus of the C2B domain. This region was originally thought to comprise a distinct domain involved in protein-protein interactions and synaptic vesicle docking (Fukuda et al., 2000), but a recent structure revealed that this region completes the C2B domain (Fernandez et al., 2001).

C. WNK1 and Syt2 exist as a native complex in subset of subcellular compartment

To investigate interactions between the native proteins, we raised highly selective anti-Syt2 antibodies (Figure 3-4) (also see Figure 3-6B). Syt1 and 2 have critical roles in Ca^{2+}-evoked exocytosis in β-cell lines, even though their function in primary islet β-cells is controversial (Lang et al., 1997; Gao et al., 2000). Syt2 is expressed in neuronal and neuroendocrine cells including pancreatic β-cell lines such as INS-1. Immunoprecipitation of endogenous Syt2 from INS-1 cells also brought down WNK1 (Figure 3-4). By comparison to WNK1 immunoprecipitates, nearly 20% of the immunoprecipitable WNK1 is in the Syt2 precipitates.

To examine whether an interaction between endogenous proteins could be detected by microscopy, WNK1 and Syt2 were localized by confocal immunofluorescence

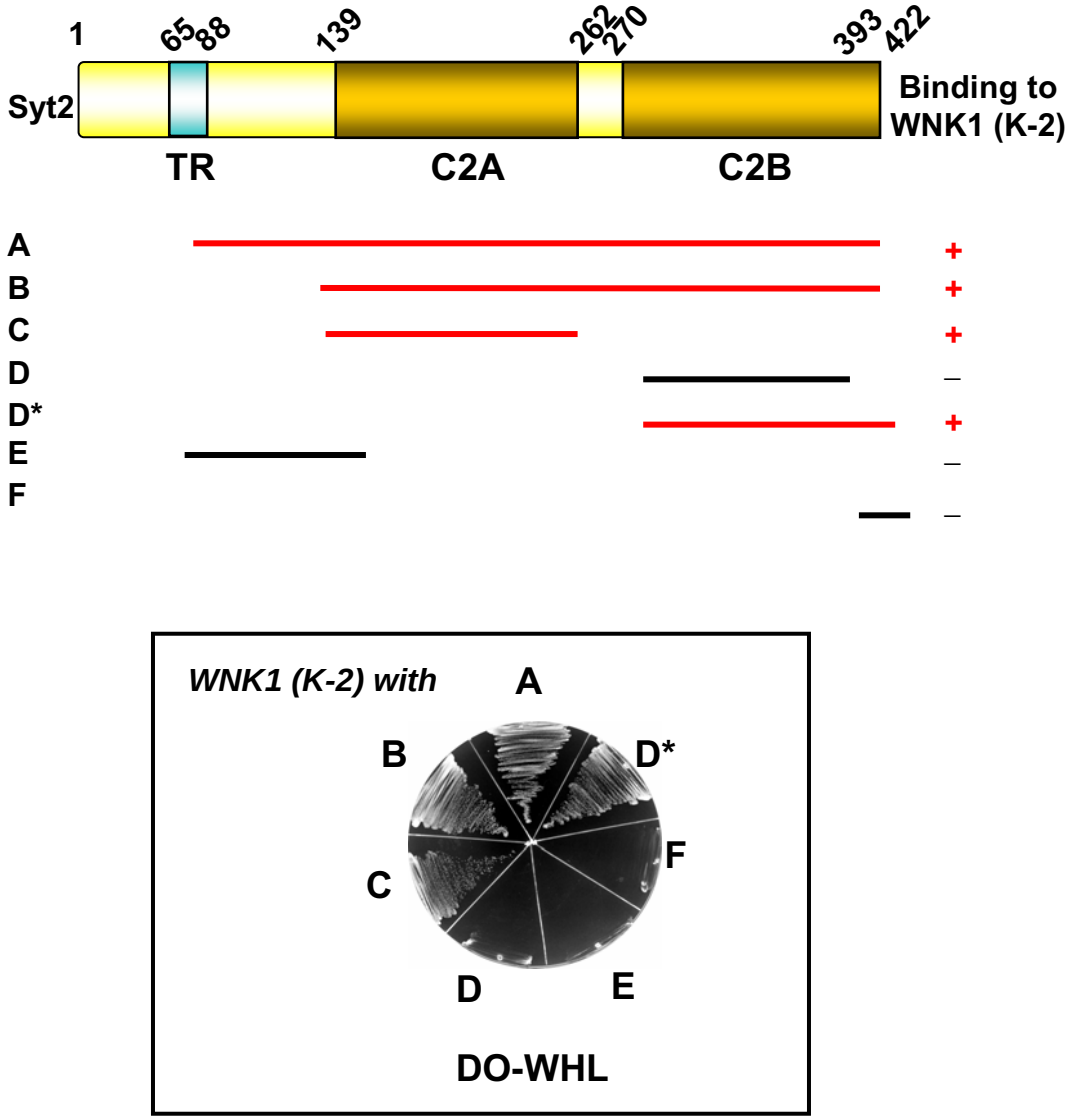

Figure 3-3. Mapping of the regions od Syt2 that bind to WNK1
Pairwise two hybrid tests of the interaction of the kinase domain of WNK1 with Syt2 fragments indicated in the top panel. In the bottom panel, interactions were detected with constructs A (81-422), B (C2A + C2B, 141-422), C (C2A, 141-268), and D* (C2B, 266-422). No interaction was detected with D (incomplete C2B, 266-399), E (linker, 81-140), or F (C-terminus, 380-422). DO, drop-out medium.

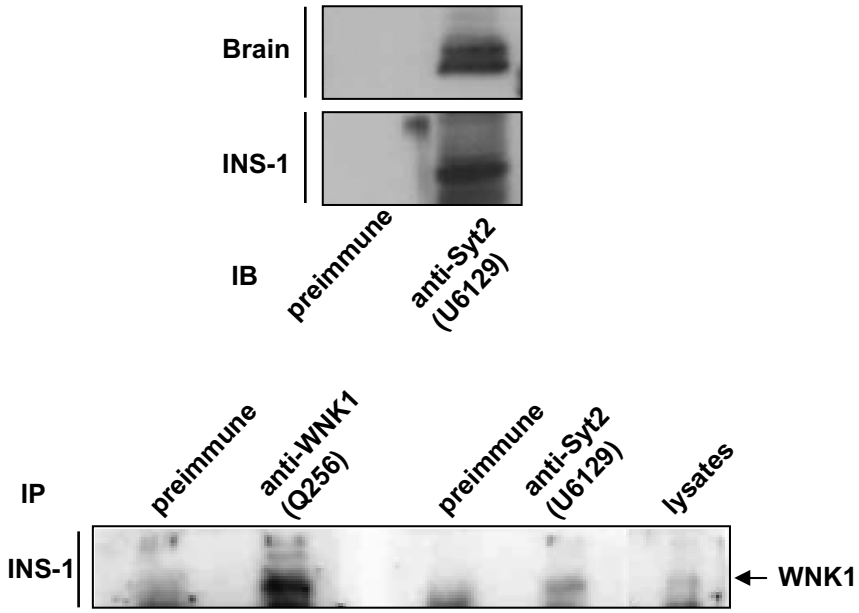

Figure 3-4. Interaction of endogenous Syt2 and WNK1
Blots of brain extracts and INS-1 cell lysates (top panels) and blots of immunoprecipitates from INS-1 cell lysates immunoprecipitated with either anti-Syt2 (U6129) or anti-WNK1 (Q256) (bottom panel).

microscopy in INS-1 cells (Figure 3-5). Each protein was detected in the cytoplasm and associated with vesicular structures; a significant fraction of the Syt2 also appeared to be localized to the plasma membrane. INS-1 cells contain large numbers of insulin secretory vesicles. To determine the relationship of the two proteins to secretory vesicles, we stained cells for insulin. Although each also has unique distributions, both WNK1 and Syt2 display significant colocalization with insulin-staining vesicles (Figure 3-5G-I). Because the size of these particles ($\leq$ 0.5 μm) is on the order of the limit of resolution of the confocal microscope, it is not clear whether they represent single particles or clusters. These results were further supported by the observation that transfected full length Syt2 also showed similar patterns of prominent colocalization with endogenous WNK1 (Figure 3-5J). Unexpectedly, cells transfected with Syt2 showed distinctive neurite-like growth. Costaining was also observed within the neurite-like extensions as well as in cytoplasmic secretory granules near the plasma membrane.

To provide additional evidence for their partial colocalization, INS-1 lysates were fractionated on sucrose density gradients (done by C. Heise). Syt2 was found in fractions in the lower half of the gradient consistent with its association with vesicular structures (Figure 3-5K). WNK1 was found near the top of the gradient, typical of soluble proteins, as well as in Syt2-containing fractions corresponding to dense core vesicles. In multiple gradients analyzed, between 20 and 40% of the WNK1 comigrated with the vesicles. These independent approaches clearly indicate that Syt2 can associate with WNK1 in the native state.

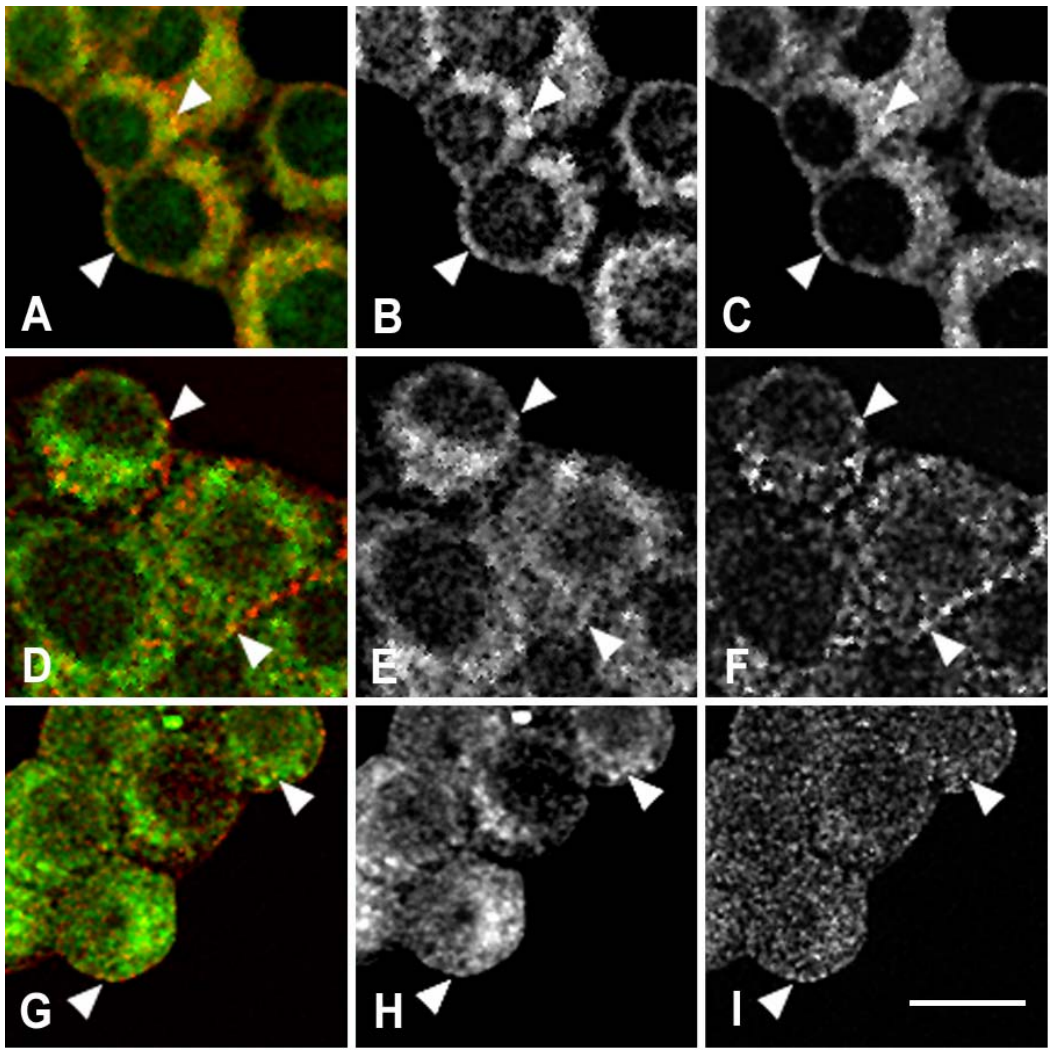

Figure 3-5. Subcellular localization of insulin, WNK1, and Syt2 in INS-1 cells
A-C. WNK1 (red) and insulin (green) were immunolabeled with Q256 (1:200) and FITC-conjugated anti-insulin (1:400). D-F. Endogenous Syt2 (red) and insulin (green) were costained with U6129 (1:500) and FITC-conjugated anti-insulin (1:400). G-I. For costaining of endogenous WNK1 (green) and Syt2 (red), Fc regions of Q256 and U6129 were directly labeled with fluorophore-conjugated Fab fragments. Bar = 10 μm. Arrowheads denote examples of discrete particles in which the two proteins co-localized at this level of resolution. *–continued-*

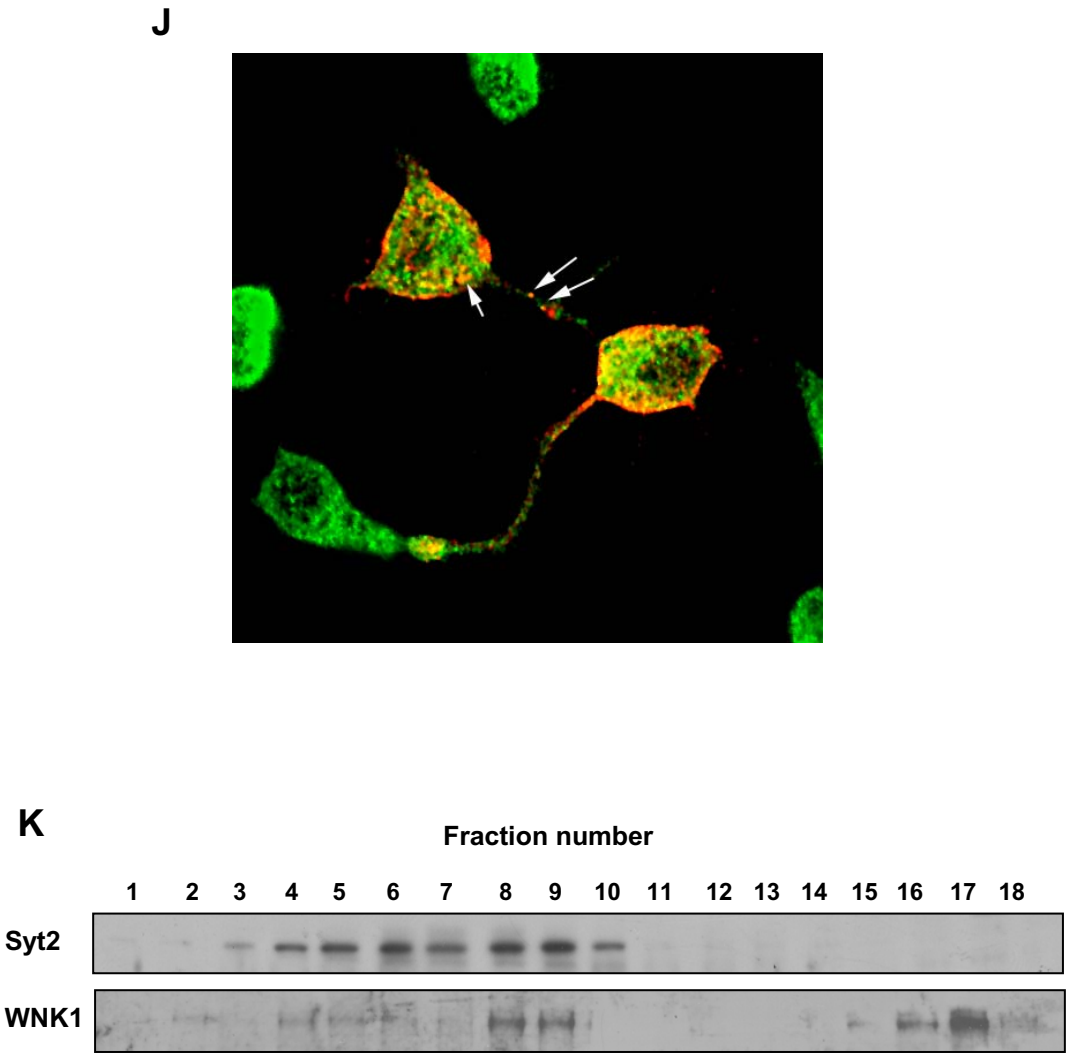

Figure 3-5. Subcellular localization of insulin, WNK1, and Syt2 in INS-1 cells
J. WNK1 (green) was detected with antiserum Q256 (1:200) and FITC-conjugated anti-rabbit secondary antibody. Flag-Syt2 (red) was stained with anti-Flag (1:500) and rhodamine conjugated anti-mouse secondary antibody. Arrowheads denote examples of colocalizations. K. Fractionation of INS-1 cell lysates on a sucrose gradient. Immunoreactivity of fractions with U6129 and Q256 (done by C. Heise).

D. WNK1 displays specificity among Syt isoforms

Syts 2, 3, and 9 were identified as WNK1 interactors, suggesting that WNK1 may also bind other Syts. To test the specificity of WNK1 binding to Syt2, we examined its interactions with Syts representing the six currently defined classes (Südhof, 2002) (Table 3-1). WNK1 specifically bound to Syts 1, 2, 3, and 9, but not to 4, 7, or 8 (Figure 3-6A). Immunoblotting with antibodies to the fusion domain showed that weak expression did not account for the lack of interaction with Syts 4 and 7 (Figure 3-6B); in fact, Syt2 expression could not be detected with anti-lexA antibody in spite of its strong interaction. In contrast, the Syt2 antibodies readily detected Syt2 and showed limited cross-reactivity only towards Syt1 (Figure 3-6B). None of Syt isoforms interacted with lamin, an abundant nuclear protein, suggesting that Syt isoforms are not promiscuous binders (Figure 3-6C).

To determine if the ability of WNK1 to bind Syts reflects more generally on a property of WNK family members, we isolated a cDNA encoding WNK4 to test its binding to Syts. Surprisingly, no interaction of WNK4 was detected with any of the seven Syts (Figure 3-6D), although it does bind to another WNK1 interactor isolated in the two-hybrid screen, designated KD-11-2 (Smad2) (Figure 3-6E). Any stable WNK4 interaction with Syts not detected in this assay is likely to be weak. These observations underscore the specificity of WNK1 binding to Syts.

E. WNK1 interacts with Syt2 through essential Ca^{2+}-binding residues in the C2 domains

Syt1 is thought to be a Ca^{2+}-sensor, triggering membrane fusion and

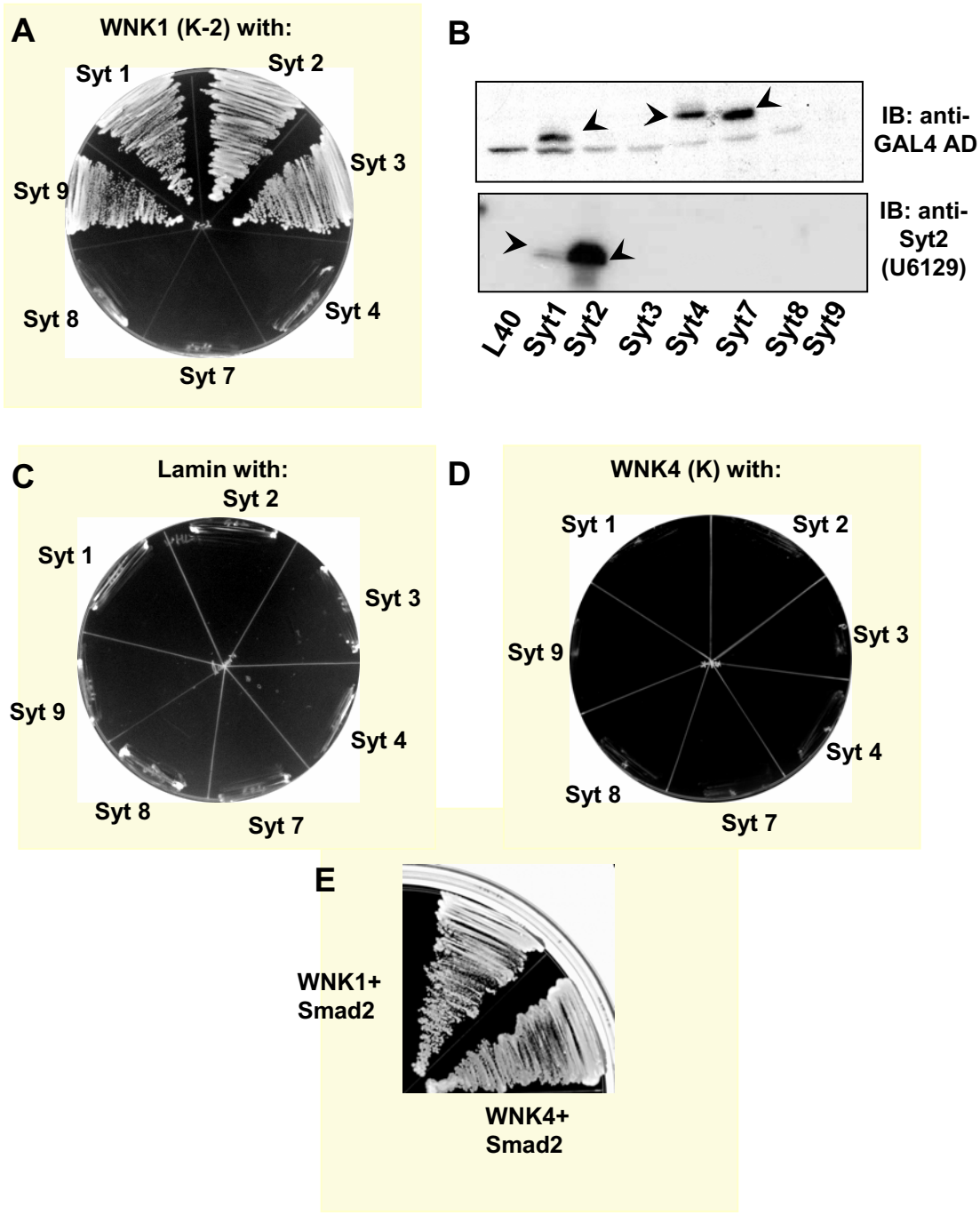

Figure 3-6. Specificity of the WNK1-Syt interaction
A. Two-hybrid test of interaction of WNK1 with Syt isoforms. B. Blot of yeast extracts showing expression of Syt fusion proteins. C. Two-hybrid test of interaction of lamin with Syt isoforms. D. Two-hybrid test of interaction WNK4 kinase domain (158-444) with Syt isoforms. E. Confirmation of the interaction of kinase domains of WNK1 and WNK4 with the positive control insert KD-11-2 by directed two-hybrid test.

neurotransmitter release at the synapse. It binds to phospholipids and effector molecules, such as syntaxin, in a Ca^{2+}-dependent manner (Yoshihara et al., 2003). Among the Syts that did not bind to WNK1 were 4 and 8, which have lost one or more of their Ca^{2+}-binding residues (see Table 3-1) and do not bind to phospholipids and effector molecules in a Ca^{2+}-dependent manner (von Poser et al., 1997; Li et al., 1995). We examined their in vitro binding to determine if Ca^{2+} influenced the association of Syt2 with WNK1. Binding of the two proteins was detectable in the absence of added Ca^{2+} or even in the presence of 5 mM EGTA, but was markedly enhanced by Ca^{2+} from submicromolar up to 1 mM (Figure 3-7A). To test the hypothesis that the Syt2 Ca^{2+}-binding residues are important for the interaction with WNK1, we created Syt2 mutants D231S and D310N with impaired Ca^{2+} binding (Figure 3-7B). Each of these mutations completely abrogated binding to WNK1 (Figure 3-7C), in spite of their comparable expression to wild type counterparts. In contrast, the mutation of S to D in Syt4 (S244D), to introduce a residue that might restore Ca^{2+} binding, did not cause it to acquire the ability to interact with WNK1, indicating that the simple substitution is not sufficient for WNK1-Syt binding (data not shown). These findings indicate that Ca^{2+} binding to Syt2 promotes its association with WNK1.

F. WNK1 contains a selective Syt binding pocket

We have solved the crystal structure of the kinase domain of WNK1 (Min et al., 2004). Molecular modeling of WNK4 based on the coordinates of WNK1 revealed a region on the substrate binding surface with provocative differences in charge between them (Figure 3-8A). Because WNK1 and WNK4 are about 85% identical in their kinase domains,

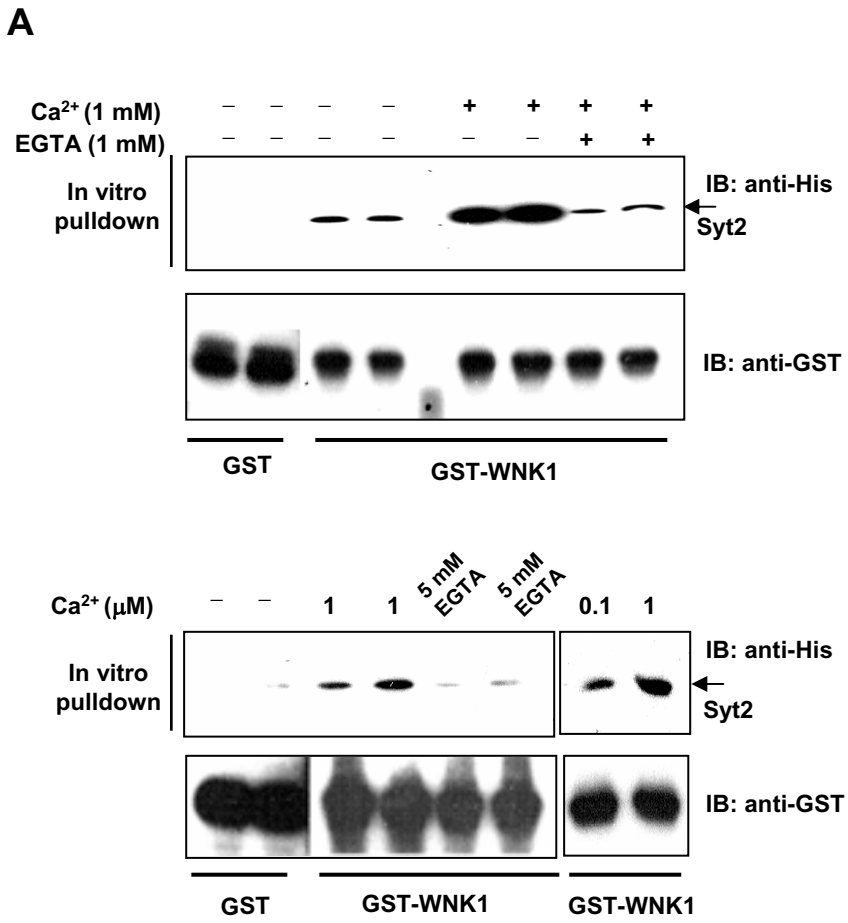

Figure 3-7. Role of Ca^{2+} in the specificity of the WNK1-Syt2 interaction
A. (Top panel) Effect of Ca^{2+} on the in vitro binding of WNK1 and Syt2 as in Figure 1B with the indicated concentrations of Ca^{2+} and EGTA. (Bottom panel) 5 mM EGTA to chelate Ca^{2+}. Interactions are shown in duplicate. No significant binding of WNK1 was observed to GST in the presence of 1 mM Ca^{2+} (not shown). *–continued-*

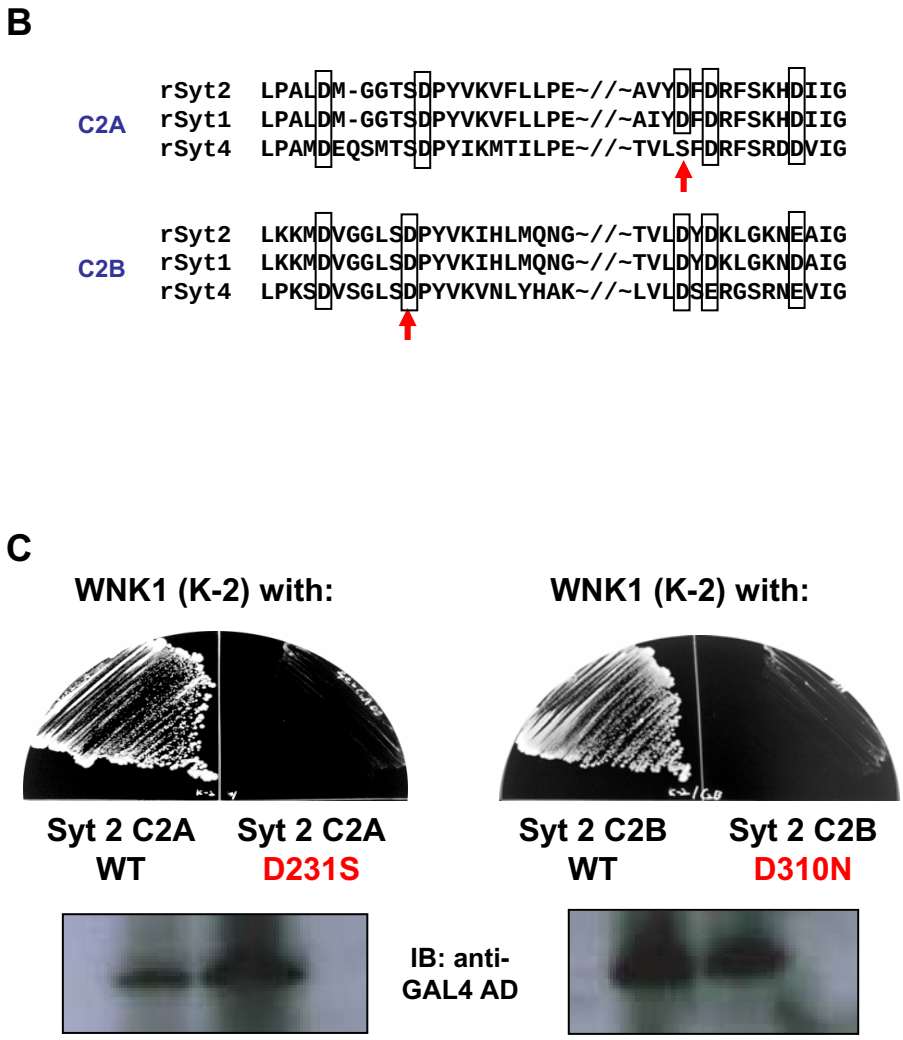

Figure 3-7. The role of Ca^{2+} in the specificity of the WNK1-Syt2 interaction
B. Partial sequences of C2A and C2B from Syts 1, 2, and 4 with indicated residues mutated. The five conserved acidic residues that coordinate Ca^{2+} ions are in open boxes. C. Two-hybrid test of interaction of WNK1 with the indicated C2 domain mutants (top) and the corresponding immunoblots with anti-GAL4 AD (bottom).

we considered the possibility that the difference in surface charge might account for the selective recognition of Syts by WNK1 and not WNK4. To test this hypothesis, we mutated a WNK1 residue contributing to this difference in surface charge, valine 318, to glutamate, and measured the ability of this WNK1 mutant to interact with Syt2. WNK1 V318E lost its capacity to bind to either the C2A or C2B domain of Syt2 (Figure 3-8B, top) but retained the ability to bind to another interactor, KD-11-2 (Smad2), indicating no gross change in WNK1 structure or stability (Figure 3-8B, middle). Other surface residues outside the expected substrate binding region that were also mutated had no effect on WNK1 binding to Syt2 (Figure 3-8B, bottom). These observations suggest that a binding pocket on WNK1 facilitates its stable association with Syts.

G. WNK1 phosphorylates Syt2 on its C2 domains

WNK1 phosphorylated Syt2, but only on fragments that contained either or both of its C2 domains (141-268 (not shown), 81-422, or 141-422) (Figure 3-9A). The stoichiometry of WNK1 phosphorylation of Syt 2 was approximately 1.2 mol of phosphate/mol of Syt2. WNK1 did not phosphorylate several other proteins that are substrates for other protein kinases, including all of the known MAP kinases and MAP2 kinases (ERK2, p38, JNK, ERK5, MEK1-7), casein, ribosomal protein S6, IκB, MEF2C and c-Jun (data not shown, (Xu et al., 2000)). Other protein kinases including p38 and JNK did not phosphorylate Syt2 (data not shown). WNK4 phosphorylated Syt2 but at a much reduced rate compared to WNK1 (Min et al., 2004). Syt1 was phosphorylated by CaMKII, CKII, and PKC, in each case within the linker region between the transmembrane and the C2A domain (Popoli,

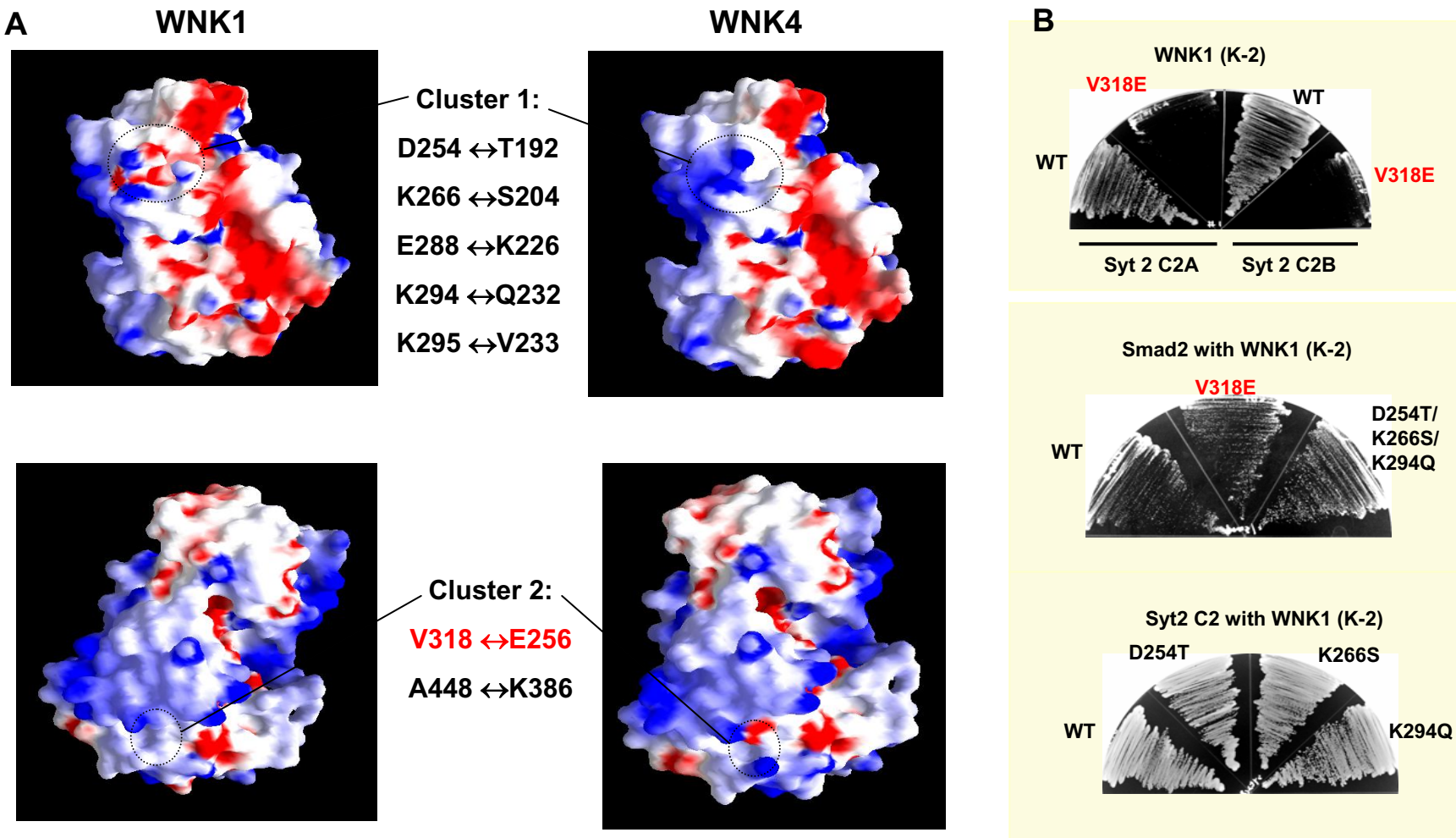

Figure 3-8. Molecular modeling of WNK4 based on WNK1 structure and mutagenesis analysis of surface residues with different charges between WNK1 and 4

A. Sequence alignment and molecular modeling of WNK4 with WNK1 coordinates revealed two clusters of different charges on the surface (done by X. Min). B. Two-hybrid test of interaction of WNK1 WT or mutants with its substrates. E288K, K295V, and A448K did not inhibit WNK1 binding to Syt2 (data not shown).

1993; Davletov et al., 1993; Hilfiker et al., 1999). In contrast, WNK1 phosphorylated Syt2 within the C2 domains (Figure 3-9B). Five phosphorylation sites were identified from mass spectrometry, and mutational analyses suggested that two sites (T202 and T386) are major and three sites (S280, S309, and S381) are minor phosphorylation sites (Figure 3-9B and data not shown). T202 is conserved among Syt isoforms, while T386 is less so. The T202A and T386A Syt 2 mutants were each phosphorylated by WNK1 to a reduced extent (60 and 40% of the wild type stoichiometry) (Figure 3-9C). Phosphorylation of a Syt2 mutant lacking the Ca^{2+} binding residues, Syt 2 C2A D231S and C2B D310N, was substantially reduced relative to wild type (Figure 3-9D). This indicates that both the stable association of Syt2 with WNK1 and its phosphorylation are enhanced by its Ca^{2+} binding.

To determine if Syt2 is phosphorylated by WNK1 in cells, I expressed Flag-Syt2 C2 (residues 141-422) without or with Myc-WNK1 kinase domain (residues 216-491), and labeled cells with [^{32}P]-orthophosphate. Syt2 immunoprecipitated from ^{32}P-labeled cells contained more radioactive label if it had been coexpressed with WNK1 (Figure 3-9E). To further confirm that T202 was a site of phosphorylation in vivo, we generated a phospho-specific antibody to phosphoT202 of Syt2 (Figure 3-9F, left panel) and found greater antiphosphoT202 reactivity if the protein had been coexpressed with WNK1 (Figure 3-9F, right panels). These findings support the conclusion that Syt2 is a WNK1 substrate and that T202 is a bona fide phosphorylation site. Together with the colocalization of the endogenous proteins, these results support the proposal that WNK1 regulates the function of Syt2 by phosphorylation of T202.

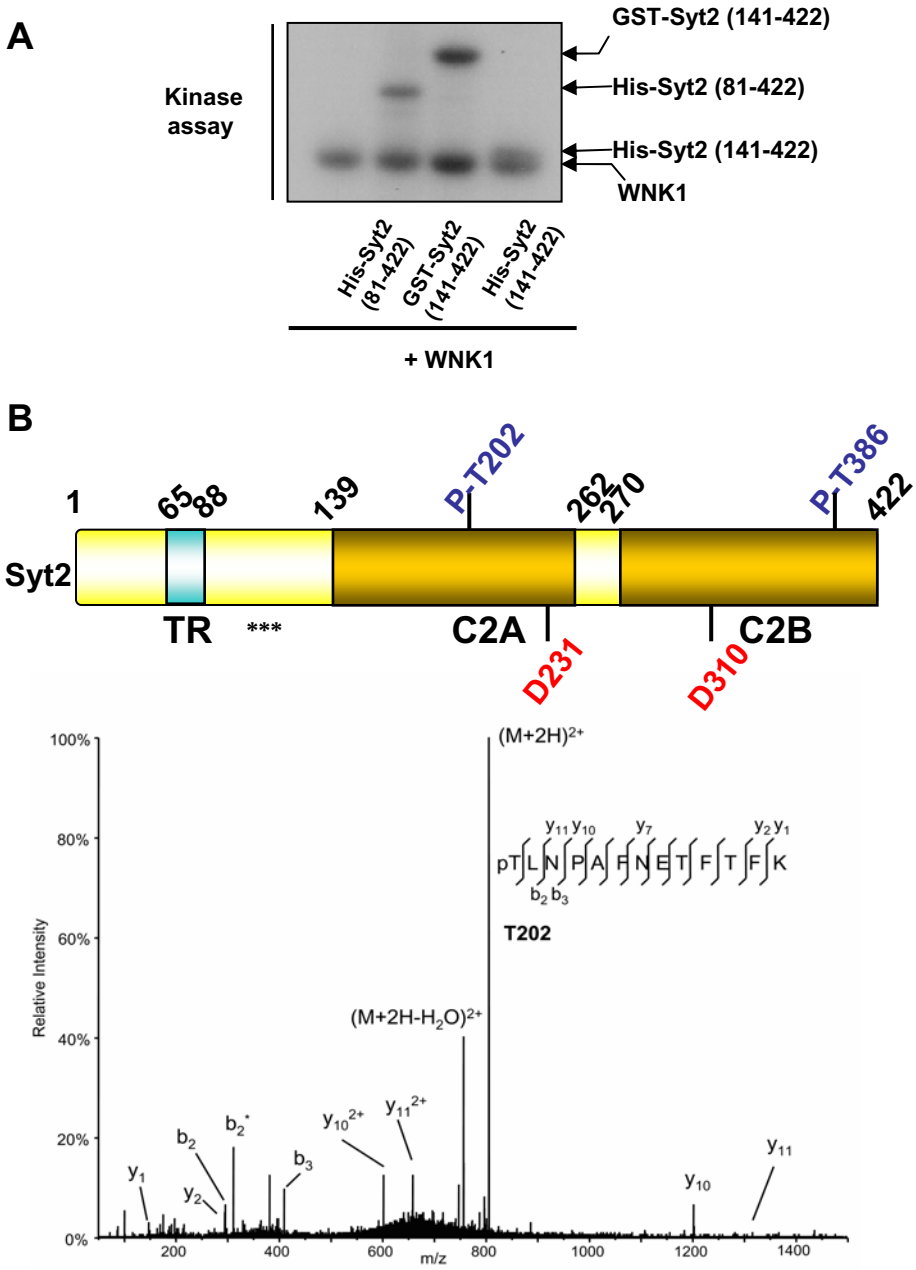

Figure 3-9. Phosphorylation of Syt2 by WNK1
A. His_6-Syt2 (81-422), GST-Syt2 (141-422), and His_6-Syt2 (141-422) were phosphorylated by WNK1 in vitro and resolved by SDS-PAGE. His_6-Syt2 (141-422) migrates just above the WNK1 band. An autoradiogram is shown. Incorporation into WNK1 is substantial because it autophosphorylates efficiently on several sites. B. Positions of phosphorylation sites found in Syt2 phosphorylated by WNK1(193-483) (top) and mass spectroscopic data indicating the sequence of the phosphopeptide containing T202 (bottom). Phosphorylation sites previously identified in Syt1 are marked with asterisks. *–continued-*

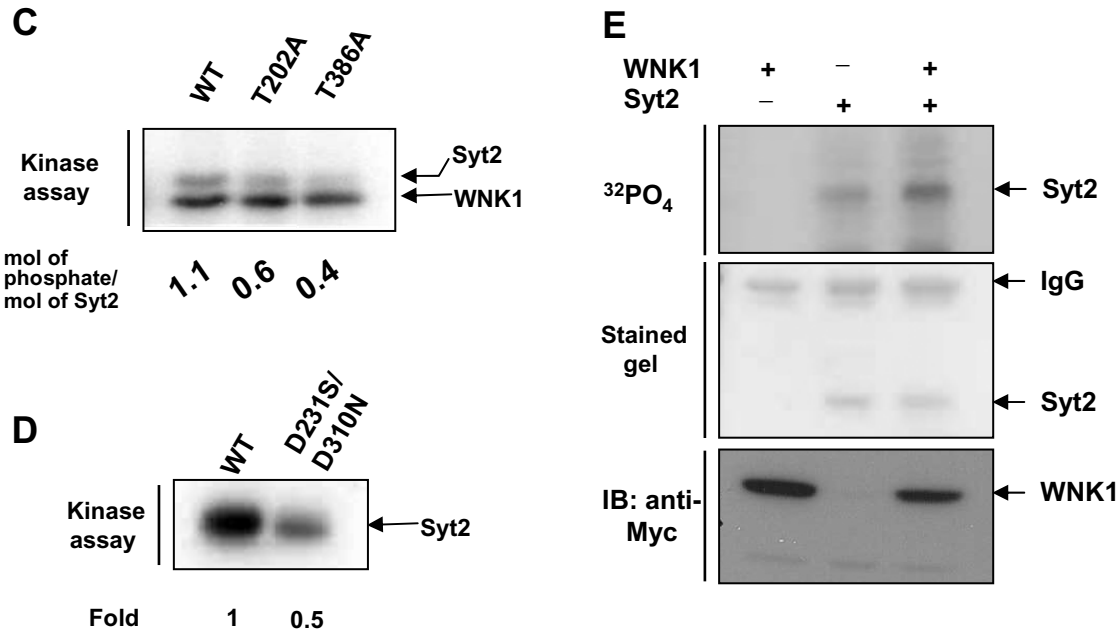

Figure 3-9. Phosphorylation of Syt2 by WNK1
C. Phosphorylation of the Syt2 mutants lacking individual phosphorylation sites compared to wild type. An autoradiogram is shown along with the calculated stoichiometries. D. Phosphorylation by WNK1 of the Syt2 C2 domain fragment with two Ca^{2+} binding residues mutated. An autoradiogram is shown along with the fold difference in phosphorylation of the mutant compared to wild type. E. ^{32}P-labeling of Syt2. 293 cells were transiently transfected with the constructs, Myc-tagged WNK1 fragment (residues 216-491) and Flag-tagged Syt2 C2 fragment (residues 141-422), and after 48 hours were labeled with [^{32}P]orthophosphate. After 3 hours, Flag-Syt2 C2 was immunoprecipitated (middle, stained gel). Phosphorylation of the Syt2 fragment was visualized by autoradiographyn (top). WNK1 expression was confirmed by immunoblotting with anti-Myc (bottom). *–continued-*

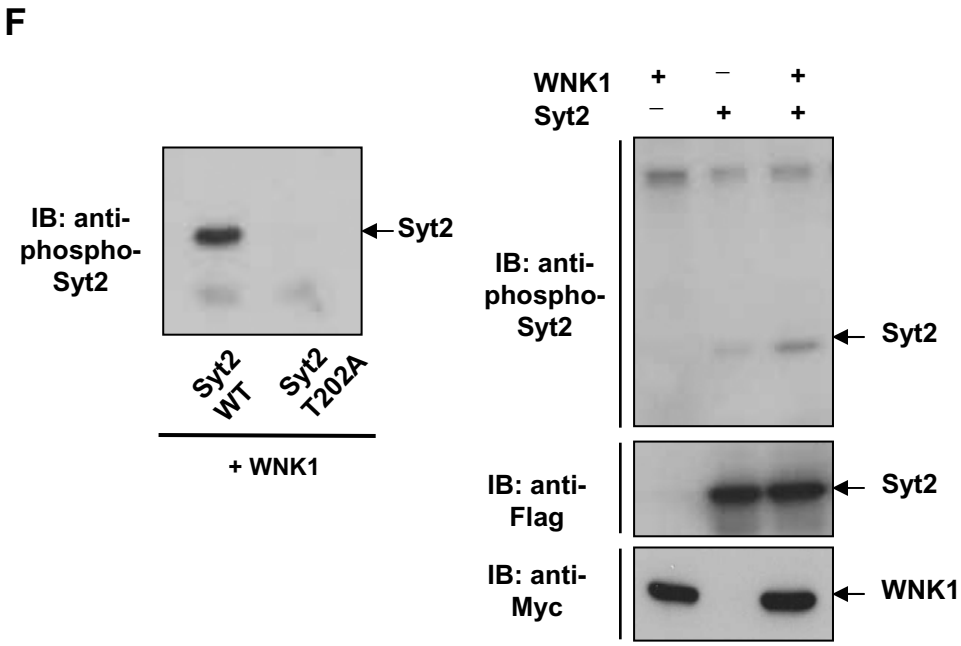

Figure 3-9. Phosphorylation of Syt2 by WNK1
F. Immunoblotting with anti-phosphoT202 Syt2. The specificity of the phosphoT202 Syt2 antibody was verified with recombinant His_6-Syt2 (81-422) WT or T202A which had been phosphorylated with WNK1 in vitro (left panel). COS7L cells expressing Myc-WNK1 (216-491) and Flag-Syt2 C2 were immunoblotted with anti-phosphoT202 Syt2 (top right panel) and with anti-Flag (middle). WNK1 expression was monitored with anti-Myc (bottom).

H. Phosphorylation by WNK1 changes the Ca^{2+} requirement for Syt2 binding to phospholipid vesicles

We explored the functional impact of Syt2 phosphorylation by measuring its binding to phospholipid vesicles (Figure 3-10A). As expected, the Syt2 C2 domains (141-422) fused to GST or His_6 bound to liposomes with an apparent affinity for Ca^{2+} of 110 μM (n=3) (Figure 3-10B). Omitting liposomes showed that sedimentation of the Syt2 C2 domain fragment was not due to aggregation. His_6-Syt2 (81-422) and His_6-Syt2 (141-422) also showed similar patterns of liposome binding (Figure 3-10C). Next, we investigated whether WNK1 could alter the properties of Syt2 binding to phospholipids (Figure 3-10D). Mixing WNK1 with Syt2 in the absence of ATP did not change its behavior (Figure 3-10E). If the Syt2 C2 domain fragment (141-422) was phosphorylated by WNK1 to a stoichiometry of one or greater, it showed a marked right shift in the Ca^{2+}-dependence of its phospholipid binding (Figure 3-10F, lane 1 to 4). Binding of phosphorylated Syt2 141-422 to phospholipid vesicles in the presence of 100 μM Ca^{2+} was reduced by approximately 80%, and a modest reduction in binding was observed even at 1 mM Ca^{2+}. In contrast, incubation of Syt2 with p38 under phosphorylating conditions did not cause any change in the behavior of the Syt2 C2 domain fragment (Figure 3-10F, lane 5 to 8).

To determine if phosphorylation of T202 or T386 contributed to the altered lipid binding, we examined effects of mutating these residues on Ca^{2+}-dependent phospholipid binding of the Syt2 C2 domains. T386A Syt2 sedimented poorly with phospholipid vesicles even at 1 mM Ca^{2+} (data not shown); therefore, its contribution to the altered behavior could not be assessed. However, T202A Syt2 141-422 showed a Ca^{2+}-dependence similar

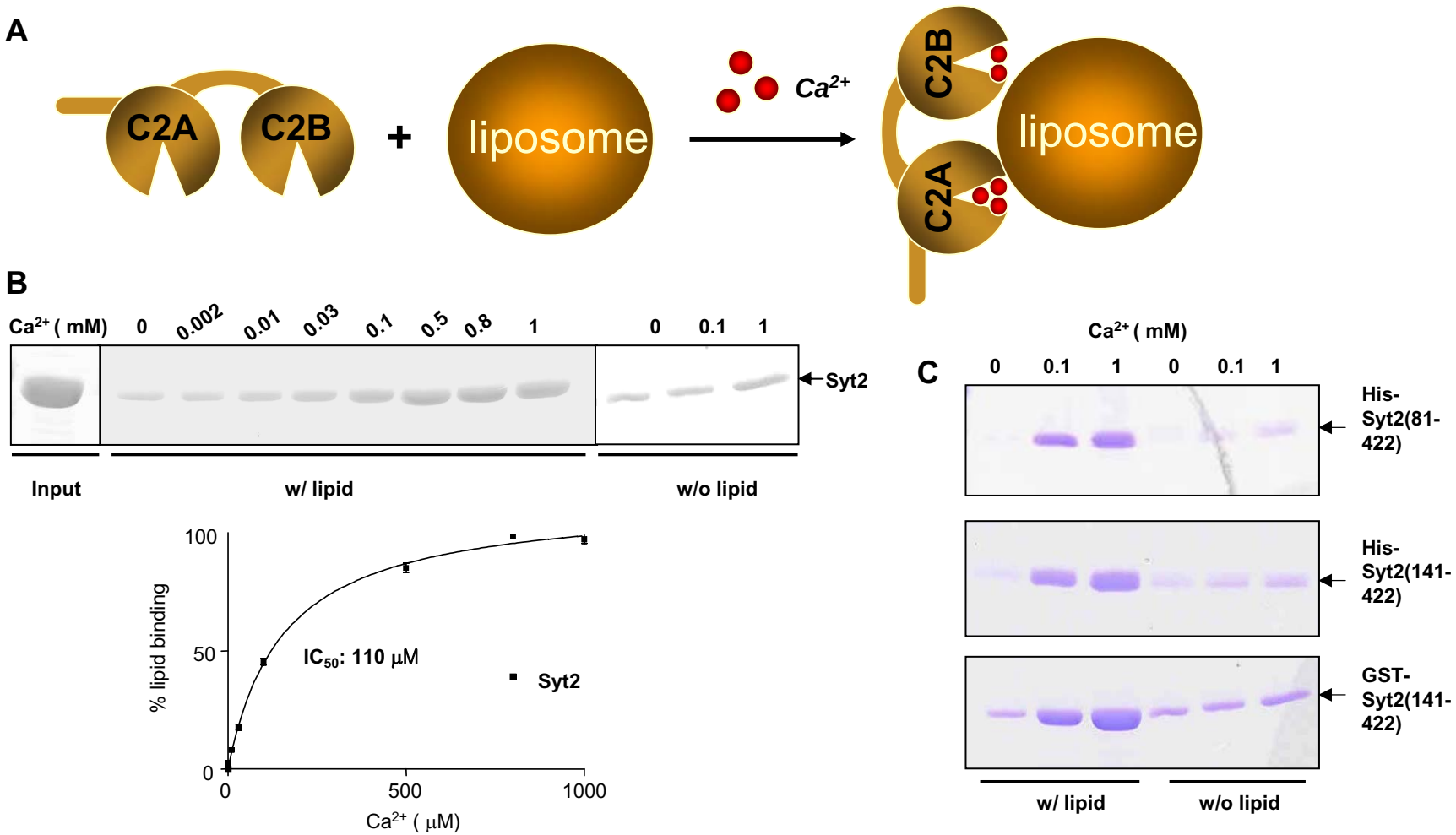

Figure 3-10. Effect of phosphorylation on the interaction of Syt2 with phospholipid vesicles
A. Schematic representation of phospholipid binding assay. B. (Top) Coomassie blue-stained gel of Syt2 C2 domains (GST-141-422) in the pellet in the presence (left) or absence (right) of phospholipid vesicles and increasing concentrations of Ca^{2+}. Input protein is shown on the far left. (Bottom) Plot of phospholipid binding of Syt2 as a function of Ca^{2+} concentration. n=3. Data are corrected for Syt2 sedimenting in the absence of phospholipids. C. Phospholipid binding with His_6-Syt2 (81-422) and His_6-Syt2 (141-422) *–continued-*

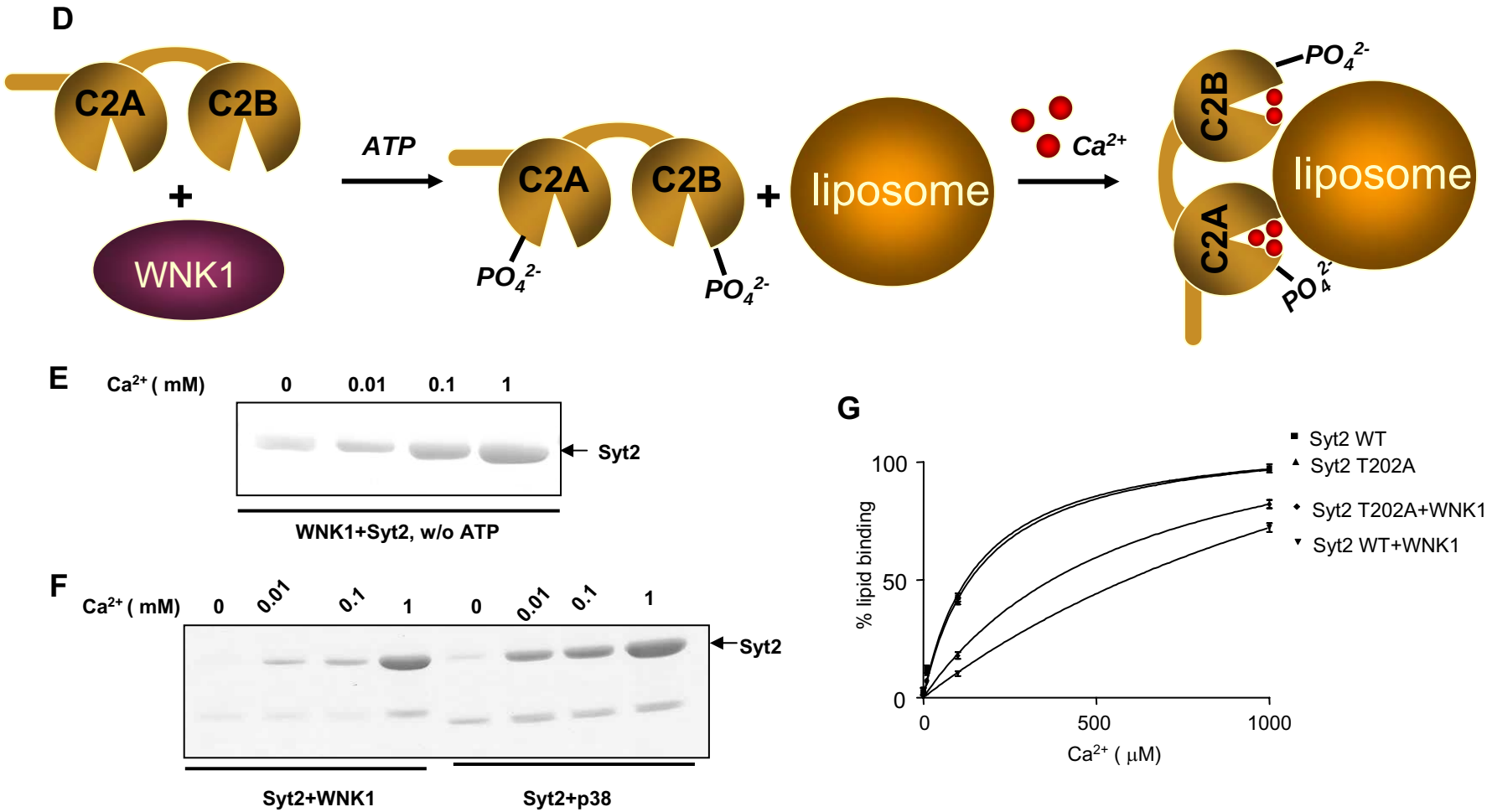

Figure 3-10. Effect of phosphorylation on the interaction of Syt2 with phospholipid vesicles ***–continued -***
D. Schematic representation of phospholipid binding assay of Syt2 phosphorylated by WNK1. E. As in panel A, except that Syt2 was mixed with WNK1 (193-483) in the absence of ATP prior to sedimentation with vesicles. F. As in top panel of A, except that Syt2 was phosphorylated (left) by WNK1 (193-483) or (right) by p38 prior to sedimentation with vesicles. G. Plot of phospholipid binding as a function of Ca^{2+} concentration of Syt2 (141-422) and Syt2 (141-422) T202A, each without or with phosphorylation by WNK1 as in F.

to that of wild type unphosphorylated Syt2 (Figure 3-10G). Following phosphorylation by WNK1, T202A Syt2 displayed behavior intermediate between that of wild type phosphorylated and unphosphorylated Syt2 141-422, consistent with its contribution to the altered behavior of Syt2 phosphorylated by WNK1 (Figure 3-10G, diamond). These observations support the conclusion that phosphorylation by WNK1 modulates the Ca^{2+}-dependence of Syt2 binding to phospholipid vesicles.

V. Discussion

Here I showed that WNK1 interacts with Syt2 and phosphorylates its C2 domains, modulating one of its most critical biochemical activities, its Ca^{2+}-dependent association with phospholipid vesicles. WNK1 also interacted with other Syt isoforms with Ca^{2+}-binding C2 domains. WNK1 is the only kinase currently known that phosphorylates Syt C2 domains; other protein kinases phosphorylate Syt1 in the linker region (Popoli, 1993; Davletov et al., 1993; Hilfiker et al., 1999). Thus, phosphorylation of C2 domains provides a heretofore undescribed mechanism for regulation of the interactions mediated by these Ca^{2+}-sensing domains.

WNK1 also interacts with other Ca^{2+} binding Syts, in agreement with the idea that WNK1 regulates the properties of the Ca^{2+}-binding forms of Syt (data not shown). The selectivity of WNK1 among Syt isoforms, the enhancement of Syt2 binding to WNK1 by Ca^{2+}, and the reduction of WNK1-Syt2 binding by mutation of critical Ca^{2+}-coordinating residues of Syt2 strongly argue that Ca^{2+} is an important regulator of and recognition determinant for the association of WNK1 with Syts. By inference from the structure of Syt1,

T202 of Syt2 lies within a beta strand of the beta sheet (Shao et al., 1998; Fernandez et al., 2001). Structural studies suggest that Ca^{2+} ions do not trigger any significant conformational change in Syt1; instead Ca^{2+} induces a change in its electrostatic potential from negative to positive (Figure 3-11A) (Shao et al., 1997; Murray and Honig, 2002). This charge reversal drives Ca^{2+}-induced interactions with anionic phospholipids (Zhang et al., 1998). Phosphorylation by WNK1 will locally increase the negative charge of Syt, which should inhibit binding to negatively charged phospholipids, a prediction validated by the increased Ca^{2+} requirement for membrane binding of phosphorylated Syt2 (Figure 3-11B). Thus, the exact position of the phosphorylation sites may not be as important as the capacity of WNK1 to place negative charges on the surface of the C2 domains. Alternatively, the phosphorylations of the C2 domains by WNK1 may affect the intramolecular conformational change of Syt2 triggered by Ca^{2+}. Godwin's group suggested that Syt1 can go through a Ca^{2+} -dependent conformational change and subsequent intramolecular interaction which is mediated by a linker region between the C2A and C2B domains (Garcia et al., 2000). However, it is not known whether intramolecular interaction of Syt1 is significant for its properties of effector binding.

The binding data suggested that Ca^{2+} positively affects WNK1-Syt2 binding in vitro, although the WNK1-Syt2 interaction occurs even without Ca^{2+}. On the other hand, competition of WNK1 with membranes for Syt2 binding was not detected, nor did WNK1 co-sediment with the Syt2-bound vesicles (not shown). These findings suggest that at low intracellular Ca^{2+}, Syt2 will be associated with WNK1 and phosphorylated if WNK1 is activated. As the Ca^{2+} concentration increases, Syt2 C2 domains will begin to associate

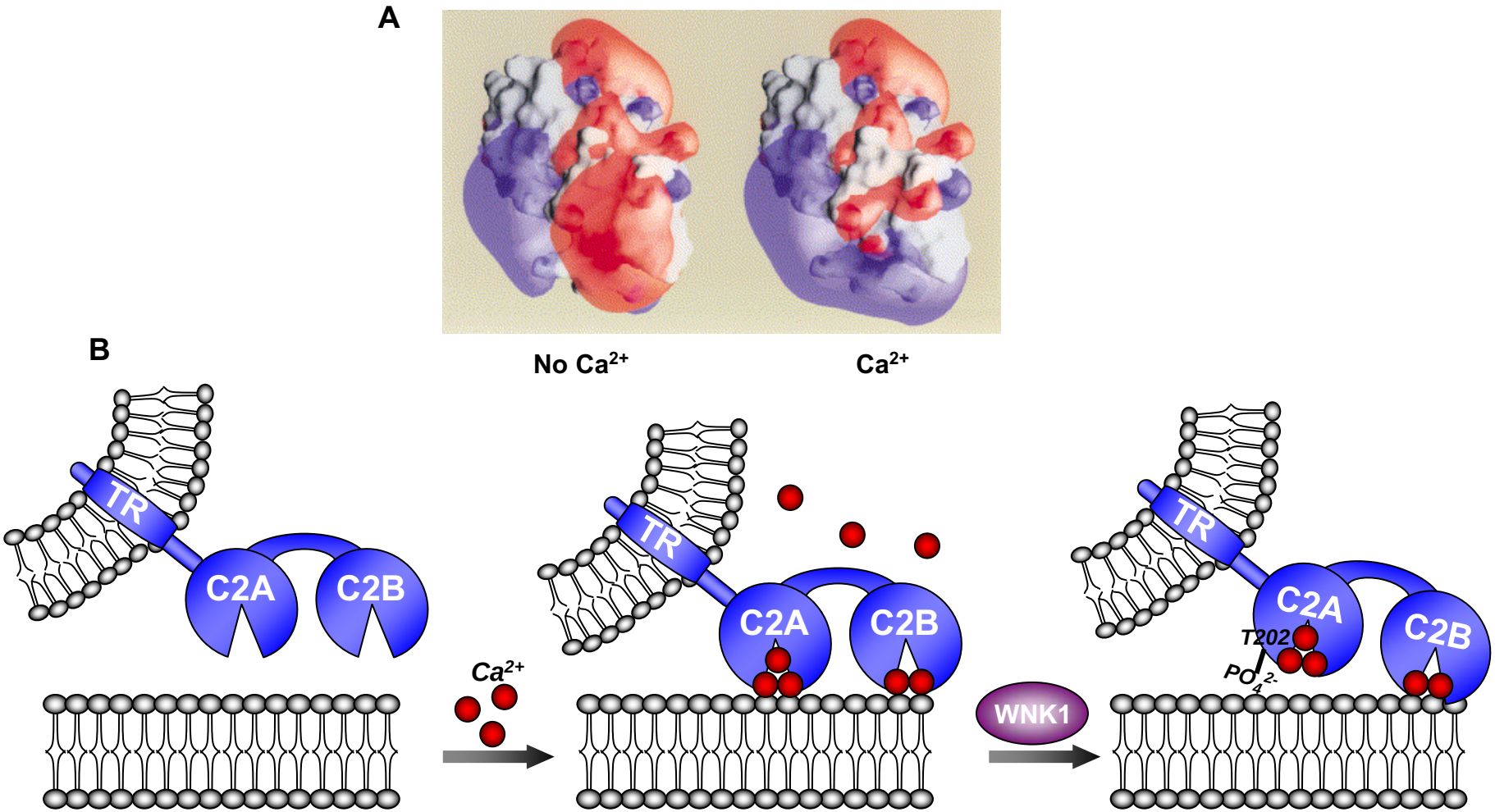

Figure 3-11. Ca^{2+}-driven electrostatic change of Syt1 C2A domain and a model for WNK1 phosphorylation effect on Syt2 phospholipid binding

A. Positive (blue) and negative (red) potentials of Syt1 C2A is contoured with or without Ca^{2+} (Murray and Honig, 2002).B. Current model for WNK1 phosphorylation of T202 site on Syt2 and its role in membrane binding.

with membranes, and association with membranes will be strongly favored over WNK1 binding. However, if Syt2 has first been phosphorylated by WNK1, more Ca^{2+} will be required to promote binding of Syt2 C2 domains to phospholipid vesicles, Dephosphorylation will cause Syt2 to again bind to membrane vesicles at lower Ca^{2+} concentrations. Phosphorylation will likely influence other electrostatic interactions mediated by C2 domains, for example, with syntaxin, a component of the SNARE complex, which interacts with Syts in a Ca^{2+}-dependent manner (Li et al., 1995). Upon Ca^{2+} binding to Syt1, the electrostatic repulsion between Syt1 and syntaxin is reversed, facilitating their binding (Shao et al., 1997). Other possible targets include SNAP-25, ion channels, AP-2, neurexins, *stoned* A/B, tubulin, calmodulin, the Rab3 effector RIM as well as Syts themselves, which are all Syt interactors binding in either a Ca^{2+}-dependent or Ca^{2+}-independent manner. The lipid composition of the plasma membrane may be another factor that influences phosphorylation-driven Syt behavior. Recent studies proposed that Syt1 binds with high affinity to phosphatidylinositol 4,5-bisphosphate (PIP_2) at the inner leaflet of the plasma membrane. The lipid steers the membrane penetration activity of Syt1 toward the target membrane (Bai and Chapman, 2004). Another question that should be investigated is whether WNK1 itself directly binds to and phosphorylate these Syt-binding molecules.

What is the biological outcome of Syt regulation by WNK1? We suggest that WNK1 will influence the rate of cycling of Syts among their Ca^{2+}-dependent binding states, by influencing the duration of individual interactions. Phosphorylation will probably shorten the time that Syt C2 domains are bound to membranes. Syts are involved in both

exocytosis and endocytosis and both processes might be affected (Ullrich et al., 1994; Martin, 2003; Wang et al., 2003; Zhang et al., 1994). The answers for this question may be partly addressed by membrane fusion analysis using a reconstituted system with defined components. Chapman's group suggested that Syt1, together with SNAREs, strongly stimulated membrane fusion in a Ca^{2+}-dependent manner. This result suggested that Syt and SNAREs are the minimal protein complement for Ca^{2+}-driven exocytosis (Tucker et al., 2004). Thus, it will be interesting to test if WNK1 phosphorylation of Syt can modulate the kinetics of Ca^{2+}-triggered membrane fusion events. Recent studies of synaptic transmission using synaptophluorin, a pH-sensitive fluorescent protein, suggest that there are three modes of synaptic vesicular recycling; kiss-and-run, compensatory, and stranded mechanisms (Gandhi and Stevens, 2003). In kiss-and-run fusion events, the synaptic vesicles remain open for only a very short period of time (tenth of a second); allowing for transient and repeated fusion rather than full vesicle collapse. Other events are more conventional extended (seconds to tens of seconds) secretory mechanisms that include collapse and retrieval of vesicles in a stimulus-dependent manner. Interestingly, according to a recent report, the choice between kiss-and-run and full fusion events appears to be dependent on the intrinsic properties of Syt, that is, the Ca^{2+}-dependence of Syt. The authors suggested that Syt1 favors full fusion, but Syt4 selectively displays a kiss-and-run mechanism (Wang et al., 2003). At fly neuromuscular junctions, selective photo-inactivation of Syt1 only blocked slow compensatory synaptic vesicle endocytosis in vivo (Poskanzer et al., 2003). Therefore, a requirement of selective interaction of WNK1 and phosphorylation by WNK1 among Syt isoforms may reflect different modes of synaptic vesicle endocytosis

by altering the kinetics, probably both duration and frequency, of specific membrane fusion events.

WNK1 is abundant in many tissues notably brain, heart, and kidney (Xu et al., 2000; Choate et al., 2003), suggesting that it plays a universal role, not limited to renal or even neuronal functions. This is further supported by the colocalization of WNK1 with Syt2 in pancreatic β-cells, a cell type specialized for regulated secretion on a relatively slow time scale. The functionality of a number of transporters is regulated by their time of residence in the plasma membrane. The regulation of insulin-sensitive glucose transporters, such as GLUT4, primarily by insertion into or removal from the membrane, shares a striking similarity with the regulated secretion of synaptic vesicles in neurons and insulin secretory vesicles (Hudson and Birnbaum, 1995; Cain et al., 1992). Syt9, for example, was proposed to have a regulatory role in the membrane insertion of transporter- and channel-containing vesicles outside of the brain (Hudson and Birnbaum, 1995). Moreover, the existence of SNARE-like molecules in many tissues, including tissues unrelated to regulated secretion, suggests roles of SNAREs in trafficking membranous organelles to expose cargos (Galli et al., 1994; McMahon et al., 1993). WNK1 is an attractive candidate to modulate these processes.

Another thought-provoking question is how might this regulatory function of WNK1 contribute to hypertension? A number of renal transporters, e.g., the Na-Cl cotransporter (NCC), the epithelial sodium channel (ENaC), and the Kir1.1 (ROMK) subtype of inward rectifier K^+ channel, are regulated by membrane insertion and/or retrieval (Snyder, 2000; Yoo et al., 2003; Wilson et al., 2003), suggesting that WNK1 causes abnormal ion

reabsorption by increasing the membrane concentration of one or more transporters, in part through phosphorylation of Syts. Although mutations in WNK1 and WNK4 have both been shown to account for different occurrences of PHAII, the mechanisms by which these two family members can lead to this disease appear be distinct. WNK4 has been shown to cause a reduction in membrane delivery of the NCC by an unknown mechanism (Wilson et al., 2003; Yang et al., 2003), and its inhibitory effects on ROMK appear to be dependent upon the endocytotic machinery, suggesting distinct mechanisms (Kahle et al., 2003). WNK4 mutations that cause PHAII are in the coding sequence and may inhibit or enhance its function (Wilson et al., 2003; Kahle et al., 2003). On the other hand, the WNK1 mutation found in PHAII causes its overexpression (Wilson et al., 2001). The idea that WNK1 and WNK4 have antagonistic functions is suggested by the finding that WNK1 inhibited the effect of WNK4 on the NCC (Yang et al., 2003). This potential antagonism may account for our least predictable findings that WNK1 and WNK4 did not share a strong interaction with Syt2, and the specificity is derived in part from a hydrophobic interaction with the extended substrate binding region of WNK1. At the least, this difference provides biochemical evidence that WNK1 and WNK4 have some distinct functions. WNK4 may have more specialized activity in regulating certain types of transporters or channels perhaps due to its lack of interaction with Syts or its recognition of its own discrete targets.

Our understanding of the regulation of WNK catalytic activity is still rudimentary (Xu et al., 2000; Xu et al., 2002). The upstream signaling molecules and stimuli for WNK pathways remain to be identified. The one stimulus currently defined for WNK1 is hypertonicity (Xu et al., 2000). In synapses, hypertonic sucrose can drive release of

synaptic vesicles by an unknown mechanism (Stevens and Williams, 2000; Chapman, 2002), leading us to speculate that WNK1 may be involved in this type of event because of its activation by hypertonicity. In addition, WNK family protein kinases may undergo cross-connections with other signaling pathways because WNKs contain multiple putative protein-protein interaction modules and motifs which allow other regulatory mechanisms that have yet to be discovered. For example, our yeast two-hybrid results and preliminary observations uncovered a wide spectrum of binding partners for WNKs with many implications in other signaling pathways (Smad2 in TGF-β signaling pathway), proper spatial localization and trafficking (dynein light chain), protein stability (E2 ubiquitin conjugation enzyme), and homo- or hetero-oligomerization (self-association and WNK1 complex formation) (see Table 3-2 and Chapter 5).

WNK1 acts upstream of WNK4 by ameliorating its inhibitory effect on NCC (Yang et al., 2003). This is consistent with the idea that overexpression of WNK1 resulted in hypertension in PHAII patients and partial loss of function of WNK1 led to the lowered blood pressure in WNK1 heterozygous mice (Wilson et al., 2001; Zambrowicz et al., 2003). However, the localization of WNK1 and WNK4 shows different patterns in tissues, and it is not known whether they can epistatically affect common effector molecules other than NCC. Moreover, WNK4 regulates many transporters and channels including the NCC, ROMK, the Na-K-2Cl cotransporter (NKCC), the Cl^-/base exchanger (CFEX) and claudin to control ion homeostasis by kinase activity-dependent or independent mechanisms. These observations strongly suggest that WNK1 and WNK4 not only epistatically act in a signaling pathway but also they independently influence different targets in a kinase activity-

dependent or independent manner. In fact, WNK1 exists as multiple spliced forms, and particularly, in kidney, a kinase-defective form is predominant (O'Reilly et al., 2003; Delaloy et al., 2003). Increased WNK1 transcript level reported in PHAII did not discriminate between full length and spliced forms. Therefore, it is possible that overexpression of the kinase-defective form of WNK1 might cause PHAII hypertension.

It is notable that PHAII is usually accompanied by hypercalciuria (high urinary Ca^{2+} excretion), suggesting that changes in the balance of certain ions may be functionally coupled to the level of other ions for adaptation. The change of ion flux (e.g. the alteration of Ca^{2+} level) might be one of the driving forces for WNK1-Syt2 effects on electrolyte homeostasis. One potential clue for this hypothesis comes with the interesting discovery that phosphatidylinositol 3-kinase (PI3K) activates the membrane trafficking of Ca^{2+} channels on the cell surface (Lhuillier and Dryer, 2002; Viard et al., 2004). It was suggested that PI3K stimulation by insulin-like growth factor (IGF-1) or angiotensin II promotes the translocation of Ca_v channels to the plasma membrane by undefined mechanisms. As noted in Chapter 2, WNK1 is a substrate of Akt, although phosphorylation of WNK1 by Akt did not change either activity or localization of WNK1 under their defined conditions (Vitari et al., 2004). Therefore, the functional links among these kinases and Ca^{2+} channels remain to be identified. In spite of much speculation, phosphorylation of Syt2 C2 domains by WNK1 provides a novel signaling mechanism to regulate membrane trafficking and subsequent cargo insertion or removal. We suggest that the capacity of WNK1 to alter the electrostatic properties of Syts will regulate their behavior as Ca^{2+} sensors.

Chapter 4: WNK1 Interacts with Smad2 and Dynein Light Chain

I. Abstract

Yeast two-hybrid screening of a mouse brain cDNA library with WNK1 fragments yielded Smad2 and an 8 KDa dynein light chain/protein inhibitor of nitric oxide synthase (LC8/PIN) as interacting proteins. An inactive form of the WNK1 kinase domain pulled down two cDNA clones of Smad2. Both WNK1 and WNK4 phosphorylated full length Smad2 as well as its individual MH1 and MH2 domains in vitro. Immunoblotting with a phosphoS465/S467 antibody showed that WNK1, but not WNK4, phosphorylates at least these two sites in vitro. Phosphorylation of these C-terminal serine residues is a key step in the transforming growth factor-β (TGF-β) signaling pathway. Mapping analysis indicated that the MH2 domain is required for Smad2 binding to the kinase domains of both WNK1 and WNK4. Overexpression of WNK1 neither enhanced phosphorylation of the C-terminal serine residues of endogenous Smad2 in several cell lines, nor induced the nuclear accumulation of the protein. Additionally, WNK1 did not alter the total amount of endogenous Smad2 protein.

LC8/PIN, a subunit of the dynein motor complex, was isolated multiple times from screening with a WNK1 bait corresponding to the autoinhibitory domain plus a coiled-coil region (residues 481-660). Interaction of WNK1 with LC8/PIN was confirmed by in vitro pulldown assays. Recombinant WNK1 proteins also phosphorylated LC8/PIN in vitro. However, the corresponding region of WNK4 did not bind to LC8/PIN, suggesting a selective interaction with WNK1. Unexpectedly, an Ala622 to Asp mutation, in WNK1

completely abolished its binding to LC8/PIN, which was proven by pairwise yeast-two hybrid interaction and in vitro pulldown assay. Because this Ala is not conserved among WNK isoforms, LC8/PIN is likely to be a WNK1-specific binding partner. On the other hand, introduction of mutations into WNK1 that were associated with hypertensions when found in WNK4 had no effect on the interaction with LC8/PIN. Interestingly, the incubation of LC8/PIN proteins with a WNK1 fragment that included its autoinhibitory domain enhanced WNK1 kinase activity toward substrates. This finding suggests that at least one function of LC8/PIN may be the relief of autoinhibitory effects on WNK1.

II. Introduction

A. TGF-β signaling and Smad

Transforming growth factor-β (TGF-β) superfamily members control a diverse array of biological processes including embryogenesis, cellular growth, differentiation, migration, and programmed cell death. Defects in ligands and signal transducers within this signaling pathway cause severe impairments in embryonic development and disorders in tissue homeostasis during adult life (Massague, 1998). Members of this superfamily are divided into the TGF-β/Activin/Nodal subfamily and the bone morphogenetic protein (BMP)/growth and differentiation factor (GDF)/Muellerian inhibiting substance (MIS) subfamily. More than forty of the cytokines are present in human, nine are in fly, and six are in worm. These ligands transduce signals by stimulating the formation of heteromeric complexes of type I and type II Ser/Thr kinase receptors. The type II receptor activates the type I receptor by

phosphorylating a specific domain known as the glycine-serine or GS domain. Activated type I receptors initiate intracellular signaling through activation of specific receptor-activated Smads (R-Smads) to relay signals into the nucleus, where they control numerous target genes (Figure 4-1). The TGF-β signaling pathway is a useful model system for signaling, due to its parsimoniousness in signal transduction routes.

Smad genes were first identified from genetic screens in fly and worm. The name of Smad reflects a fusion of *Drosophila* mothers against decapentaplegic (Mad) and *C. elegans* small (Sma) (Derynck et al., 1996). Smad proteins fall into three subfamilies; R-Smads, common mediator Smads (Co-Smads), and inhibitory Smads (I-Smads) (Figure 4-2A). R-Smads (Smad1, 2. 3, 5, and 8) specifically interact with and are phosphorylated by the type I receptors. Subsequently, activated R-Smads recruit Co-Smads (Smad4), and they form heteromeric complexes to enter the nucleus. By contrast, I-Smads (Smad6 and 7) act as negative regulators. They compete for activated type I receptors with R-Smads, thus preventing R-Smad-mediated signaling. However, Smad6 also exerts its inhibitory effects on signaling by competing with Smad4 for heteromeric complex formation with activated Smad1 (Massague, 1998; Hata et al., 1998). R-Smads and Co-Smads share highly conserved domains at their N- and C-termini, known as Mad homology domains (MH1 and MH2). These characteristic domains are separated by a less conserved proline-rich linker of diverse length. The MH2 domain is highly conserved among all Smads, and it resembles the forkhead-associated domain (FHA), a phosphoserine/threonine binding domain. The MH2 domain is important for hetero- or homo-oligomerization among Smads and recognition by phosphorylated type I receptors. This domain is also involved in binding

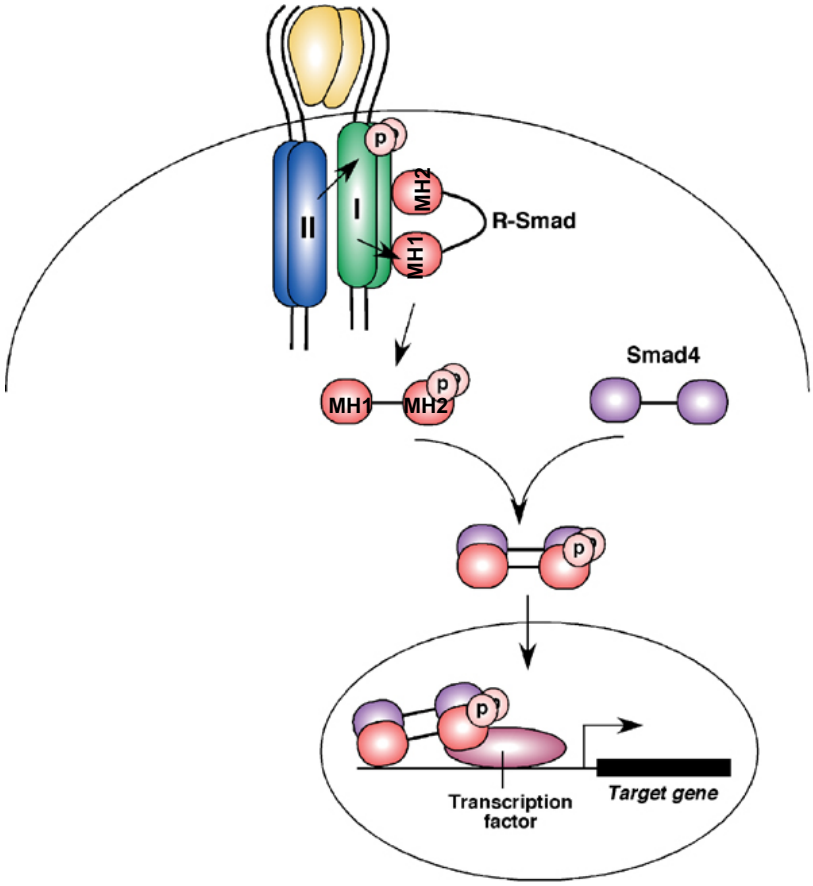

Figure 4-1. Schematic representation of TGF-β signaling pathway
Figure is from Izzi and Attisano, 2004.

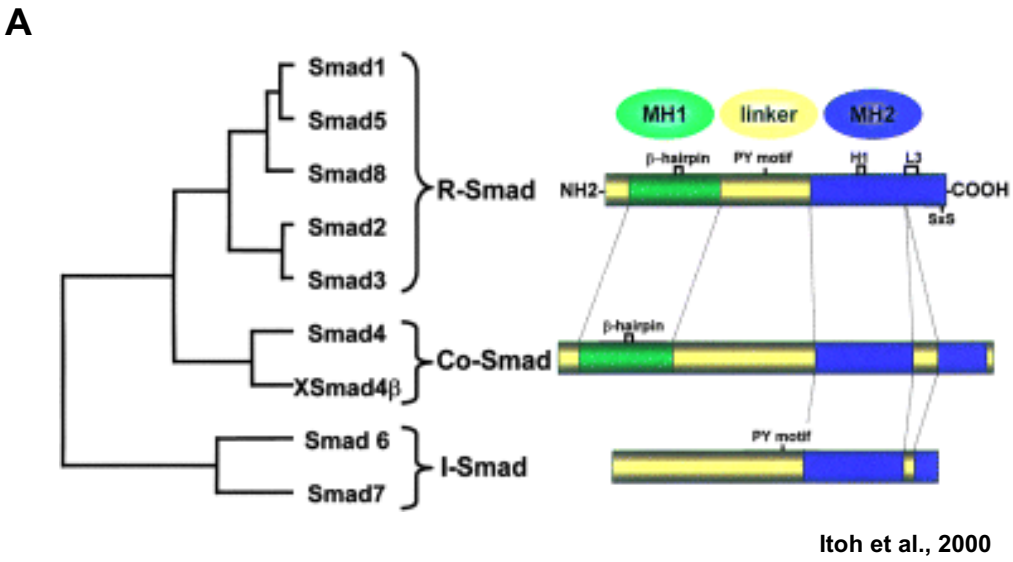

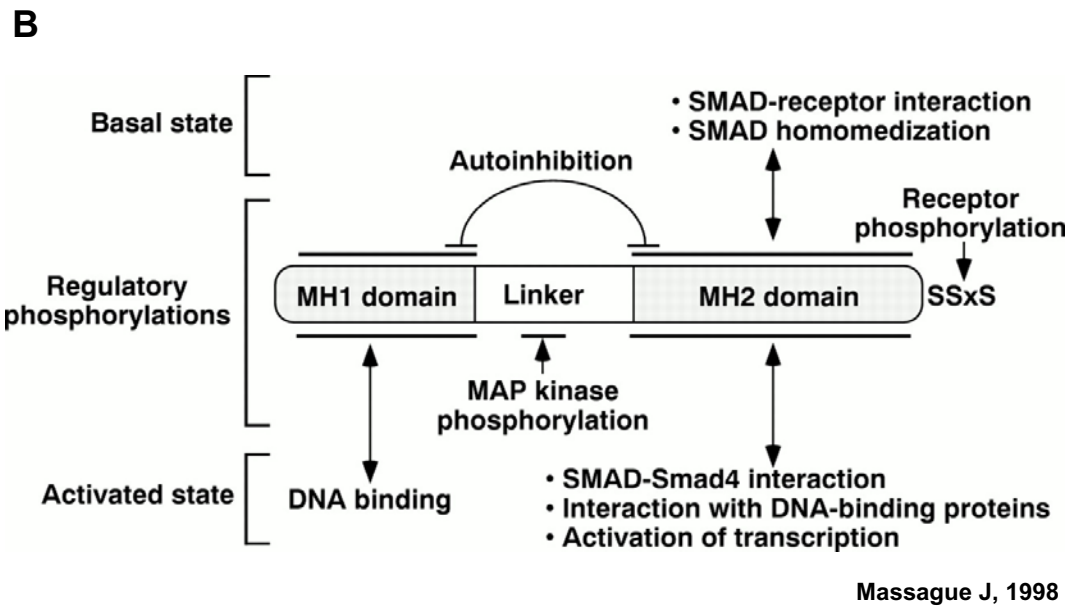

Figure 4-2. The Smad family and their domains
A. Phylogenetic dendogram of vertebrate Smads. The highly conserved domains and motifs are indicated. B. The functional organization of Smad.

to cytoplasmic regulators, and in transcriptional activation or repression (Li et al., 2000; ten Dijke et al., 2000). The MH1 domain shows remarkable sequence homology between R-Smads and Co-Smads, but the N-terminal region of I-Smads lacks sequence similarity to MH1 domains. MH1 domains have intrinsic DNA binding activities and also bind to MH2 domains intramolecularly probably for autoinhibition (Figure 4-2B) (Hata et al., 1997).

R-Smads, such as Smad2, interact with the TGF-β type I receptor (TβRI) and the Smad anchor for receptor activation (SARA) protein before nuclear translocation. SARA is a cytoplasmic protein that specifically interacts with unphosphorylated Smad2 and the receptor complex (Tsukazaki et al., 1998). This adaptor protein contains a Smad-binding domain (SBD) for Smad2 binding and a phosphatidylinositol 3-phosphate binding FYVE motif for anchoring Smad2 to the plasma membrane or endosomal vesicles. Once phosphorylated by TβRI, Smad2 forms a complex with Smad4. Smad2 is then released from TβRI and SARA, and accumulates in the nucleus. Structural studies showed that this event occurs through mutually exclusive protein-protein interactions, because the regions of the Smad2 MH2 domain that bind to TβRI and SARA are also required for the formation of homomeric or heteromeric Smad2-Smad4 complexes (Shi and Massague, 2003). In the nucleus, Smad complexes interact with transcription factors, co-activators, or repressors. For example, the *Xenopus* FoxH1 family member Fast1 is the first known transcription factor that binds to the Smad complex (Chen et al., 1997). Further studies identified a common and short, proline-rich Smad interaction motif (SIM) among the transcription factors. This SIM motif specifically binds to the MH2 domain of R-Smads, and interestingly shares significant homology with a short region within SBD domain of SARA (Wu et al.,

2000). Smads proteins also regulate transcription both positively and negatively by selectively binding to co-activators and repressors. Co-activators include the pX oncoproteins of hepatitis B virus (pXHBV), p300/CBP, and p300- and CBP-associated factor (P/CAF), and repressors include histone deacetylase (HDAC), the homeodomain DNA-binding protein 5'TG'-interacting factor (TGIF), and the proto-oncogene products Sloan-Kettering avian retrovirus/ski-related novel gene (Ski /SnoN). Smads themselves have transcriptional activity (Massague and Wotton, 2000). The MH1 domain of Smad3 and Smad4 directly binds to the Smad-binding element (SBE) on DNA with low affinity. Due to this low affinity, Smads count on interactions with other transcription factors and regulators to target specific genes (Wrana, 2000).

B. Regulation of Smad signaling

Phosphorylation of the C-terminal serine residues (e.g. Ser465 and 467 in mouse Smad2) in R-Smads by the type I receptor is a crucial step in TGF-β signaling. The outcome of R-Smad phosphorylation is the dissociation of this protein from SARA and the receptor, and the formation of an oligomeric complex with Co-Smad, allowing the newly formed complex into nucleus (Moustakas et al., 2001). However, signaling through receptor tyrosine kinases (RTKs) also activates Smads (de Caestecker et al., 1998). Indeed, Smads have been known to be phosphorylated by other protein kinases including ERK1/2, CaMKII, PKC, MAP2K kinase 1 (MEKK1), stress-activated protein kinase/c-Jun NH_2-terminal kinase (SAPK/JNK), and probably more (Moustakas et al., 2001; Derynck and Zhang, 2003). For example, ERK2 phosphorylates serine residues in the linker region of R-Smads and

appears to inhibit nuclear accumulation of the Smad complex (Kretzschmar et al., 1997; Kretzschmar et al., 1999). Similarly, CaMKII phosphorylates R-Smads and Co-Smads in vitro, and inhibits TGF-β induced signaling pathways (Wicks et al., 2000). PKC phosphorylates the MH1 domains of R-Smads and negatively regulates transcription (Yakymovych et al., 2001). In contrast, MEKK1 and SAPK/JNK phosphorylate R-Smads, inducing their nuclear translocation and transcriptional activation (Brown et al., 1999; Engel et al., 1999). SAPK/JNK phosphorylates unknown sites outside the C-terminal SSXS motif. I-Smads are phosphorylated, not by type I receptor kinases, but by unknown kinases, but. However, the importance and roles of these phosphorylations are not fully understood (Pulaski et al., 2001).

The intensity and duration of TGF-β and Smad signaling are tightly regulated by diverse mechanisms. The rate of turnover of Smads can be controlled by ubiquitin-proteasomal mediated degradation. The E3 ubiquitin ligases, Smad ubiquitination regulatory factor 1 (Smurf1) and Smurf2, downregulate TGF-β mediated signaling by targeting R-Smads for degradation. Smurf1 binds to Smad1 and Smad5 to antagonize BMP responses, whereas Smurf2 interacts with diverse R-Smads. R-Smads that have been phosphorylated in the SSXS motif and imported into the nucleus also undergo ubiquitination probably after completion of their transcriptional roles. In addition to R-Smads Smurf1 and Smurf2 also have additional targets including the TGF-β receptor complex and the transcriptional repressor SnoN (Derynck and Zhang, 2003; Moustakas et al., 2001). E3 ligases other than Smurf1 and Smurf2 also mediate R-Smad downregulation. These include Itch E3 ligase and neural precursor cell expressed, developmentally down-

regulated 4-2 (NEDD4-2) (Bai et al., 2004; Kuratomi e al., 2004).

The fate of the TGF-β signaling pathway can be determined by subcellular compartmentalization through different internalization routes of the TGF-β receptor-Smad complex. For example, SARA and the adaptor protein disabled 2 (Dab2) bind both receptors and R-Smads, and they promote clathrin-dependent internalization into endosomes. This trafficking into endosomes may be required for efficient TGF-β signaling through Smads. By contrast, the receptor complexes also associate with caveolin in lipid rafts of the plasma membrane. The receptor complexes bound to I-Smad and Smurf can be internalized into caveolin-enriched vesicles for degradation by the ubiquitination pathway. The receptor invagination pathway may be important for control of the duration and intensity of Smad signaling (Derynck and Zhang, 2003; ten Dijke and Hill, 2004).

C. LC8/PIN (dynein light chain)

Two different streams of studies have converged on the highly conserved, small protein, the 8 KDa dynein light chain. Snyder's group identified an 89-amino acid protein from their yeast-based genetic screening with neuronal nitric oxide synthase (nNOS) as the bait. This protein originally appeared to inhibit the activity of nNOS, and thereby designated as protein inhibitor of nNOS (PIN) (Jaffrey and Snyder, 1996). PIN binds to N-terminal region of nNOS, but its inhibitory effects were later challenged with contradictory evidence (Rodriguez-Crespo et al., 1998; Hemmens et al., 1998). A separate line of efforts was directed towards uncovering the components of the dynein motor complexes. The analysis of the microtubule-associated motor protein complexes revealed the same protein, dynein

light chain of 8 KDa (LC8, also called DLC1 or DLC8), as a subunit of cytoplasmic and flagellar dynein (King and Patel-King, 1995).

There are three major classes of molecular motor complexes; these are kinesin, dynein, and myosin. The compositions and mechanisms of these cellular motors have been described in detail (Hirokawa, 1998; Karcher et al., 2002; Vale, 2003). Dynein is a super complex of about 1.2 MDa and consists of two heavy chains, and several intermediate, light intermediate and light chains (Figure 4-3A). This motor complex is primarily involved in the retrograde transport of membranous organelles and cargo-containing vesicular structures, such as endosomes. Currently, at least four dynein light chains have been identified; Tctex-1 and -2 (or Tctex-1 and rp3), LC8/PIN, and LC7/roadblock. They often form a homo- or heterodimer (King et al., 2002).

LC8/PIN is one of the most conserved proteins among evolutionarily distant species and its actual mass is 10 KDa. The solution structure showed that this protein is composed of one beta strand, two alpha helices, and four antiparallel beta strands (N- to C-terminus). An invariant residue Trp54 appears to be important for stabilizing the structure (Tochio et al., 1998). Later, a crystal structure bound to nNOS peptides suggested that LC8/PIN is actually dimeric and the binding site for peptide substrate is formed adjacent to the interface between two beta sheets (Figure 4-3B) (Liang et al., 1999).

Currently, the known cytoplasmic LC8/PIN-associated proteins include nNOS, IκBα, the proapoptotic member of Bcl-12 family Bim, Swallow, myosin V, a guanylate kinase domain-associated protein (GKAP), and the postsynaptic scaffolding protein gephyrin (Crepieux et al., 1997; Puthalakath et al., 1999; Schnorrer et al., 2000; Naisbitt et al., 2000;

A

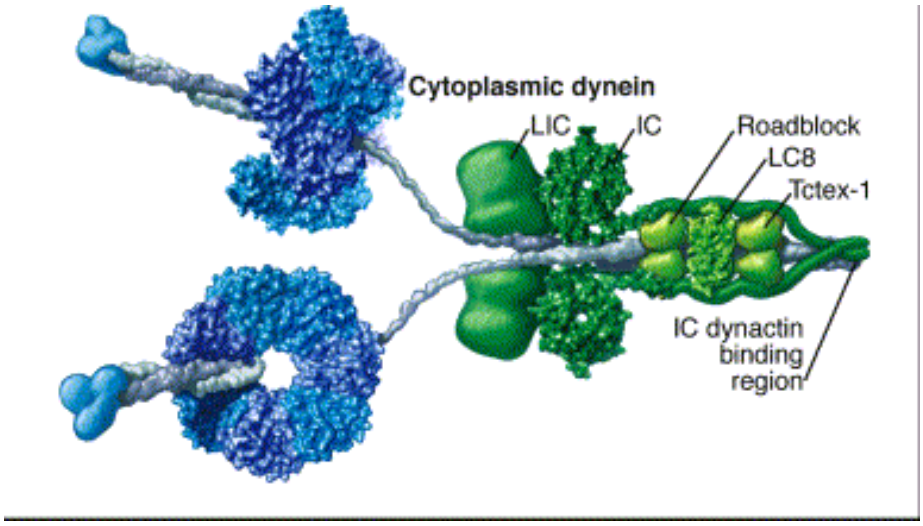

Vale, 2003

B

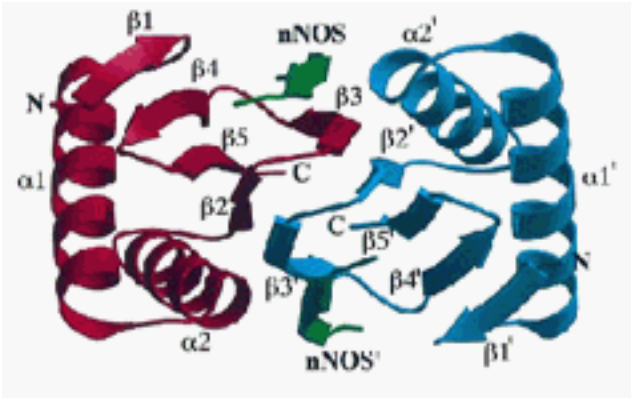

Liang et al., 1999

Figure 4-3. The dynein motor complex and structural organization of the LC8 dimer
A. The motor head of dynein is shown in mixed purple and blue shading to illustrate the distinct domains. The stalks extending from the ring bind to microtubules at their globular tips. Tightly associated motor subunits (intermediate chains (ICs), light intermediate chains (LICs), and light chains (LCs)) are shown in green. B. Crystal structure of LC8 dimer with two peptides derived from nNOS.

Espindola et al., 2000: Fuhrmann et al., 2002J). Interestingly, several viral proteins (mostly phosphoproteins) also interact with LC8/PIN, probably due to their association with the dynein motor complex during retrograde movement into nucleus (Jacob et al., 2000; Raux et al., 2000). Rodriguez-Crespo's group developed a library of overlapping dodecapeptides synthesized on a cellulose membrane (pepscan technique) and identified two putative consensus motifs, (K/R)*X*TQT and G(I/V)QVD, among most, if not all, known interacting proteins (Rodriguez-Crespo et al., 2001). However, it is still not clear how LC8/PIN is able to achieve its binding specificity among different and seemingly unrelated target proteins with significantly low sequence similarity.

To date, the physiological function of this small polypeptide is not well understood. In unicellular organisms, loss-of-function of LC8/PIN did not affect viability and only showed very limited phenotypes. By contrast, in fly, partial loss-of-function mutations of this protein caused morphological abnormalities in bristle and wing, female sterility, and defects in axonal projections during development. Moreover, LC8 null mutations resulted in embryonic lethality caused by massive apoptosis (Dick et al., 1996; Phillis et al., 1996). These observations suggest that LC8/PIN may play a significant role especially in multicellular organisms.

III. Materials and methods

Yeast two-hybrid screen

Yeast two-hybrid screens were performed as described in Chapter 3. From 10^6

yeast transformants screened with an inactive form of the WNK1 kinase domain (residues 216-494) as a bait, eight colonies were recovered whose insert interactions were confirmed by reintroducing isolated prey plasmids into bait-containing host strains. Smad2 cDNAs were encoded in two of the isolated positive candidates. LC8/PIN cDNAs were identified as multiple times (31 clones) with a bait containing an autoinhibitory domain plus a coiled-coil region (residues 481-660) from $3X10^6$ yeast transformants screened.

Subcloning and mutagenesis

Two-hybrid vectors of WNK1 and WNK4 were generated as described in Chapter 3. Mouse and frog Smad and Fast1 cDNAs (gift from J. Graff) were used as templates to create prey constructs containing full length and fragments of each isoform in pGADGH vector. For full length LC8/PIN, the original clones from screens were used since all of them contained the full length cDNA.

All of the bacterial and mammalian WNK vectors are as described in Chapter 3, except pCMV5- Myc-WNK1 (216-491) D368A (an inactive form) which was generated using the full length kinase dead WNK1 as a template. pGEX-KG-Smad2 full length, MH1, MH2, ΔMH1, and ΔMH2 (residues 1-467, 1-190, 241-467, 206-467, and 1-240, respectively) were generated by PCR-based subcloning using pCS-Smad2 full length as a template. The corresponding Smad2 clones in p3xFlag-CMV and pCMV5-Myc vectors were made similarly. pHis$_6$Parallel- and pRSETA-LC8/PIN (residues 1-89) were also generated in a similar manner.

Site-directed mutagenesis was done with the QuikChange kit (Stratagene) according to the manufacturer's instructions. All constructs and mutants were confirmed

by sequencing.

Expression of recombinant proteins, in vitro pulldown assays, and protein kinase assays

Expression of the recombinant proteins, in vitro pulldown assays, and kinase assays were as described in Chapter 3. For kinase assays, GST-Smad and His-LC8/PIN proteins were used at 0.6 – 1 μM and 3 μM, respectively.

Cell culture, immunoblotting, and immunoprecipitation

Maintenance, transfection, and lysis of HEK293, COS7L, DCT, or HeLa cells were as described in Chapter 3. HepG2 cells were grown in minimal essential medium (MEM) containing 10% FBS, 1 mM sodium pyruvate, and 0.1 mM nonessential amino acid. For immunoblotting Smad2 and LC8/PIN, 1:125 of an anti-Smad2 polyclonal antibody (Zymed), 1:500 of anti-Smad2/3 monoclonal antibody (BD Transduction), 1:500 of an anti-phosphoSmad2 (Ser465/467) antibody (Cell Signaling), 1:1000 of an anti-phosphoSmad2 antibody (Thr8) (Biosource), and 1:250 of an anti-PIN monoclonal antibody (BD Transduction) were used.

Human TGF-β was purchased from R&D Systems and reconstituted to 1 μg/ml in 4 mM HCl plus 0.05% BSA. Cells were treated with TGF-β for 30 min to 1 hr after serum starvation.

For subcellular nuclear and cytoplasmic fractionations, cells were washed twice with PBS , swollen in ice-cold hypotonic lysis buffer (10 mM Hepes, pH 7.9, 10 mM KCl, 1.5 mM $MgCl_2$, 0.5 mM dithiothreitol, 1 μg/ml leupeptin, 10 mM benzamidine, 1 μg/ml pepstatin A, 10.5 μg/ml aprotinin, and 1 mM phenylmethylsulfonyl fluoride), and broken using Dounce

homogenizer. Lysed cells were centrifuged at 228 g for 5 min, and the nuclear pellets were resuspended in 3 ml of 0.25 M sucrose and 10 mM $MgCl_2$, and layered over 3 ml of 0.35 M sucrose and 0.5 mM $MgCl_2$. Nuclei were collected by sedimentation at 1430 g for 5 min. The final pellets were resuspended in high salt buffer (hypotonic buffer plus 500 mM NaCl) or RIPA buffer (50 mM Tris, pH 8.0, 150 mM NaCl, 1% NP-40, 0.5% deoxycholate, and 0.1% SDS) with protease inhibitors.

IV. Results

A. The kinase domains of WNK1 and 4 interact with Smad2

Yeast-based screening of a neonatal mouse brain cDNA library with an inactive form of WNK1 kinase domain as the bait identified two clones encoding Smad2, a signal transducer in the TGF-β signaling pathway,. The Smad2 cDNAs originally isolated contained the intact MH2 domain, a linker region, and about one third of the MH1 domain. These clones showed reproducible binding to the WNK1 bait after being reintroduced into yeast. Furthermore, Smad2 is not found in the list of common false positives at “Interaction Trap At Work” (http://www.fccc.edu/research/labs/golemis/InteractionTrapInWork.html).

To verify the interaction between the WNK1 kinase domain and Smad2, I generated Smad2 full length, MH1, MH2, ΔMH1, ΔMH2, and linker region fragments in the prey vector. Pairwise yeast-two hybrid interaction tests showed that the MH2 domain is required for WNK1 binding to Smad2 (Figure 4-4). Interestingly, the kinase domain of WNK4 also bound to Smad2 in a similar manner, suggesting that this R-Smad may be a

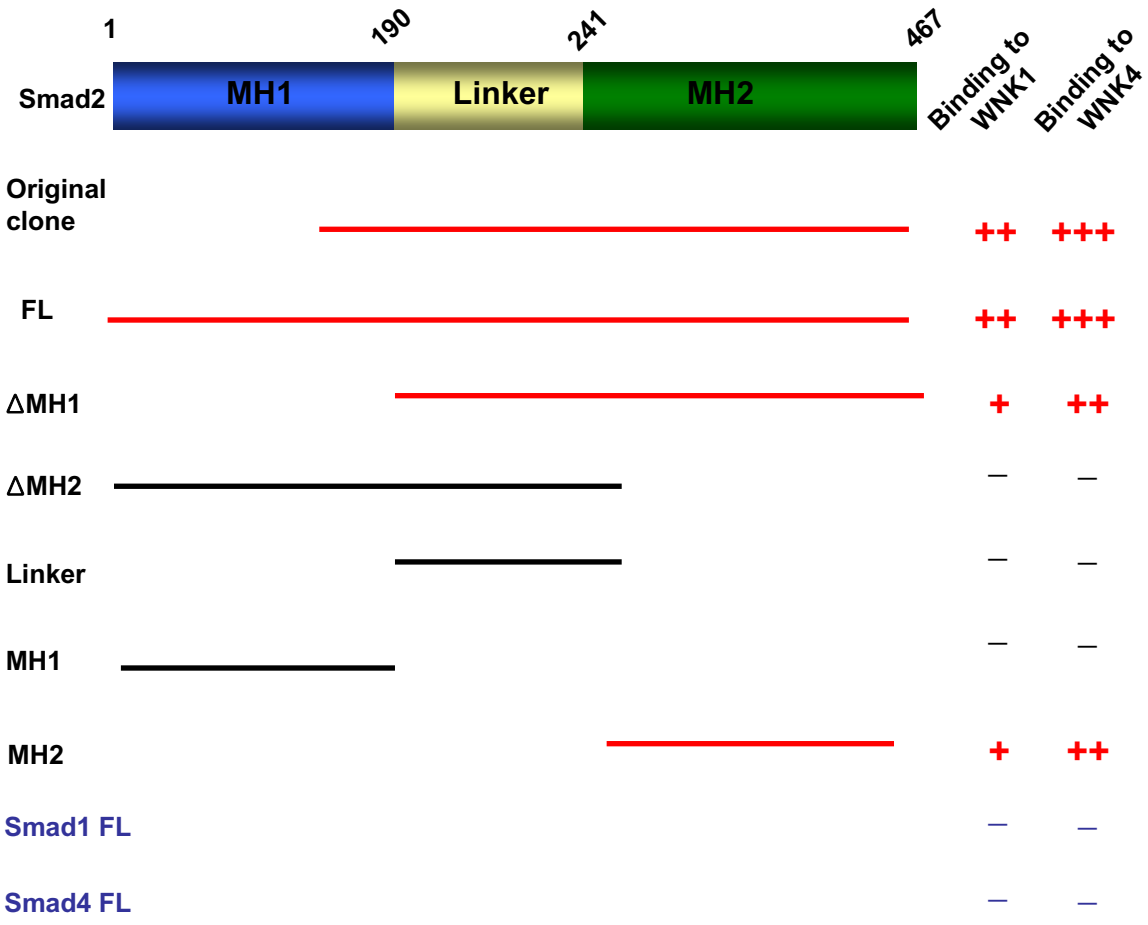

Figure 4-4. Mapping of the regions in Smad2 that bind to WNK1 and WNK4
Pairwise two hybrid tests of the interaction of the kinase domains of WNK1 and WNK4 with Smad2 fragments are indicated.

common player for both WNK1- and WNK4-mediated pathways. To exclude the possibility that Smad2 may nonspecifically bind to MAP4K level protein kinases, I tested the interaction of Smad2 with the protein kinases one thousand and one 2 (TAO2) and oxidative stress-responsive 1 (OSR1), which are Ste20p-related kinases, also used for yeast two-hybrid screening in the lab (M. Raman and M. Cobb, unpublished data; Chen et al., 2004). Neither of them displayed association with Smad2. In addition, another R-Smad, Smad1 and the Co-Smad, Smad4 did not bind to either WNK1 or WNK4, further supporting the specificity of the interactions of WNK1 and WNK4 with Smad2.

B. Both WNK1 and WNK4 phosphorylate Smad2

To determine whether Smad2 is a substrate for WNK1 and WNK4, I performed in vitro kinase assays with full length and truncated forms of GST-Smad2. All of the recombinant Smad2 proteins were phosphorylated by both WNK1 and WNK4. The results showed the most incorporation of phosphate into ΔMH2, among equally loaded protein samples (Figure 4-5A). Kinase assays with individual GST-Smad2 MH1 and MH2 also produced similar results in that the MH1 domain was more highly labeled than the MH2 domain (Figure 4-5B), suggesting that the MH1 fragment is a better substrate or may contain more phosphorylation sites than the MH2 domain. However, the phosphorylation of full length Smad2 was less than the sum of phosphate incorporations into the individual MH1 and MH2 domains. The poor phosphorylation of the full length protein is probably due to an autoinhibitory state of inactive Smad2 caused by intramolecular interactions between the MH1 and MH2 domains (Massague, 1998). It is not currently clear whether these

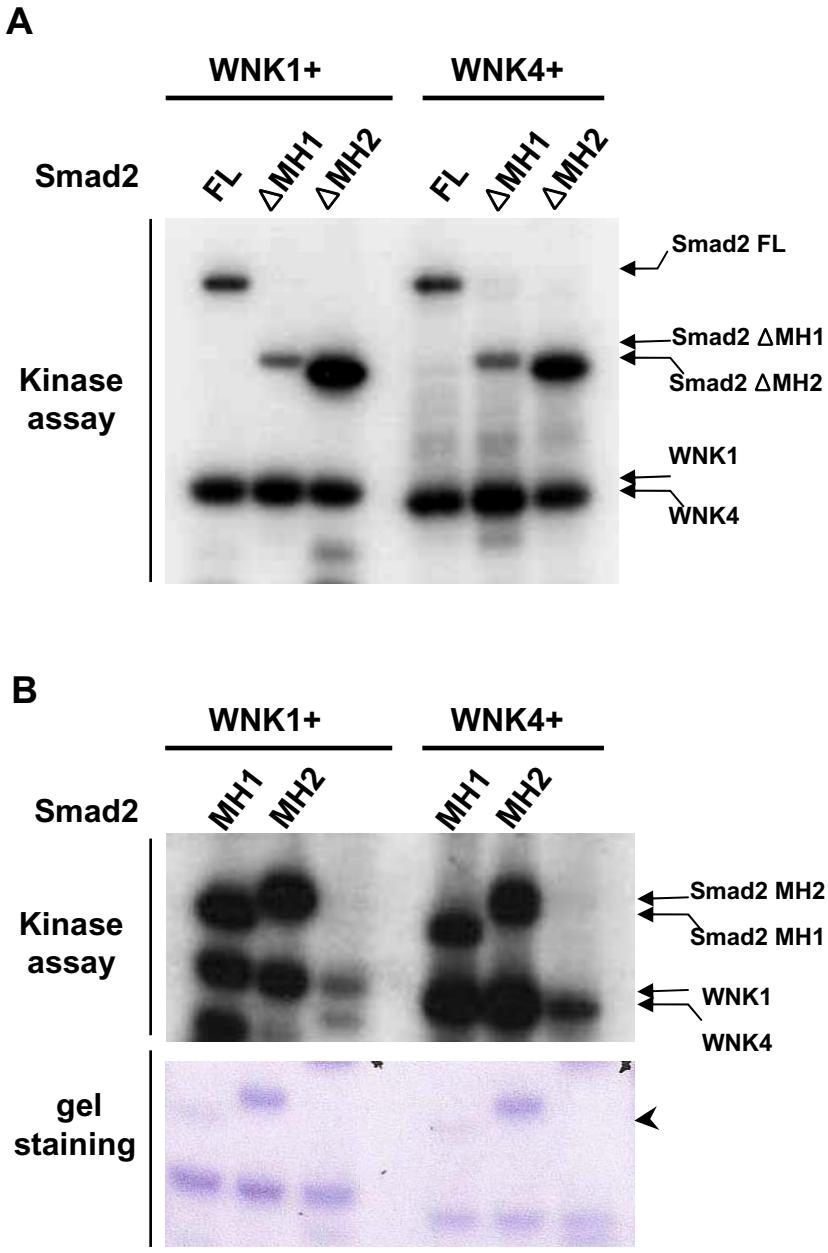

Figure 4-5. Phosphorylation of Smad2 by WNK1 and WNK4
A. GST-Smad2 full length, ΔMH1, and ΔMH2 were phosphorylated by WNK1 and resolved by SDS-PAGE for autoradiography. B. GST-Smad2 MH1 and MH2 were phosphorylated by WNK1. Note that significantly less amount of GST-Smad2 MH1 was used for kinase assay (arrow head), but showed comparable phosphate incorporation to GST-Smad2 MH2.

recombinant proteins behave in a manner similar to their physiological states in vivo. Interestingly, the anti-phosphoSmad2 (Ser465/467) antibody recognized the Smad2 MH2 domain phosphorylated by WNK1, but not by WNK4 (Figure 4-6). As noted above, phosphorylation of these two serine residues by the type I receptor is a critical event in the TGF-β signaling pathway. The full length Smad2 by the anti-phosphoSmad2 (S465/467) antibody following phosphorylation by WNK1 also showed significantly reduced signal intensity compared to the isolated MH2 domain (Figure 4-6, lane 2). This finding is consistent with the idea that poor phosphorylation on these key serine residues in the full length Smad2 by WNK1 partly explains the decreased phosphate incorporation in the kinase reaction in Figure 4-5. It is noteworthy that WNK4 did not phosphorylate these C-terminal serine residues, in spite of the comparable amount of Smad2 phosphorylation by WNK1 and WNK4 shown in Figure 4-5. Thus, the selectivity between WNK1 and WNK4 for Smad2, at this time, may be determined by the mode of phosphorylation of WNK protein kinases, not by binding specificity as in the case of Syt2 and WNK. Additionally, another antibody, anti-phosphoThr8, which detects the site on Smad2 phosphorylated by ERK, did not show any crossreactivity to Smad2 phosphorylated by WNK1 (data not shown). This suggests, not surprisingly, that WNK and ERK do not share conserved phosphorylation site motifs among their substrates. However, the significance of Smad2 phosphorylation by WNKs awaits further investigation.

C. WNK1 did not affect the activity or stability of Smad2 in cells under currently defined conditions

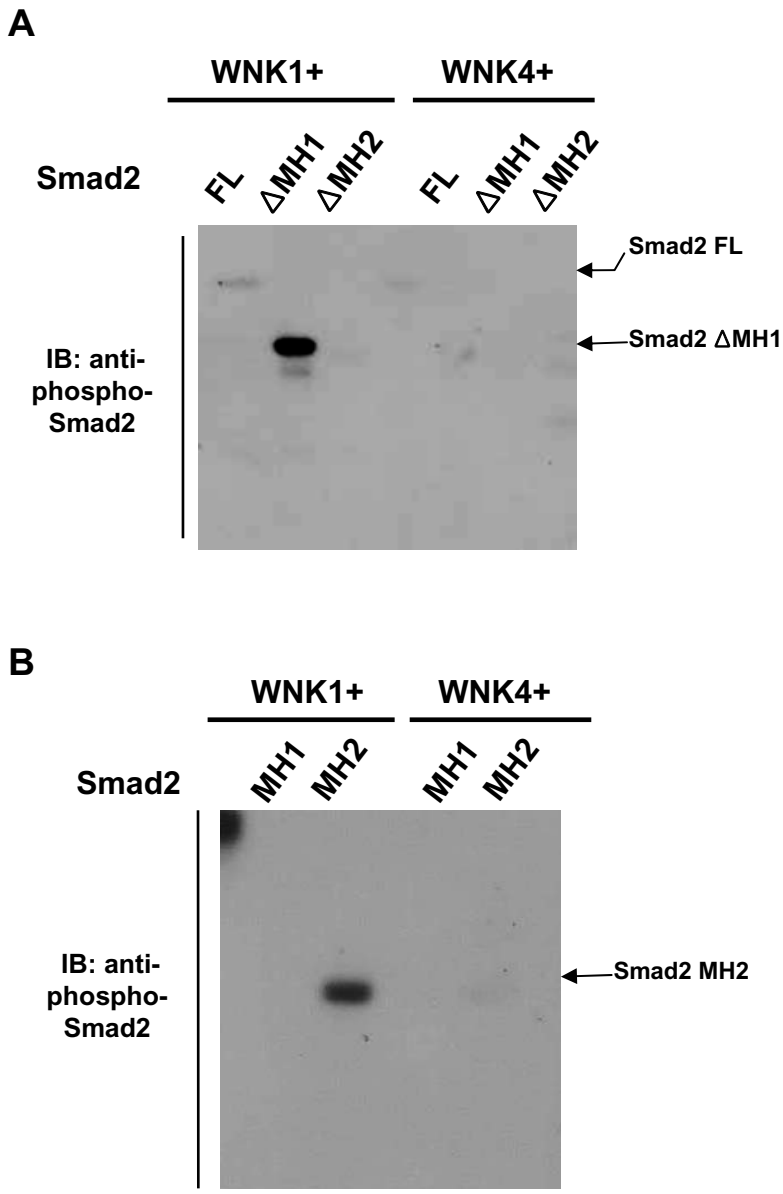

Figure 4-6. The selective phosphorylation of C-terminal serine residues on Smad2 by WNK1 relative to WNK4

A, B. GST-Smad2 full length, ΔMH1, ΔMH2, MH1, and MH2 were phosphorylated by WNK1 as described in Figure 4-5 and were used for immunoblotting by phospho-specific Smad2 (Ser465/467) antibody.

To further investigate the functional relationship between Smad2 and WNK1, we tested several cell lines by treating with TGF-β and also transiently expressing the WNK1 kinase domain. It is already known that endogenous WNK1 activity is not significantly changed by TGF-β treatment (L. Lenertz, unpublished data). Most of the cell lines I tested showed TGF-β responsiveness, and HepG2 cells were the best among them. HEK293 and COS7L cells responded relatively less (Figure 4-7A), but they were more efficiently transfected than other cell lines. The amount of endogenous phosphoSmad2 (Ser465/467) did not change by expressing WNK1, and TGF-β treatment of WNK1-transfected cells also did not alter the amount of phosphoSmad2 (Figure 4-7B). Additionally, WNK1 did not affect phosphorylation of the transfected Smad2 (data not shown).

My early data showed that when simultaneously cotransfected, WNK1 might decrease the total Smad2 protein. However, this decrease was not reproduced under different conditions, e.g. sequential transfection (data not shown). Furthermore, overexpression or knockdown of WNK1 did not change the amount of endogenous Smad2 in several cell lines tested (Figure 4-7B, C, and D). Thus, perhaps the effect of WNK1 on the stability of Smad2, if any, should be investigated under a wide variety of conditions. To examine whether the nuclear translocation of Smad2 can be promoted by WNK1, I subjected cells which had been cotransfected with WNK1 and Smad2 to subcellular fractionation. There was no obvious difference in the accumulation of Smad2 in the nucleus in the absence or presence of WNK1, in spite of the fact that WNK1 was able to phosphorylate the C-terminal serine residues of Smad2 in vitro (Figure 4-8). Under the conditions tested, we found no effect of WNK1 on the signaling properties of Smad2. Again,

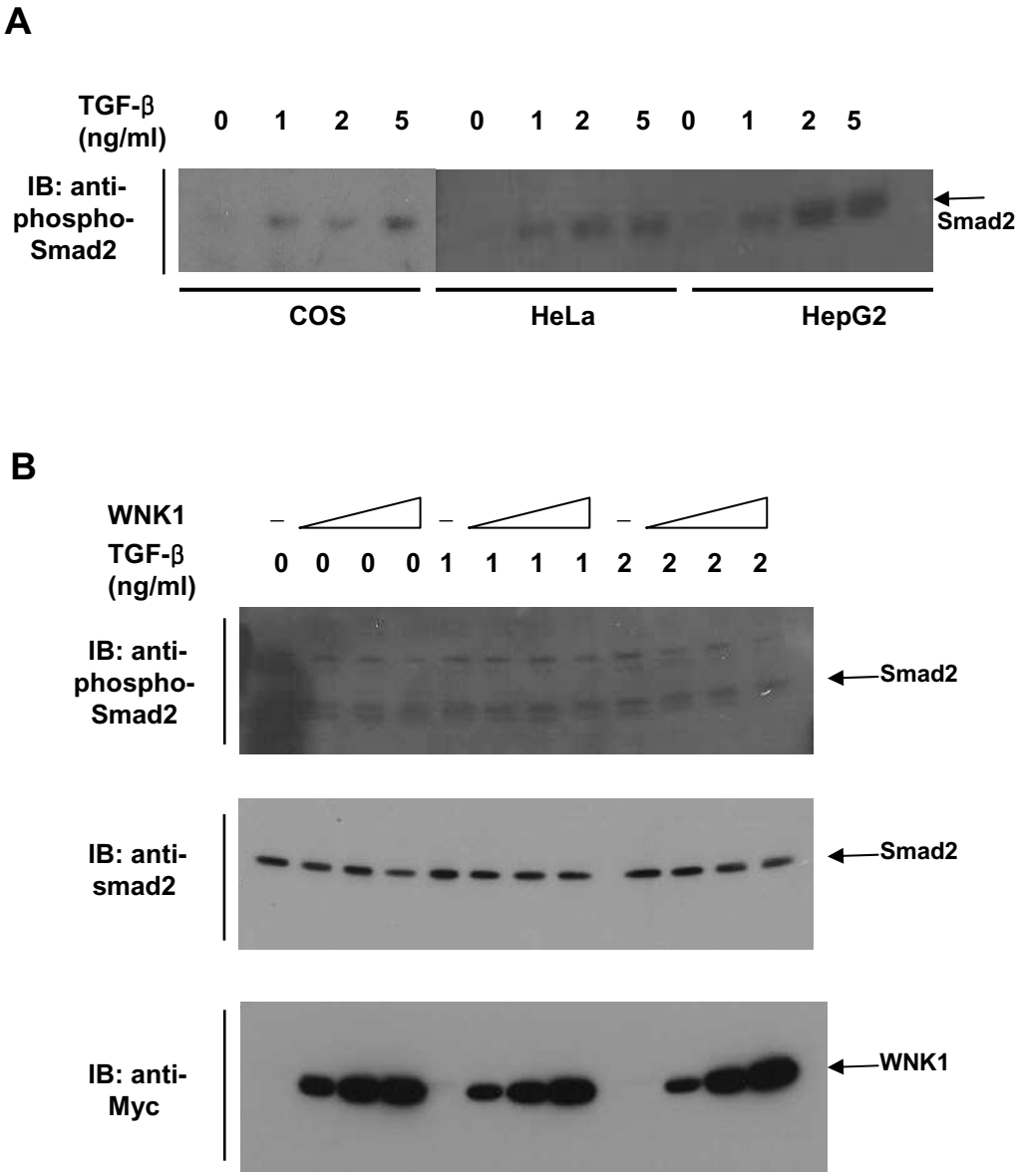

Figure 4-7. Effects of WNK1 on endogenous Smad2 protein level
A. COS, HeLa, and HepG2 cells were treated with TGF-β for 30 min and the cell lysates were immunoblotted by anti-phosphoSer465/467 Smad2 antibody. B. COS cells were transfected by sequential amount of Myc-WNK1 kinase domain DNA (0, 0.1, 0.2, and 0.5 μg) and, at the next day, were treated with TGF-β at the indicated concentrations for 30 min. COS cell lysates were immunoblotted with phospho-specific Smad2 (Ser465/467) (Top), anti-Smad2 (Middle), and anti-Myc (Bottom) antibodies. *–continued-*

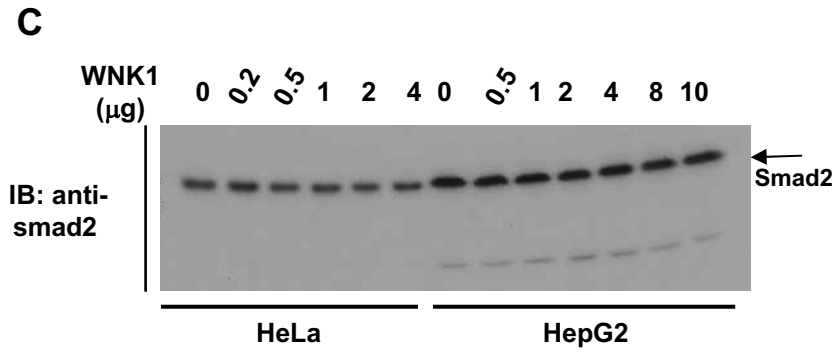

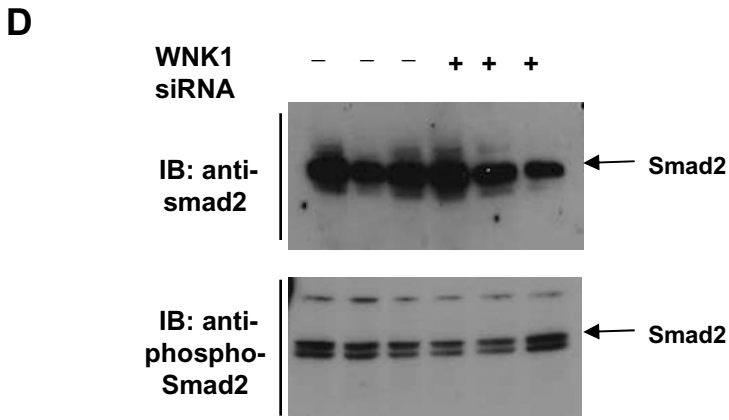

Figure 4-7. Effects of WNK1 on endogenous Smad2 protein level
C. HeLa and HepG2 cells were transfected with Myc-WNK1 kinase domain plasmids and were used for immunoblotting by anti-Smad2 antibody. D. 293 cells treated with WNK1 dsRNA were used for Western blots with phospho-specific Smad2 (Ser465/467) (Top) and anti-Smad2 (Middle) antibodies. The lysates were prepared and validated for WNK1 knockdown by BE. Xu.

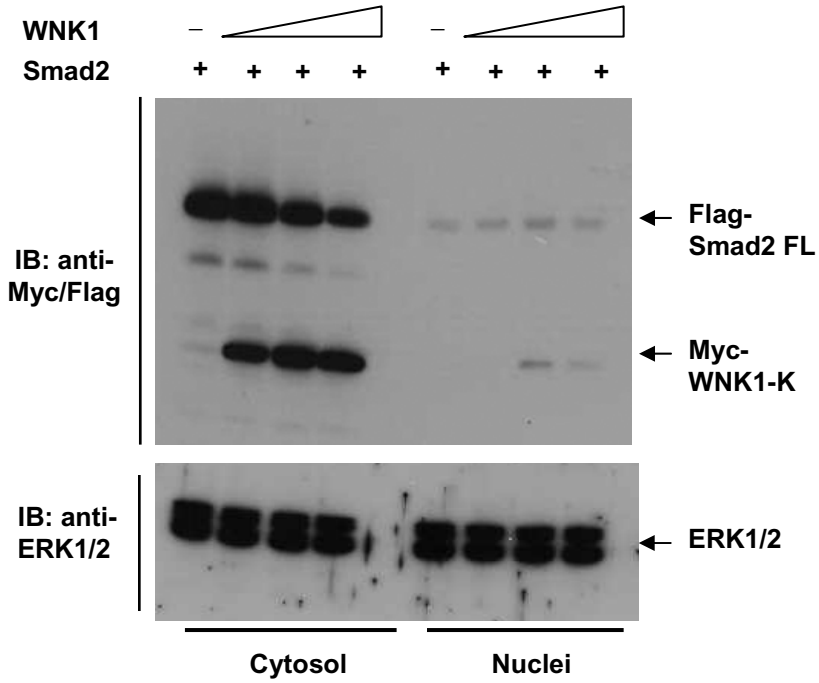

Figure 4-8. No change in Smad2 nuclear translocation caused by WNK1
COS cells were co-transfected with 1 μg of Flag-Smad2 full length and 0, 0.2, 0.5, and 1 μg of Myc-WNK1 kinase domain DNAs. The cell lysates were fractionated as described in Materials and methods, and each of cytosol and nuclei fractions was used for immunoblotting by anti-Flag/Myc (Top) and anti-ERK1/2 (Bottom) antibodies.

certainly more conditions need to be tested.

D. WNK1 binds to and phosphorylates LC8/PIN

I performed yeast two-hybrid screens of a mouse brain cDNA library with a WNK1 fragment containing an autoinhibitory domain plus a coiled-coil region (residues 481-660, hereafter called 1C) as the bait. From around $3X10^6$ yeast transformants screened, the WNK1 1C bait identified more than thirty positive clones containing LC8/PIN; all of them encoded the full length LC8/PIN protein (Figure 4-9A). When cotransformed with the 1C bait into yeast host strains, LC8/PIN clones showed reproducible binding to WNK1 1C, but not to the corresponding region of WNK4, suggesting that the interaction is WNK1-specific. Moreover, LC8/PIN is not in the list of common false positives at "Interaction Trap At Work" (http://www.fccc.edu/research/labs/golemis/InteractionTrapInWork.html).

To validate the interaction between WNK1 and LC8/PIN by a separate approach, I expressed and purified recombinant His_6-LC8/PIN proteins, and performed in vitro pulldown assays with full length GST-WNK1 and GST-WNK1 (490-640) along with GST alone as a negative control. As shown in Figure 4-9B, His_6-LC8/PIN bound to both GST-WNK1 full length and GST-WNK1 (490-640) in a dose-dependent manner, but not to GST.

Although the WNK1 kinase domain itself did not bind to LC8/PIN, I investigated if LC8/PIN is a substrate for WNK1 using in vitro kinase assays. The WNK1 kinase domain as well as WNK1 full length and WNK1 (193-610) phosphorylated LC8/PIN (Figure 4-10A). Surprisingly, the extension of the WNK1 kinase domain with 1C, that is, WNK1 (193-660), enhanced LC8/PIN phosphorylation over that by the WNK1 kinase domain alone (Figure 4-

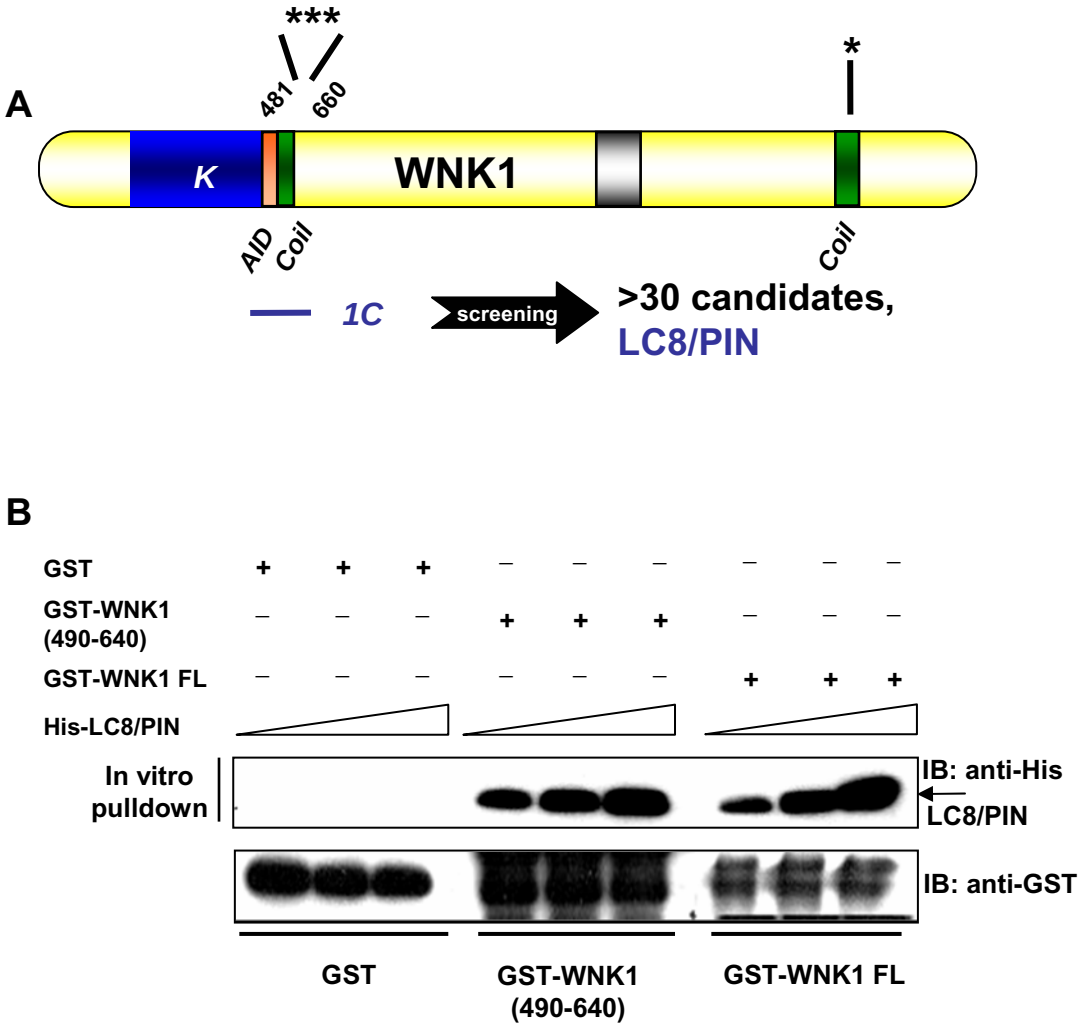

Figure 4-9. WNK1 interacts with LC8/PIN
A. Summary of the results of yeast two-hybrid screening with WNK1 1C bait. An autoinhibitory domain (AID) and coiled-coil regions (Coil) are depicted. The locations of the conserved residues mutated in WNK4 in PHAII patients were marked as asterisks. B. Immobilized GST, GST-WNK1 (490-640), or GST-WNK1 full length was incubated with His_6-LC8/PIN (0.5, 1, and 2 μg). The associated LC8/PIN proteins were immunoblotted with anti-His_6 antibody (Top). The membrane was stripped and reprobed with an anti-GST antibody (Bottom).

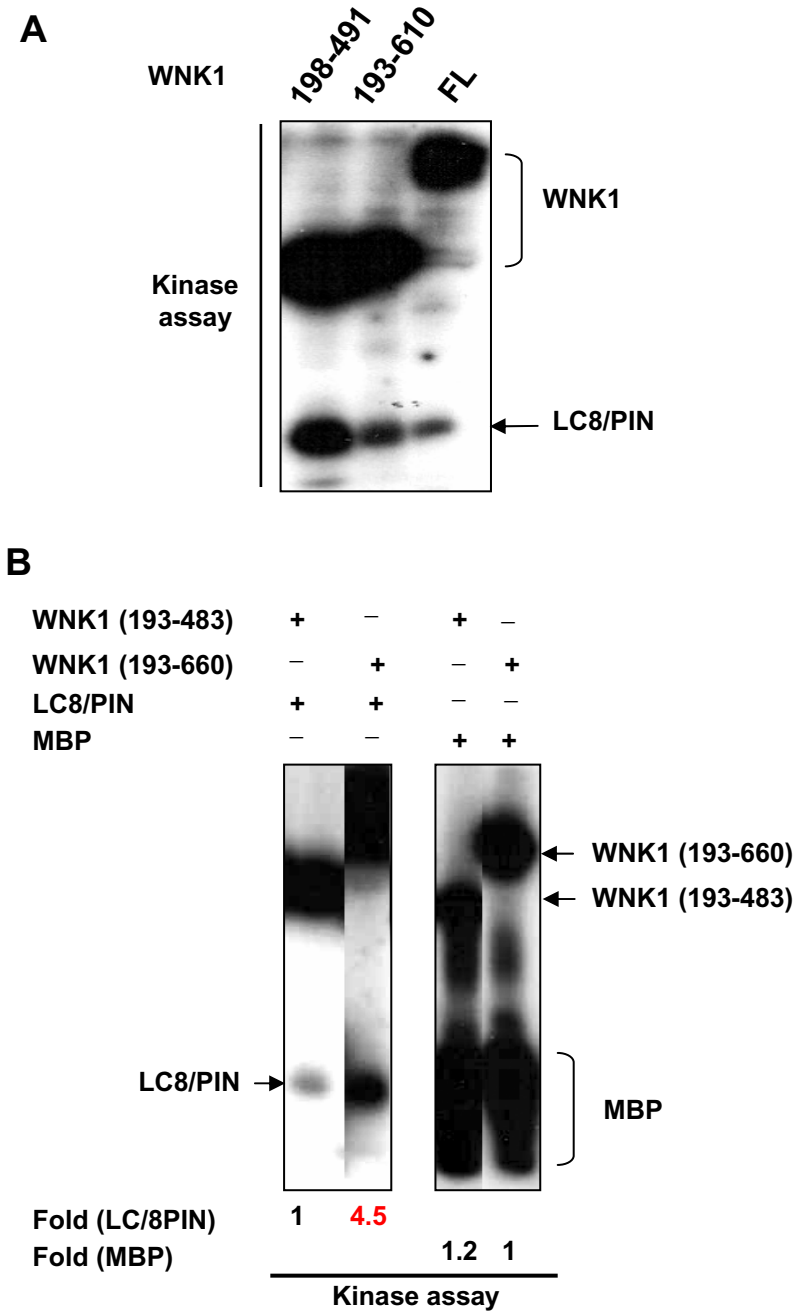

Figure 4-10. WNK1 phosphorylates LC8/PIN
A, B. Equal amount of proteins (each 1 μg) were used for the standard kinase assays, except 0.5 μg of GST-WNK1 full length (FL) was used. *–continued-*

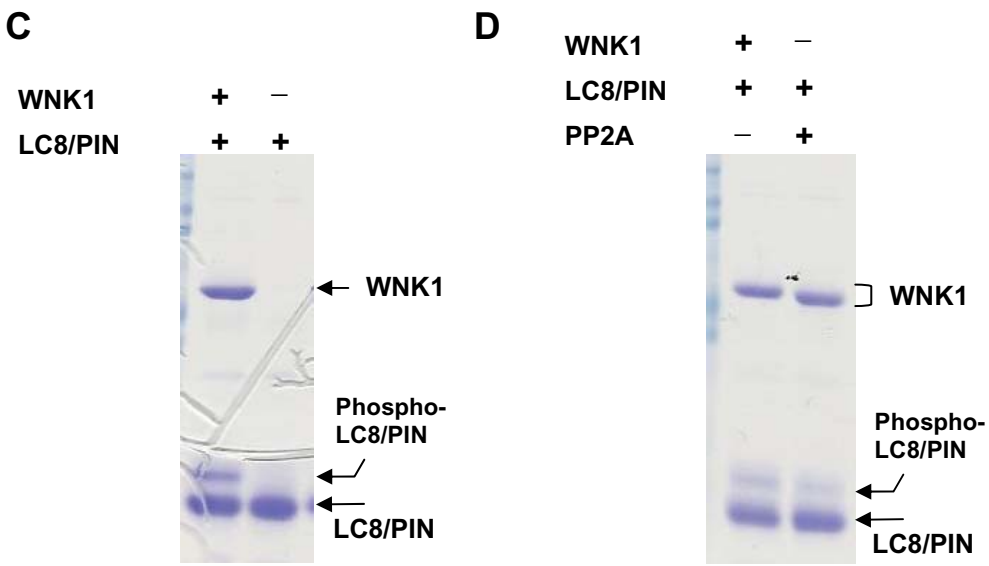

Figure 4-10. WNK1 phosphorylates LC8/PIN
C. Kinase assays were performed in the presence of 4 mM ATP for 12 hr to see the mobility shift of the phosphorylated LC8/PIN. 1 μg of WNK1 kinase domain (193-483) and 2 μg of LC8/PIN were used for the reactions. D. In vitro kinase assays were as described in Figure 4-10C and then PP2A was treated for 45 min.

10B). This was probably due to their interaction through the 1C region. Both WNK1 (193-483) and WNK1 (193-660) exhibited comparable activities toward MBP. I also examined the stoichiometry of LC8/PIN phosphorylation by WNK1 under incubation conditions of 4 mM ATP for around 12 hr at 30 ^{o}C. Generally 0.5 or less mol of phosphate was incorporated into mol of protein. Interestingly, phosphorylated LC8/PIN showed a mobility shift on the gel, and this shift was partially reversed to the normal form by treatment with PP2A, suggesting that the shift is due to phosphorylation (Figure 4-10C and D).

E. Mutation of Ala622 to Asp abolished WNK1 binding to LC8/PIN

The WNK1 1C bait contains an autoinhibitory domain and a coiled-coil region. Three out of four of the WNK4 mutations associated with hypertension were found within a short highly conserved segment near this coiled-coil region from PHAII patients (Wilson et al., 2001). The comparable residues in WNK1 are E634K, D636A, and Q637E (see Figure 2-6). Although all of the missense mutations were only identified in WNK4, the residues are all conserved among WNK isoforms. The fact that each of these mutations change the residue charge tempted me to investigate the possible relationship between the hypertension-causing mutations and WNK1-LC8/PIN binding. None of these mutations affected WNK1-LC8/PIN association; this was confirmed by both pairwise yeast-two hybrid interaction tests and in vitro pulldown assays (Figure 4-11). However, I found that a completely unexpected mutation, Ala622 to Asp, completely disrupted WNK1 binding to LC8/PIN (Figure 4-11). This alanine residue is not conserved among WNK isoforms, further suggesting that LC8/PIN may be a WNK1-specific interactor. The A622D mutation is not

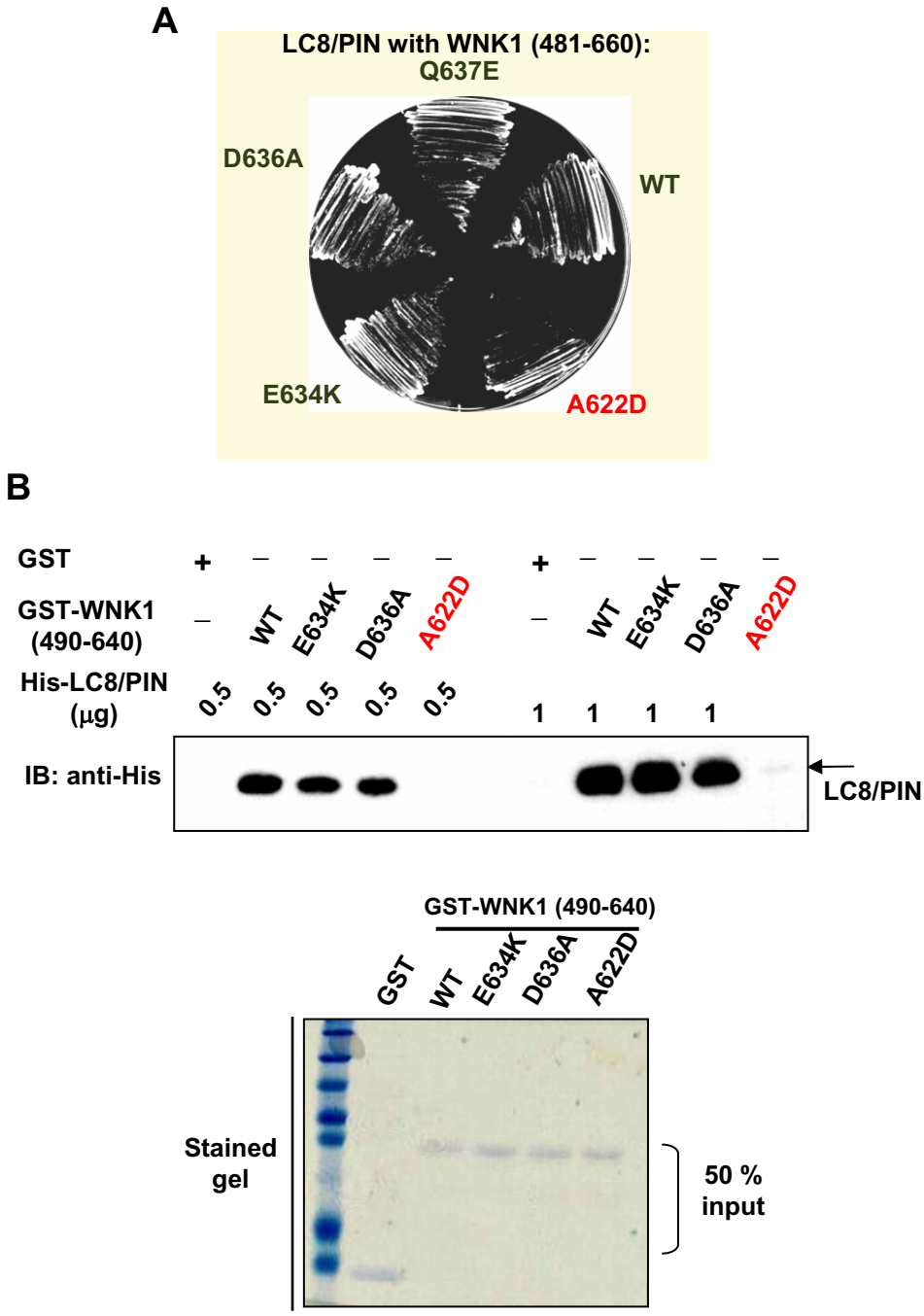

Figure 4-11. LC8/PIN binding to WNK1 and mutants
A. Pairwise two-hybrid tests of the interaction of LC8/PIN with WNK1 WT and mutants. B. In vitro pulldown assay. GST and GST-WNK1 (490-640) were used at 1 μg for the binding assay (Top). 50% (0.5 μg) of the inputs for binding assay were stained on the gel (Bottom).

likely to cause unwanted functional or conformational alterations of the WNK1 protein since this mutation did not have any effects on WNK1 interactions with other binding partners (further discussed in Chapter 5).

F. LC8/PIN may attenuate the autoinhibitory effects of WNK1 on substrates

Ala622 is in between the autoinhibitory domain and a coiled-coil region of WNK1. The location of this residue near the autoinhibitory domain and its importance for WNK1-LC8/PIN association raised a possibility that LC8/PIN may relieve the autoinhibitory state of WNK1 by binding in the vicinity of the autoinhibitory domain. Consistent with the previously characterized behavior of the autoinhibitory domain, WNK1 containing the autoinhibitory domain (residues 193-660) showed less phosphorylation of Syt2 compared to WNK1 kinase domain (residues 193-483) (Figure 4-12). Interestingly, the addition of LC8/PIN in the kinase reaction significantly enhanced the phosphorylation of Syt2 by WNK1 (193-660); increases ranged from 2- to 3-fold, depending upon the recombinant Syt2 protein used. This type of disinhibition caused by LC8/PIN should be further confirmed with other substrates.

V. Discussion

It is too preliminary to deduce a specific functional link between WNK1 and Smad2 or between WNK1 and LC8/PIN, due to limited data. The exact location and functional significance of phosphorylation sites should be determined for both of substrates. Our current state of knowledge offers no obvious insights into how these seemingly unrelated

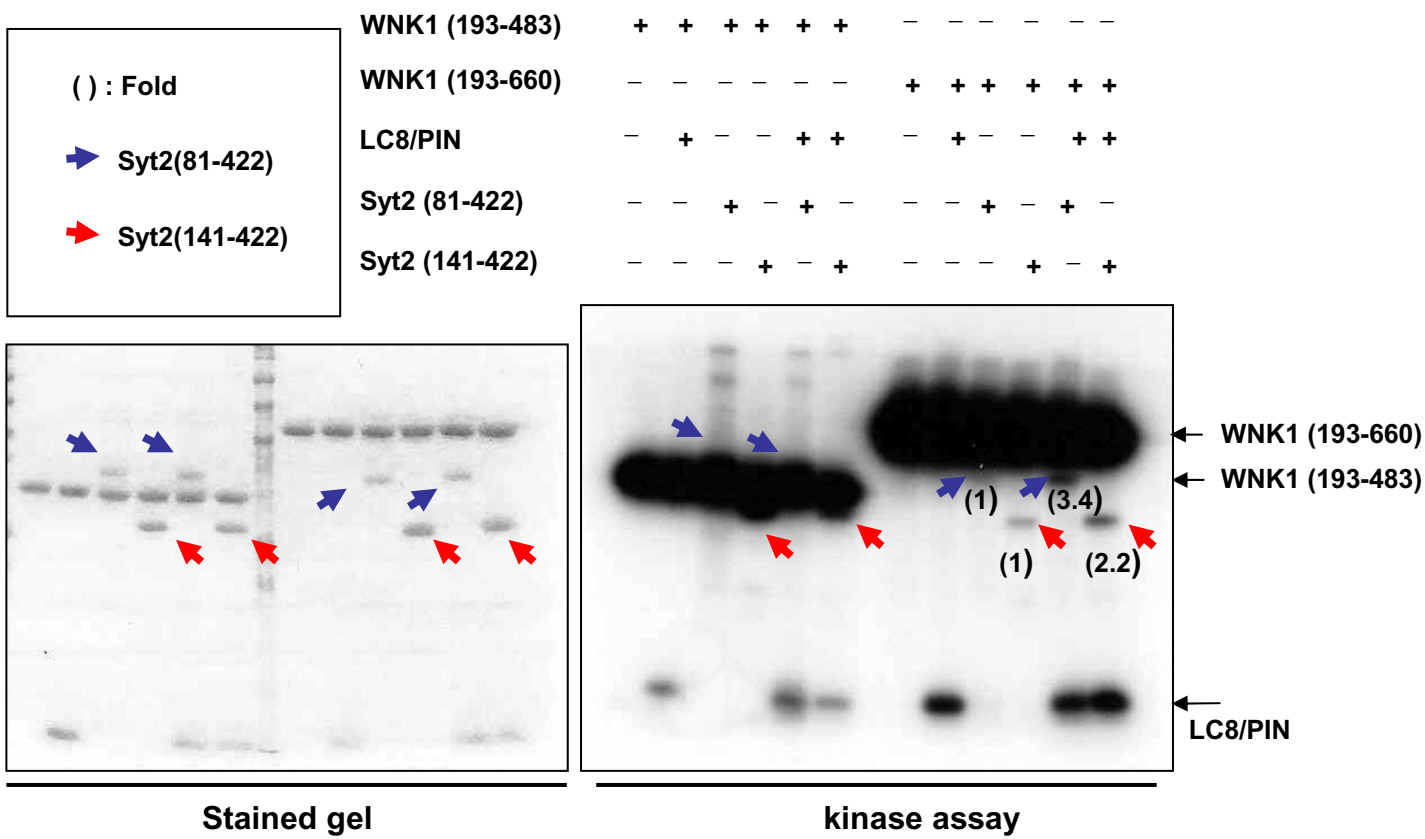

Figure 4-12. Attenuation of the autoinhibitory effects of WNK1 by LC8/PIN
The standard kinase assays were performed as described in Materials and methods. Syt2 (81-422) and (141-422) were used as the substrates for WNK1 (193-483) and (193-660) in the absence or presence of LC8/PIN. Phosphorylation of LC8/PIN was enhanced by WNK1 (193-660), probably due to its binding to 1C region and the presence of LC8/PIN increased the phosphorylation of Syt2 by WNK1 (193-660).

signaling pathways, as Smad2 in TGF-β signaling, LC8/PIN for retrograde trafficking, and WNK for blood pressure control, can be related to one another. Nonetheless, I reasoned that the consistent binding and reproducible phosphorylation of these substrates by WNK that I found may imply potentially critical signaling events that have yet to be identified.

A. WNK and Smad2

Smad2 is a signal mediator in one of the best known cytokine-induced pathways, the TGF-β signaling pathway. Based on the known observations, TGF-β activates other signaling cascades, including MAPK pathways, for example. Other stimuli, such as epidermal growth factor (EGF) or hepatocyte growth factor (HGF), can activate the Smad signaling pathway (Derynck and Zhang, 2003). These data suggest that there are substantial cross-connections among Smad-dependent and independent and TGF-β-dependent and independent pathways. In fact, phosphopeptide analyses of endogenous Smads revealed more than ten different phosphopeptides in addition to phosphopeptides containing the C-terminal phospho-serine residues whose phosphorylation is catalyzed by TβRI, implying roles for additional protein kinases in Smad signaling (Souchelnytskyi et al., 1997; Yakymovych et al., 2001). WNK1 may be one of these candidate kinases, although several other kinases have been reported to phosphorylate Smads in vitro or in vivo. Based on my data, WNK1 not only interacts with Smad2 through its MH2 domain, but also phosphorylates it on both MH1 and MH2 domains. Phosphorylation of both of these conserved domains may reflect as yet unknown regulatory mechanisms controlled by WNKs. Perhaps more surprising, WNK1, but not WNK4, phosphorylates the same key

residues phosphorylated by the type I receptor Ser/Thr protein kinases at least in vitro. The basis and significance of the apparent selectivity of WNK1 over WNK4, the settings in which WNK1 rather than the type I receptor might phosphorylate these sites, and the functional consequences of phosphorylation outside the C-terminus by WNK1 and WNK4 should be more investigated.

Regulation of the subcellular localization and compartmentalization of TβRI-Smad complex appears to be important for Smad signaling pathways. WNK1 might be involved in these types of events to regulate signaling intensity and duration of Smad signaling. For example, WNK1 binds to the MH2 domain of Smad2, and this domain is also the place where the mutually exclusive binding occurs among TβRI-Smad2-SARA and oligomeric Smad complexes upon TGF-β stimulation. Therefore, WNK1 binding to the MH2 domain and subsequent phosphorylation of both MH1 and MH2 domains may exert additional regulatory effects on the known spatiotemporal regulation. It is becoming clear that there are two distinct internalization routes for TβRI-Smad complexes that determine activation or inhibition of signaling (Di Guglielmo et al., 2003). However, the underlying mechanisms to determine the fates of these two different invagination events are not clear. As discussed in Chapter 3, WNK1 may act as a molecular switch to regulate membrane trafficking events for retention or retrieval of the plasma membrane proteins or possibly vesicles themselves by altering electrostatic properties of Syt proteins. Thus, WNK1 might participate in membrane events relevant to Smad signaling. Furthermore, WNK1 appears to regulate the ubiquitination-mediated downregulation of a specific type of membrane transporter by acting as an upstream inducer of NEDD4-2 phosphorylation (Xu et al., in revision). NEDD4-

2 is an E3 ligase recently reported to downregulate Smad2 (Kuratomi et al., 2004). I also identified a specific type of ubiquitin conjugation enzyme as a WNK1 interactor from yeast two-hybrid screening (see Table 3-2). All these possible connections that may influence Smad2 stability require further investigation.

Smads function early in vertebrate development. In animal cap explants from *Xenopus* embryos, Smad2 induces the expression of muscle actin (as a component of mesodermal induction), thus phenocopying the effects of activin (Graff et al., 1996). My preliminary animal cap experiments with fertilized *Xenopus* oocytes injected with the full length cRNAs of WNK1 and WNK4 in collaboration with E. Fortuno in J. Graff's group suggested that both WNK1 and WNK4 may turn on a subset of mesodermal markers, xBra and globin, among the markers tested; other markers that did not show any induction include xCA (mesodermal), xSox17α (early endodermal), goosecoid (late mesodermal), LFABP (endodermal), and NCAM (neural ectodermal) (see http://www.xenbase.org/WWW/Marker_pages/Marker_index.html for the details about the markers) (data not shown). EF-1α, an ectodermal housekeeping protein in animal cap, was used as a positive control. Additionally, injections of WNK1 or WNK4 into *Xenopus* embryos showed very heterogeneous (mixed) morphological defects during frog oocyte development, as well as accompanying growth defects and lethality before the tadpole stage (data not shown). Because these phenotypes could be due to spurious activities or overdose effects of WNKs, these studies need to be repeated with appropriate controls. Smad2-deficient mice die around E7.5 to E8.5 and display a failure in gastrulation, mesodermal formation, and egg cylinder elongation (Weinstein et al., 2000). It is noteworthy that WNK1 null mice

also showed embryonic lethality before day 13 of gestation (Zambrowicz et al., 2003). Indeed, WNK1 transcripts can be detected as early as the two-cell stage during animal development (http://www.ncbi.nlm.nih.gov/UniGene). As previously noted, the distribution of WNK1 is ubiquitous. These observations raise an interesting possibility that the fundamental function of WNK1 may be traced back to early organogenesis. Defects in blood pressure control by WNK dysregulation might be a subset of phenotypes or one of the subsidiary effects that WNK can impose. For example, we do not know whether secretion or production of hormones that are important for blood pressure control, such as angiotensin, can be regulated by WNK1 in extrarenal tissues. The failure of hormonal balance due to a loss of WNK1 outside the kidney might also affect renal functions.

Signaling from the TGF-β pathway plays an antiproliferative role in many cell types, and in that context the receptors and signal transducers act as tumor suppressors. Mutations in TβRII, for instance, account for approximately 10% of nonpolyposis colorectal cancers (de Caestecker et al., 2000; Hata et al., 1998). A number of mutations in Smad genes have been linked to cancer as well. Mutations are largely distributed in either MH1 or MH2 domains (especially, the MH2 domain) and include small deletions, nonsense or missense mutations, and frameshift mutations. Even though many mutations probably affect the folding or structural integrity of the proteins, or heteromeric Smad2-Smad4 binding, it is still conceivable that some of them might influence the interactions of Smads with other proteins. WNK might be one of the candidates. Interestingly, partial cDNAs of WNK1 and WNK2 were isolated from malignant prostate tissues and pancreatic cancer cells (Moore et al., 2000; Ito et al., 2001). However, any roles of WNK in tumorigenesis are

not yet known.

Recently, two groups reported interesting observations about the crosstalk between Akt/PKB and TGF-β pathways in determining cell fate - either cell death or cell survival (Remy et al., 2004; Conery et al., 2004). They suggested that Akt inhibits Smad3 by sequestering it and preventing TGF-β mediated phosphorylation leading to a cell survival pathway. Notably, this event was independent of Akt kinase activity and did not occur with Smad2. I speculate that there may be similar mechanisms for other Smads including Smad2. Interestingly, one study proposed that Akt phosphorylates WNK1 on a Thr site in its N-terminus (Vitari et al., 2004). Because this phosphorylation did not alter either the kinase activity or subcellular localization of WNK1, this event may affect other aspects of WNK1 behavior, like interaction with its molecular targets. In this regard, the effect of the N-terminus of WNK1 should be investigated on the binding of the kinase domain to one or more of its substrates.

B. WNK and LC8/PIN

LC8/PIN is one of the subunits of the cytoplasmic dynein holoenzyme. This protein has been implicated in a wide spectrum of interactions with many proteins, some of which reflect a role for LC8/PIN in cargo binding and others of which may implicate it in other functions. In particular, only a small fraction of the total pool of LC8/PIN is directly bound to dynein and the majority of this protein is present in the cytoplasm in a microtubule-independent manner (King et al., 1996). Furthermore, LC8/PIN also exists as a subunit for another motor protein, myosin V (Espindola et al., 2000). These observations led to the

notion that LC8/PIN may act as “multitasking player” or “molecular glue” in cells. Peptide library-based screening among known LC8/PIN interacting proteins resulted in identification of two potential consensus motifs, (K/R)XTQT and G(I/V)QVD (Rodriguez-Crespo et al., 2001). However, these motif sequences were not found within the WNK1 1C bait. In fact, these two consensus motifs do not account for all of the previously known interactors, such as IκBα and myosin V. Therefore, the diversity of binding partners of LC8/PIN, in spite of its relatively simple structural organization, makes it difficult to understand how this protein could achieve binding specificity among cargo and non-cargo molecules.

I identified LC8/PIN as a WNK1 interacting protein from yeast two-hybrid screens. WNK1 reproducibly bound to LC8/PIN in an in vitro pulldown assay. Certainly, the primary inference from this binding is that WNK1 is a cargo molecule for the retrograde transporter (dynein) or the actin-based organelle motor (myosin V). Proper trafficking and spatial localization of WNK1 may be significant for exerting its specific roles as a signaling mediator, because at least one function of WNK1 is the regulation of resident time of transporters and channels in apical or basolateral membranes in epithelial cells by altering the kinetics of membrane events. The association between WNK1 and LC8/PIN may bear resemblance to the interaction of Sunday driver (Syd) with a kinesin light chain. Syd was first genetically identified from mutant flies which showed a larval paralysis defect caused by impaired axonal transport (Bowman et al., 2000). Syd turned out to be one of the JIP family proteins, a neuronal-enriched scaffolding protein for SAPK/JNK modules, which was independently isolated from by two other groups (Ito et al., 1999; Kelkar et al., 2000). Subsequently, it was reasoned that Syd protein plays dual roles of a motor receptor and

also a scaffolding protein. Similarly, LC8/PIN probably may allow dynamic redistribution of WNK1 within specific subcellular compartments, where WNK1 may act as a docking platform for signal mediators and regulators as well as transducing signals on its own. As described earlier, WNK1 contains numerous potential protein-protein interaction modules and motifs; and, therefore, it is likely to function as a scaffolding protein.

LC8/PIN is among the most highly conserved proteins; this protein displays more than 90% sequence identity between *Chlamydomonas* and mammals. The small size, diverse target molecules, and remarkable sequence conservation of LC8/PIN suggest parallels with ubiquitin. Otherwise, the biological functions of LC8/PIN are just beginning to be understood. The extremely well conserved sequence of LC8/PIN may imply that this small protein has evolved not to tolerate mutational changes or structural deformations, since an alteration in LC8/PIN may cause many compensatory mutations in its multiple molecular target proteins. This assumption may also imply that post-translational regulatory mechanisms of LC8/PIN, if any, should be tightly controlled. Interestingly, WNK1 not only binds to but also phosphorylates LC8/PIN. These observations strongly suggest that WNK1 is just not a cargo molecule. Rather, WNK1 may also tightly regulate the trafficking of vesicular structures and membrane organelles by acting as a motor receptor. There has been no other evidence of post-translational regulation of LC8/PIN until most recently Kumar's group reported that LC8/PIN is a physiological substrate for p21-activated protein kinase 1 (PAK1) (Vadlamudi et al., 2004). They proposed that PAK1 associates with the LC8/PIN-BimL complex and phosphorylates both of them to regulate cell survival and cell death. BimL is a proapoptotic protein, and it was previously known that LC8/PIN can

relocalize BimL to an antiapoptotic protein Bcl-2 to turn on apoptotic signaling pathways (Puthalakath et al., 1999). Thus, Kumar's group suggested that PAK1 phosphorylation of LC8/PIN-BimL complexes prevents them from access to Bcl-2 and promotes cancerous phenotypes. WNK1 might be involved in this signaling pathway or also others by phosphorylating LC8/PIN. A potentially interesting link can be deduced from the discoveries by our group in which PAK1 was identified from yeast two-hybrid screening as a substrate for OSR1. OSR1 is a putative MAP4K of unknown function activated by osmotic stimuli (Chen et al., 2004). Subsequent studies demonstrated that OSR1 interacts with WNK1 through its conserved PF2 domain. WNK1 also phosphorylates OSR1 (A. Anselmo and M. Cobb, unpublished data). These observations suggest that WNK1, PAK1, and OSR1 may form a complex. Strikingly, the PF2 domain shares significant sequence homology with the WNK1 1C region (residues 481-660) where LC8/PIN binds, raising a testable hypothesis that LC8/PIN might also interact with OSR1 via its PF2 domain. All of these correlations probably suggest that the kinases form a signaling machinery core in which LC8/PIN plays a role as a common multifunctional protein and individual kinases act as a switch upon different inputs to regulate distinct cellular functions, such as cytoskeletal reorganization, differentiation, cell survival or apoptosis, and regulation of membrane transporters. Additionally, it was recently shown that the PAK1-LC8/PIN interaction initiates macropinocytosis (pinosome formations), which provides further evidence for potential implications for WNK1 in a PAK1-LC8/PIN pathway (Yang et al., 2004).

Chapter 5: WNK1 and Other Observations

I. Abstract

For a functional study in a whole organism, I cloned the genomic DNA and cDNA of the worm WNK1 orthologue based on its sequence in the worm database. A transgenic ceWNK1-green fluorescent protein (GFP) worm was generated to localize the site of WNK1 expression. WNK1 was detected in the H-shaped excretory cell and the hypodermal cells. RNA interference (RNAi) was used to observe the loss-of-function of ceWNK1. WNK1 double-strand RNA (dsRNA)-injected worms did not show any obvious phenotypes under a series of conditions.

Because it seemed likely that WNK1 formed a complex through protein-protein interactions, I performed gel filtration chromatography with cell lysates containing endogenous WNK1 or truncated forms of WNK1 that I expressed. Both endogenous and transiently expressed WNK1 eluted in earlier fractions than predicted from the calculated mass of each protein, suggesting that WNK1 does not exist in a monomeric state. Partially purified WNK1 proteins from gel filtration were subsequently immuno-enriched and purified to identify putatively co-immunoprecipitated associated proteins by mass spectrometry. A few proteins were identified and await further investigation.

I also examined whether WNK1 and WNK4 undergo homomeric or heteromeric interactions that might lead to complex formation. Pairwise yeast two-hybrid analysis was adopted to confirm the putative direct interactions between WNK1 and WNK1, WNK1 and WNK4, and WNK4 and WNK4. Interestingly, the WNK1 N-terminus (residues 1-222)

reproducibly bound to a region near and just C-terminal to the kinase domain of WNK1. Otherwise, there were no obvious homo- or heteromeric associations among the WNK pairs that I tested. Additionally, I did not observe any effects of WNK1 hypertension-causing mutants on WNK1 interactions with its binding partners such as Syt2, Smad2, WNK1 N-t, and LC8/PIN. One of the mutants (Q637E), however, appears to decrease the kinase activity.

II. Material and methods

Pairwise yeast two-hybrid interactions

Pairwise yeast two-hybrid analysis and Western blotting of bait and prey proteins were as described in Chapter 3.

Subcloning, RNA synthesis, and mutagenesis

Two-hybrid vectors of WNK1 and WNK4, and all of the bacterial and mammalian WNK vectors were generated as described in Chapter 3.

For creating worm WNK1-GFP, around 3 Kb of the promoter region plus 1.4 Kb of genomic DNA of ceWNK1 was introduced into the GFP vector pPD95.77 (gift from A. Fire). 1 to 10 ng/μl of pPD-ceWNK1 DNA along with 100 to 150 ng/μl of marker DNA pRF4 (rol-6 gene) was injected into wild type N_2 worms. To synthesize dsRNA for RNAi experiments, approximately 0.8 Kb of ceWNK1 cDNA from the 5'-terminus was first obtained by RT-PCR and subsequently subcloned into the pGEM-T Easy vector (Promega). pGEM-T Easy-ceWNK1 plasmids were used to produce sense and anti-sense RNAs with T7 and T3 RNA

polymerase, respectively, for later annealing into dsRNA. Injection of dsRNA was as described above but without marker construct.

Site-directed mutagenesis was performed with the QuikChange kit (Stratagene) according to the manufacturer's instructions. All constructs and mutants were confirmed by sequencing.

Cell culture, immunoblotting, and immunoprecipitation

Maintenance, transfection, lysis, immunoblotting, and immunoprecipitation of HEK293 and COS7L cells were as described in Chapter 3.

Gel filtration chromatography

COS or 293 cells were harvested in lysis buffer containing 20 mM Tris, pH 7.5, 150 mM KCl, 0.5% NP-40, 1 mM dithiothreitol, and protease inhibitors. Approximately 5 mg of the cleared lysates were fractionated on a Superose-6 gel filtration column (Amersham Pharmacia) which was pre-optimized with the HMW Gel Filtration Calibration Kit (Amersham Pharmacia). Each eluted fraction was analyzed for the presence of WNK1 protein by immunoblotting. The elution of the protein standards was determined by staining with Coomassie blue.

III. Results and discussion

A. Analysis in *C. elegans*

Based on the sequence homology of rat WNK1, I searched the worm database and identified a cosmid clone c46c2.1 that contains the WNK ortholog. Additionally, I also found

a single fly WNK ortholog (clone CG7177) in the Flybase. There were no descriptions about mutant phenotypes and no other isoforms were detected. Since only one WNK1 exists in *C. elegans*, I expected to see phenotypes by disrupting ceWNK1 gene expression. As a first step for a functional study in nematodes, I cloned a partial genomic DNA of the ceWNK1 gene to generate a WNK1-GFP transgene. Using a 3 Kb promoter fragment plus a 1.4 Kb gene fragment of ceWNK linked to GFP, the nematode WNK protein was localized primarily to H-shaped excretory cells and the external epithelia (hypdodermis). Some neuronal staining was also observed (Figure 5.1). Both larval and adult stages of animals showed strong GFP expression, but expression was not detected in embryonic stages. The excretory cell and hypodermal cells are important for animals to adapt to environmental stimuli and for electrolyte homeostasis. This localization pattern is consistent with the idea that WNK1 may function in ion balance. Similar observations were also made by Hope's group with different regions of ceWNK (http://bgypc086.leeds.ac.uk/).

To understand the potential roles of WNK1, the RNAi method was employed to create worm WNK1 loss-of-function phenotypes. I generated about 800 bps of dsRNA for injection into worm, which was prepared from the 5'-coding region of the ceWNK cDNA by in vitro transcription. The effectiveness of ceWNK dsRNA to reduce WNK expression was validated by its successful inhibition of expression of GFP when injected into ceWNK-GFP transgenic worms. However, worms injected with dsRNA to suppress ceWNK did not display any obvious developmental or behavioral phenotypes. Generally, the effects of RNAi, if any, become observable from 4 to 7 hrs after injection and decline after 27 to 40 hrs; normally the effects are not transmitted past F1 generation (Fire et al., 1998). Thus, I

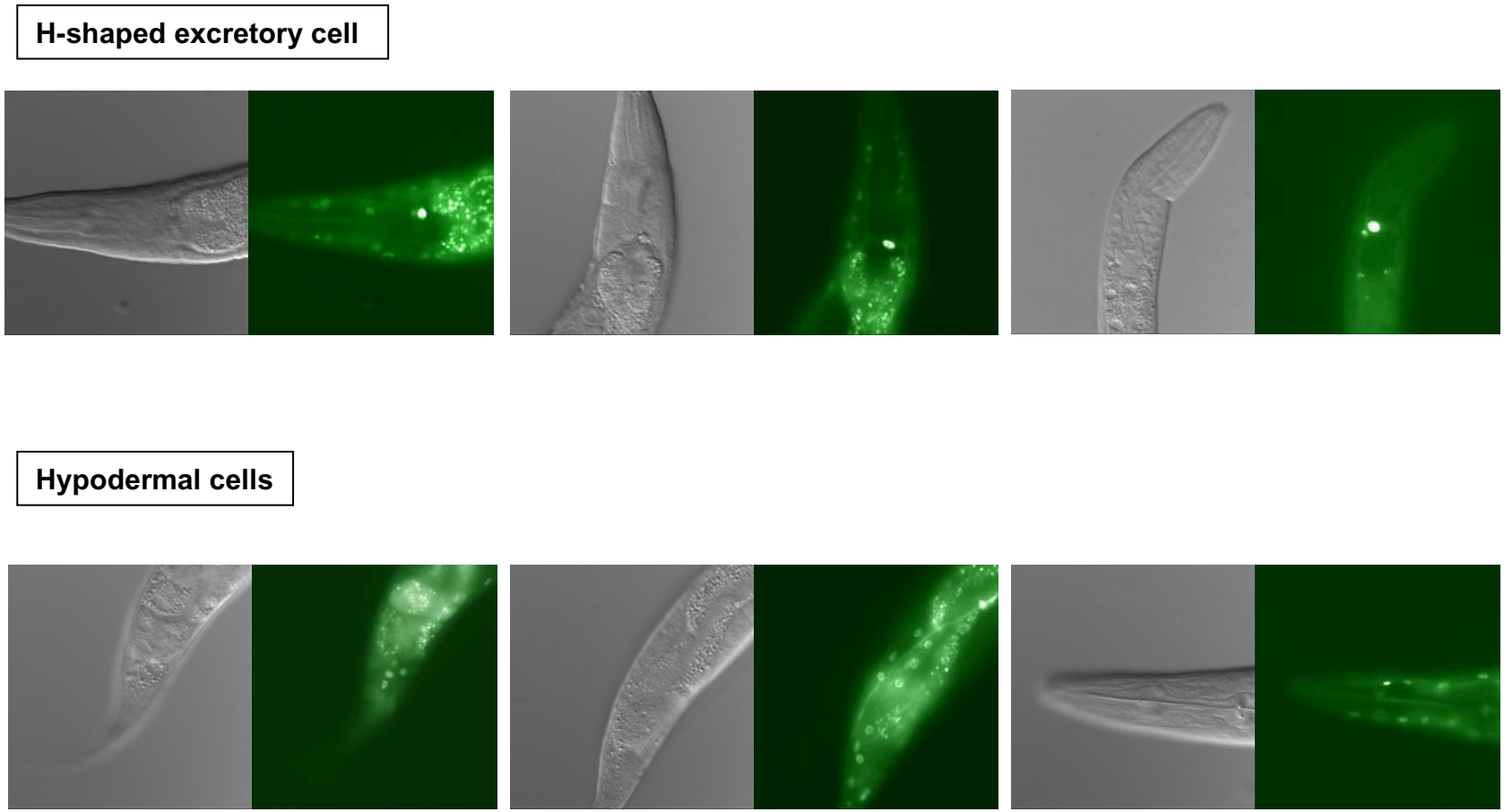

Figure 5-1. Expression of WNK1 in *C. elegans*
A 3 Kb ceWNK promoter plus 1.4 Kb WNK1 genomic DNA was fused to DNA encoding GFP. The construct was injected into nematodes. The localization of ceWNK1 was seen in the H-shaped excretory cell (Top) and hypodermal cells (Bottom).

first analyzed the morphological abnormalities of injected mothers and their F1 progeny, and also scored the brood size. Most of them were indistinguishable from their buffer-injected control counterparts. Only a few of worms showed morphological defects; these were hard to interpret due to their low penetrance and highly heterogeneity. I also tested the dsRNA-injected worms and their F1 progeny by challenging with osmotic stresses (8 M glycerol, 6 M sucrose, and 0.5 M high salt) and toxic materials (metal ions), but there was not any remarkable difference between control and dsRNA-injected worms. The worms injected with WNK dsRNA appeared to show only slight retardation of growth and hatching (data not shown). It is surprising that the knockdown of ceWNK did not produce any obvious phenotypic changes, because the worm has only one WNK ortholog and WNK1 loss-of-function in mouse resulted in embryonic lethality. The absence of defects might be due to the problem of dsRNA delivery. Many neuronal proteins in worms, for instance, are believed to be refractory to RNAi effects. This resistance problem is likely to be at least partly solved out by using currently available RNAi-sensitive strains. Intriguingly, the updated Wormbase reports showed that one study of RNAi for ceWNK1 displayed an egg laying defect (Egl) and slow growth (Gro), which is coincident with my earlier observation of subtle defects described above. However, the other four of RNAi analyses showed normal phenotypes (http://dev.wormbase.org/db/gene/gene?name=c46c2.1#Function). Additionally, ceWNK deletion mutants that we originally obtained from gene knockout consortium apparently possessed a gene duplication, and therefore could not be analyzed (http://celeganskoconsortium.omrf.org/).

B. Analysis by gel filtration

All of WNK isoforms are larger than 1200 amino acids in size and contain multiple potential protein-protein interaction modules including many PXXP SH3 binding motifs, coiled-coil domain, and locally conserved regions. This probably suggests that WNKs may act as a docking platform or scaffold that allows many signaling molecules as well as WNKs themselves to physically interact and functionally associate for specific signaling pathways. To understand the biochemical properties of WNK1 further, I performed gel filtration chromatography using a Superose-6 chromatography column which has a wide range of resolution. The source of WNK1 was mammalian cell lysates containing either endogenous WNK1 or transiently transfected WNK1 (1-1001) or (1-1193). The calibration of the column with size markers displayed a typical pattern of size exclusion in which blue dextran (2 MDa) appeared in the void volume and proteins eluted in consecutive order consistent with their masses (Figure 5-2A). Based on the estimation from these size standards and assuming all globular proteins, endogenous WNK1 eluted in fraction 12, placing it between the 2 MDa and 669 KDa standards. This clearly elutes earlier than would be predicted based on the calculated mass of WNK1 (around 225 KDa). Furthermore, the truncated forms of WNK1 (1-1193) and (1-1001) also eluted near or before 670 KDa, while they have molecular masses of 130 KDa and 110 KDa, respectively (Figure 5-2B), In contrast, the WNK1 kinase domain protein (residues 196-491) behaved in a manner expected based on its predicted mass (X. Min, unpublished data). These observations strongly suggest that WNK1 may form a complex through regions outside the kinase domain by oligomeric association or also possibly interaction with other molecules. The

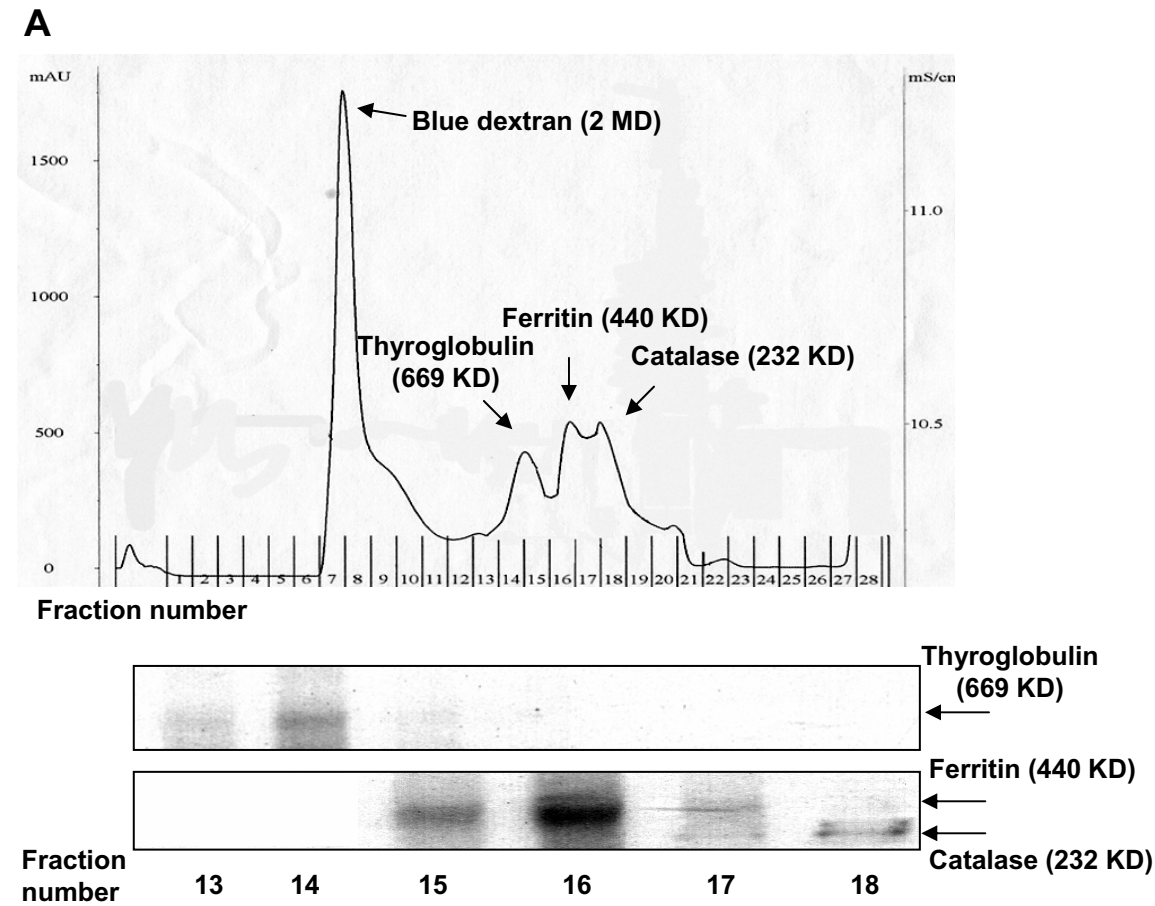

Figure 5-2. WNK1 does not exist as a monomer
A. Protein standards were fractionated (Top, chromatogram) and were stained by Coomassie blue (Bottom). B. COS or 293 cells were fractionated on a Superose-6 column. The fractions were immunoblotted to detect the WNK1 proteins. Myc-WNK1 (1-1193) and (1-1001) were also confirmed by immunoblotting with anti-Myc antibody (data not shown).

absence of detection of endogenous WNK1, WNK1 (1-1193) and (1-1001) in fractions corresponding to their monomeric sizes probably implies that WNK1 forms a complex stoichiometrically among themselves or with other interactors at any given time.

Based on the assumptions that WNK1 may act as a scaffold for other target molecules and regulators, I employed a proteomic approach to immunopurify the WNK1 complex to identify putative interacting proteins by mass spectrometry. Immuno-enrichment and subsequent immunoprecipitation with an anti-WNK1 antibody (Q256) and an anti-tag antibody partially purified WNK1-containing fractions from gel filtration. The precipitates displayed a number of candidate bands on silver stained gels, relative to pulldowns using mock transfected controls, preimmune serum or unrelated antibodies (Figure 5-3 and data not shown). Some of the proteins could not be recovered from the gel and therefore could not be analyzed, but a few proteins were identified. Notably, one of the immunoprecipitated proteins was a small piece of WNK1 itself. Assuming that this small piece does not arise from degradation during the purification, this small WNK1 may be an alternatively spliced form. As described earlier, WNK1 is post-transcriptionally regulated and exists as multiple spliced forms. Two groups reported that among the naturally existing forms of WNK1 is a short splice variant corresponding to the WNK1 N-termius, which terminates at exon 4 in kinase subdomain VII (Delaloy et al., 2003; O'Reilly et al., 2003).

C. Analysis by pairwise two-hybrid

Self-association of protein kinases is often important for their activities, regulation, and localization. Based on the previous observations, I investigated whether WNK1 and

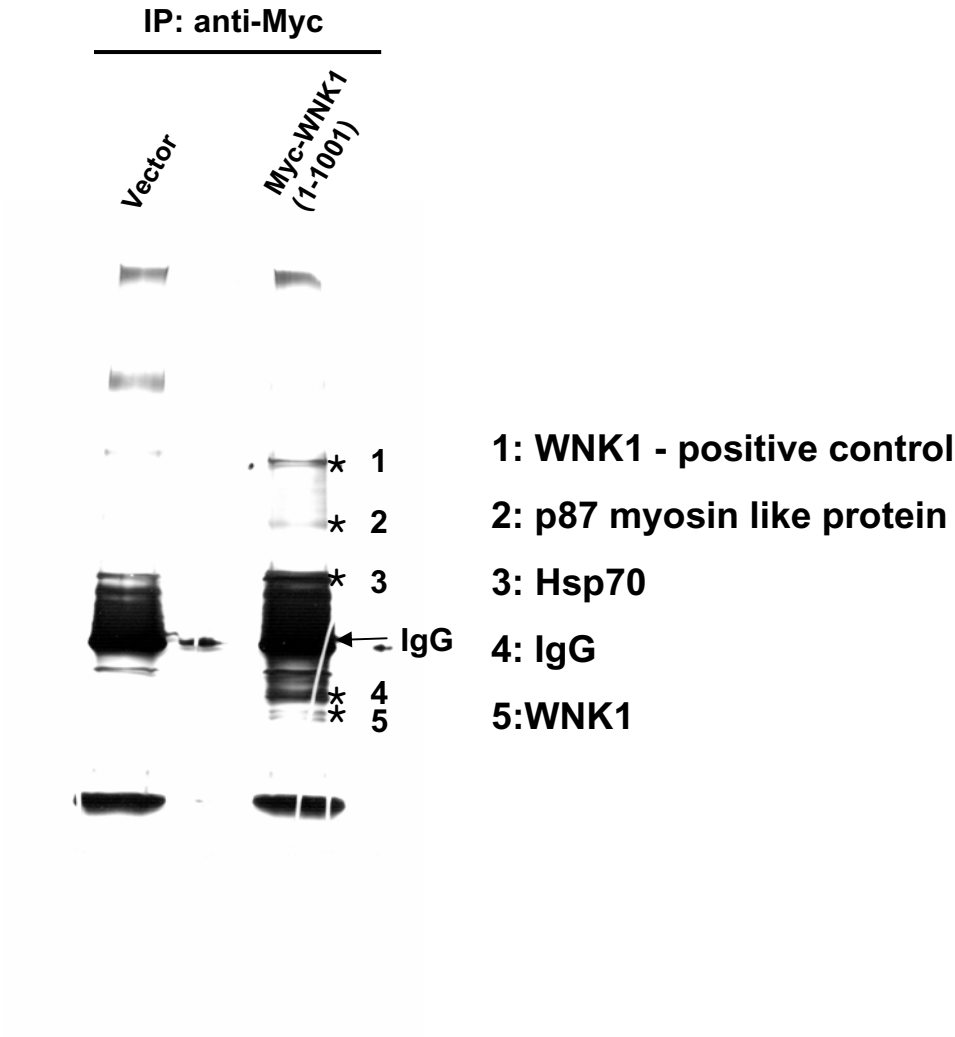

Figure 5-3. One representative silver-stained gel of the WNK1-associated proteins

Myc-WNK1 (1-1001)-containing fractions from gel filtration were combined and immunoprecipitated by anti-Myc antibody. The immunocomplex were resolved on a SDS-PAGE gel and subsequently silver-stained for mass spectrometric analysis.

WNK4 directly interact. Pairwise yeast two-hybrid interaction tests did not show interactions between WNK1 and WNK4 or of WNK4 with itself. The indicated combinations in Table 5-1 were tested. Since most of WNK4 fragments for the study are within the N-terminal half of the kinase (residues 1-748), binding may occur through more C-terminal residues of WNK4. In contrast, pairwise binding tests of WNK1 with itself suggested that the N-terminus of WNK1 (residues 1-222, hereafter called WNK1 N-t) interacts with WNK1 through a region just C-terminal to the kinase domain. This region contains an autoinhibitory domain and a coiled-coil segment (Table 5-2 and 5-3; Figure 5-4). This binding was further confirmed by switching WNK1 from bait to prey or prey to bait and retesting the repositioned pairs (see Table 5-3). Interestingly, this region is the site of LC8/PIN binding and also is a focal point of known regulatory mechanisms; autoinhibition and mutations in WNK4 causing hypertensions. The interaction of WNK1 N-t was not observed with WNK1 itself containing N-terminus, probably suggesting that intramolecular binding by the N-terminus prevents intermolecular binding of the protein. Interactions of the WNK1 N-t could be detected with fragments as long as 217-940, but longer forms of WNK1 (e.g. 217-2126) no longer bound to WNK1 N-t (Figure 5-4). Protein expression was not the cause of loss of binding (A. Anselmo, personal observation). Based on the data, I speculate that WNK1 appears to be under the influence of multiple intra- and intermolecular interactions (Figure 5-5). A certain region between 940 and the C-terminus of WNK1 probably participates in another intramolecular (and also possibly intermolecular) interaction with the WNK1 1C (residues 481-660) (see Figure 5-5). Maybe part of answer is suggested by the recent discovery by our group that the PF2 domain of OSR1 pulled down WNK1 as an interactor (A. Anselmo

Bait	Prey	Result	Comment
WNK4 1C (431-584)	WNK1 N-t (1-222)	++	Bait autoactivating
	WNK1 K-2 (217-494)	++	Bait autoactivating
	WNK1 1C (481-660)	++	Bait autoactivating
WNK1 N-t (1-222)	WNK4 1C (431-584)	-	
WNK1 K-1 (151-494)		-	
WNK1 K-2 (217-494)		-	
WNK1 K-2 (217-494, K233M)		-	
WNK1 1C (481-660)		-	
WNK1 K-2-1C (217-660)		-	
WNK1 (217-940)		-	
WNK1 (571-810)		-	
WNK1 (931-1313)		-	
WNK1 (1311-1542)		-	
WNK1 (1541-1812)		-	
WNK1 2C (1811-1910)		-	
WNK4 K (158-444)		-	
WNK4 K (158-444)	WNK1 N-t (1-222)	-	
	WNK1 K-2 (217-494)	-	
	WNK1 (1-1910)	-	
WNK1 N-t (1-222)	WNK4 K (158-444)	-	
WNK1 K-1 (151-494)		-	
WNK1 K-1 (151-494, K233M)		-	
WNK1 K-2 (217-494)		-	
WNK1 K-2 (217-494, K233M)		-	
WNK1 1C (481-660)		-	
WNK1 K-2-1C (217-660)		-	
WNK1 (217-940)		-	
WNK4 K (158-444)		-	
WNK1 N-t (1-222)	WNK4 N-t (13-171)	-	
WNK1 1C (481-660)		-	
WNK1 K-2-1C (217-660)		-	
WNK4 (431-748)	WNK1 N-t (1-222)	-	
	WNK1 K-2 (217-494)	-	
	WNK1 1C (481-660)	-	
	WNK1 (481-2126)	-	
WNK4 1C (441-600)	WNK1 N-t (1-222)	++	Bait autoactivating
	WNK1 K-2 (217-494)	++	Bait autoactivating
	WNK1 1C (481-660)	++	Bait autoactivating
	WNK1 (481-2126)	++	Bait autoactivating
WNK1 (217-2126)	WNK4 N-t (13-171)	-	
	WNK4 K (158-444)	-	
	WNK4 1C (431-584)	-	

Table 5-1. Pairwise yeast two-hybrid interactions between WNK1 and WNK4 and between WNK4 and WNK4

Bait	Prey	Result	Comment
WNK1 K-2 (217-494)	WNK1 K-2 (217-494)	-	
WNK1 K-1 (151-494)		-	
WNK1 1C (481-660)		-	
WNK1 K-2 (217-494)	WNK1 1C (481-660)	-	
WNK1 K-1 (151-494)		-	
WNK1 K-2-1C (217-660)	WNK1 K-2-1C (217-660)	-	
	WNK1 K-1-1C (151-660)	-	
WNK1 K-1-1C (151-660)	WNK1 K-2-1C (217-660)	-	
	WNK1 K-1-1C (151-660)	-	
WNK1 (571-810)	WNK1 (1-800)	-	
WNK1 (815-932)		+	Bait autoactivating
WNK1 (931-1313)		-	
WNK1 (1311-1542)		-	
WNK1 (1541-1812)		-	
WNK1 (1-800)		-	
WNK1 (1-1200)		-	
WNK1 K-2 (217-494)		-	
WNK1 K-1 (151-494)		-	
WNK1 K-2 (217-494, K233M)		-	
WNK1 K-1 (151-494, K233M)		-	
WNK1 K-2-1C (217-660)		-	
WNK1 K-1-1C (151-660)		-	
WNK1 1C (481-660)		-	
WNK1 2C (1811-1910)		-	
WNK1 C-t (2031-2126)		+	Bait autoactivating
WNK1 (571-810)	WNK1 (1-1200)	-	
WNK1 (815-932)		+	Bait autoactivating
WNK1 (931-1313)		-	
WNK1 (1311-1542)		-	
WNK1 (1541-1812)		-	
WNK1 (1-800)		-	
WNK1 (1-1200)		-	
WNK1 K-2 (217-494)		-	
WNK1 K-1 (151-494)		-	
WNK1 K-2 (217-494, K233M)		-	
WNK1 K-1 (151-494, K233M)		-	
WNK1 K-2-1C (217-660)		-	
WNK1 K-1-1C (151-660)		-	
WNK1 1C (481-660)		-	
WNK1 2C (1811-1910)		-	
WNK1 C-t (2031-2126)		+	Bait autoactivating

Table 5-2. Pairwise yeast two-hybrid interactions between WNK1 and WNK1 *–continued-*

Bait	Prey	Result	Comment
WNK1 (571-810)	WNK1 K-2-1C (217-660)	-	
WNK1 (815-932)		+	Bait autoactivating
WNK1 (931-1313)		-	
WNK1 (1311-1542)		-	
WNK1 (1541-1812)		-	
WNK1 (1-800)		-	
WNK1 (1-1200)		-	
WNK1 K-2 (217-494)		-	
WNK1 K-1 (151-494)		-	
WNK1 K-2 (217-494, K233M)		-	
WNK1 K-1 (151-494, K233M)		-	
WNK1 K-2-1C (217-660)		-	
WNK1 K-1-1C (151-660)		-	
WNK1 1C (481-660)		-	
WNK1 2C (1811-1910)		-	
WNK1 C-t (2031-2126)		+	Bait autoactivating
WNK1 (571-810)	WNK1 K-1-1C (151-660)	-	
WNK1 (815-932)		+	Bait autoactivating
WNK1 (931-1313)		-	
WNK1 (1311-1542)		-	
WNK1 (1541-1812)		-	
WNK1 (1-800)		-	
WNK1 (1-1200)		-	
WNK1 K-2 (217-494)		-	
WNK1 K-1 (151-494)		-	
WNK1 K-2 (217-494, K233M)		-	
WNK1 K-1 (151-494, K233M)		-	
WNK1 K-2-1C (217-660)		-	
WNK1 K-1-1C (151-660)		-	
WNK1 1C (481-660)		-	
WNK1 2C (1811-1910)		-	
WNK1 C-t (2031-2126)		+	Bait autoactivating

Table 5-2. Pairwise yeast two-hybrid interactions between WNK1 and WNK1

Bait	Prey	Result	Comment
WNK1 N-t (1-222)	WNK1 (1-800)	-	
	WNK1 (1-1200)	-	
	WNK1 N-t (1-222)	-	
	WNK1 K-2 (217-494)	-	
	WNK1 (217-590)	-	
	WNK1 K-2-1C (217-660)	++	Real
	WNK1 K-1-1C (151-660)	++	Real
	WNK1 1C (481-660)	+	Real
	WNK1 (151-2126)	-	
	WNK1 (217-2126)	-	
	WNK1 (481-2126)	-	
	WNK1 (571-2126)	-	
	WNK1 (1-480)	-	
	WNK1 (1-660)	-	
	WNK1 (1-940)	-	
	WNK1 (1-1313)	-	
	WNK1 (1-1542)	-	
	WNK1 (1-1812)	-	
	WNK1 (1-1910)	-	
WNK1 K-2-1C (217-660)	WNK1 N-t (1-222)	++	Real
WNK1 1C (481-660)		+	Real
WNK1 (217-590)		-	
WNK1 (1-590)		-	
WNK1 (217-810)		+	Real
WNK1 (217-940)		+	Real
WNK1 (217-2126)		-	

Table 5-3. Pairwise yeast two-hybrid interactions between WNK1 and the WNK1 N-terminal region (residues 1-222)

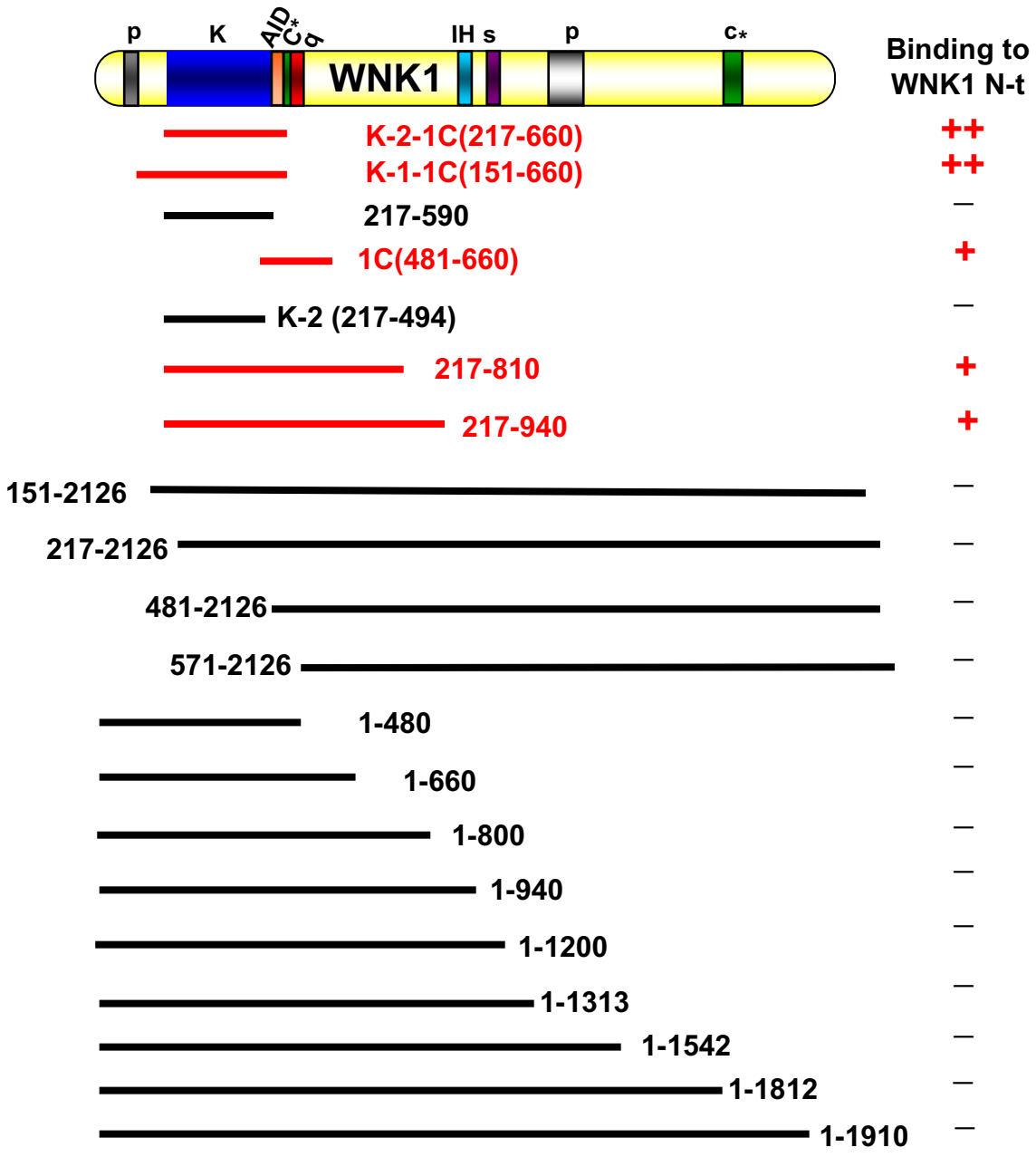

Figure 5-4. Schematic representation of the self assembly of WNK1 proteins
See the text for the details.

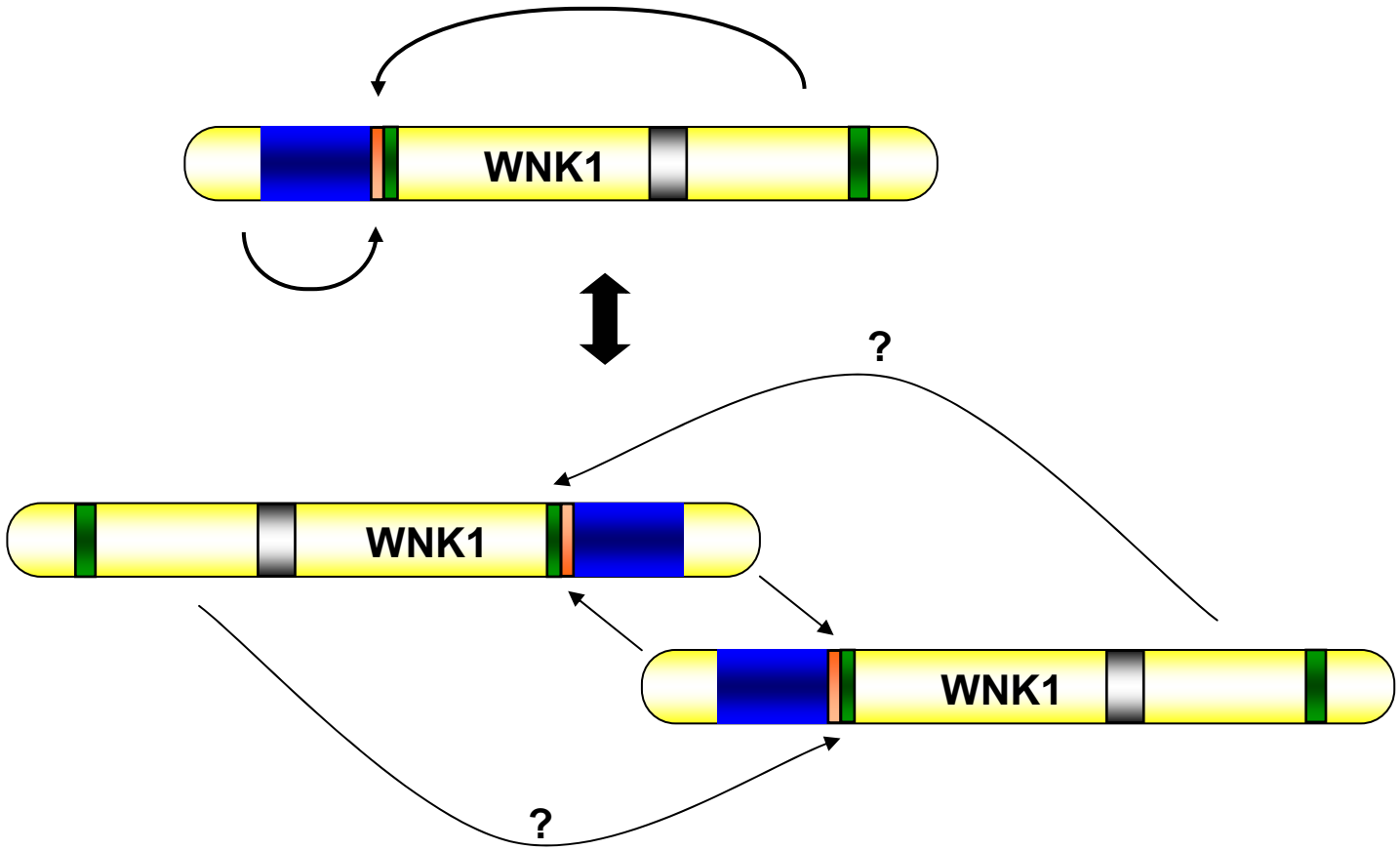

Figure 5-5. Current models concerning intermolecular and intramolecular interactions of WNK1
In this model, WNK1 N-t and 1C may bind each other for intramolecular interaction (Top). However, the same regions may also mediate intermolecular interactions among WNK1 proteins (Bottom). These interactions may be interwoven with other interactions with a certain region of C-terminus of WNK1 or also possibly with different molecules such as LC8/PIN and OSR1. See the text for discussion.

and M. Cobb, unpublished data). Interestingly, the PF2 domain binds to a specific C-terminal region of WNK1 (residues 1680-1833). An iterative PSI-BLAST search showed sequence homology between the PF2 domain and a segment within WNK1 1C region. These data hint that WNK1 (1680-1833) is also able to bind WNK1 1C. Because I cannot exclude the possibility that WNK1 (217-2126) did not fold properly, I may need to examine other truncated forms along with positive binding controls. These yeast-based interaction data further support the idea of self-association of WNK1 gathered from gel filtration experiments.

D. Analysis of hypertension-causing mutations

The previously noted, hypertension-causing mutations of WNK4 are found in a highly conserved segment near the coiled-coil domain, and the mutated residues are conserved among WNK isoforms. All four of them cause the change of residue charge (see Figure 2-6), and their conversion might result in loss of interaction with their binding partners. To investigate whether these hypertension-causing mutations affect the interactions of WNK1 with its binding partners, I tested Syt2, Smad2, WNK1 N-t, and LC8/PIN with WNK1 1C by yeast two-hybrid interaction; the binding results with LC8/PIN were described in Chapter 4 (see Figure 4-11). The results showed that WNK1 binding to its interactors is not detectably altered by the hypertension-causing mutations (Table 5-4 and data not shown). Other possible consequences of the hypertension mutations are a gain of interactions with unwanted protein molecules (or enhancement of binding affinity of weak interactors) or altered kinase activities of WNKs. The former possibility has yet to be

Bait	Prey	Result	Comment
WNK1 1C (481-660)WT	WNK1 N-t (1-222)	+	Real
WNK1 1C (481-660)EK		+	Real
WNK1 1C (481-660)DA		+	Real
WNK1 1C (481-660)QE		+	Real
WNK1 1C (481-660)AD		+	Real
WNK1 K-2-1C (217-660)WT	WNK1 N-t (1-222)	++	Real
WNK1 K-2-1C (217-660)EK		++	Real
WNK1 K-2-1C (217-660)DA		++	Real
WNK1 K-2-1C (217-660)QE		++	Bait autoactivating
WNK1 K-2-1C (217-660)AD		++	Real

Bait	Prey	Result	Comment
WNK1 K-2-1C (217-660)WT	WNK4 N-t (13-171)	-	
WNK1 K-2-1C (217-660)EK		-	
WNK1 K-2-1C (217-660)DA		-	
WNK1 K-2-1C (217-660)QE		+	Bait autoactivating
WNK1 K-2-1C (217-660)WT	WNK4 K (158-444)	-	
WNK1 K-2-1C (217-660)EK		-	
WNK1 K-2-1C (217-660)DA		-	
WNK1 K-2-1C (217-660)QE		+	Bait autoactivating
WNK1 K-2-1C (217-660)WT	WNK4 1C (431-584)	-	
WNK1 K-2-1C (217-660)EK		-	
WNK1 K-2-1C (217-660)DA		-	
WNK1 K-2-1C (217-660)QE		+	Bait autoactivating

Table 5-4. Pairwise yeast two-hybrid interactions between WNK1 or 4 and hypertension-causing mutants of WNK1

investigated. To test the latter possibility, I expressed WNK1 WT and hypertension mutant proteins and characterized their protein kinase activities. As shown in Figure 5-6A, GST-WNK1 (1-640) Q637E showed reduced WNK1 autophosphorylation, while E634K and D636A displayed activities almost comparable to WT. The reduced activity of WNK1 Q637E was further confirmed by in vitro kinase assay with a distinct WNK1 fragment, WNK1 (193-660) Q637E (Figure 5-6B). However, the hypertension-causing mutants were originally found in WNK4, not WNK1, in spite of the sequence conservation of the residues. Therefore, it should be investigated whether the Q to E mutation generally attenuates the kinase activities of all WNK isoforms. In addition, more biochemical and genetic studies need to be done to understand the roles of other hypertension mutants.

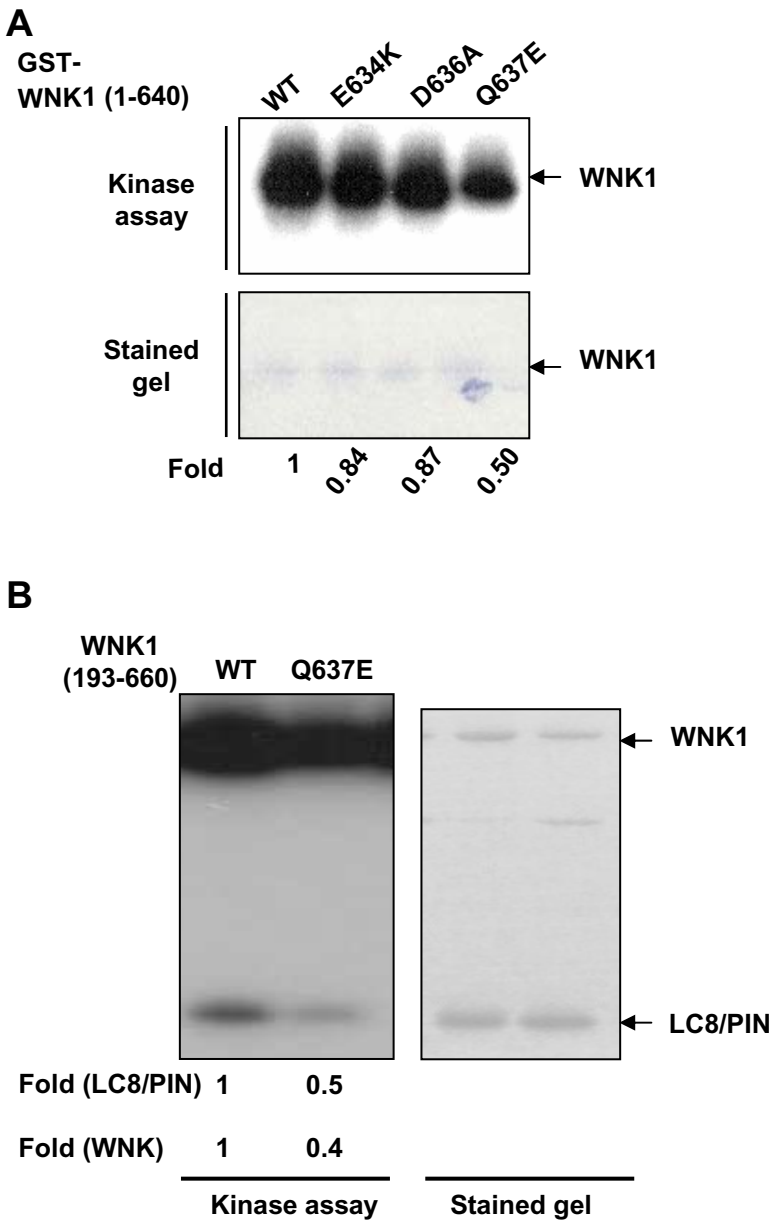

Figure 5-6. WNK1 Q637E displayed decreased activity
A, B. The standard kinase assays were performed with 0.5 μg of GST-WNK1 (1-640) WT and mutants, 1 μg of WNK1 (193-660) WT or Q637E, and 1.5 μg of LC8/PIN proteins.

Future Directions

The WNK protein kinase family is gaining attention not only due to their unique active site organization but particularly because of their pathophysiological link to human hypertension. The defining feature of WNK kinases is the unique repositioning of the catalytic lysine. The three-dimensional structure of WNK1 demonstrated that the invariant lysine is located in β2 strand rather than the usual β3 strand, still positioning into the active site for catalysis. We do not yet have answers for how and why this striking positioning was acquired only among WNK kinases or what exactly is the catalytic mechanism for WNK. What is noteworthy here is that the catalytic lysine in WNK1 is rather exposed to the outer surface (Min et al., 2004). In fact, the C2 domain of Syt forms a very rigid β-barrel structure and is not likely to be a substrate for ordinary protein kinases. Perhaps WNKs have evolved to act specifically on this type of molecule by adopting a more surface-exposed active site. This hypothesis is consistent with my observations that WNK1 interacting molecules largely include certain Syt isoforms and a protein of unknown function that contains three tandem C2 domains. Additionally, my recent preliminary data showed that WNK1 is also able to phosphorylate the C2 domains of Munc13 (data not shown). WNK1, however, is not a promiscuous protein kinase. WNK1 showed high selectivity among Syt isoforms and it did not phosphorylate c-Jun, GST, Mef2c, Chk2, Mayven, BSA, and Vps4a (previous Chapters and unpublished data from Cobb lab). Consequently, the catalytic and regulatory mechanisms of WNK1 kinase are likely to be different from other protein kinases. WNK1 may be a very attractive drug target, such as for hypertension disorders, no only due to its

highly specialized active site organization, but also because there is apparently no functional redundancy among WNK isoforms, suggested by embryonic lethality of WNK1 null mice. To validate these ideas, co-crystallization of WNK1 with one or more of its substrates would be valuable. Also determination of the sequence motifs for its substrates through peptide library screening would be informative.

WNK proteins are involved in blood pressure control probably by regulating membrane dynamics. However, the underlying mechanisms by which WNK1 can cause hypertension are not well understood yet. Interestingly, our group recently found that WNK1 can activate the sodium- and glucocorticoid-activated protein kinase 1 (SGK1), and activated SGK1, in turn, inhibits the E3 ubiquitin ligase NEDD4-2 (Xu et al., in revision). Consequently, NEDD4-2 is not able to downregulate the epithelial sodium channel (ENaC), leading to increased sodium reabsorption. Another significant clue for the question came with my discovery that WNK1 may alter membrane fusion dynamics by regulating Syt, a potential Ca^{2+} sensor (Lee et al., 2004). These events probably contribute to the control of the density of membrane transporters and channels. However, the functional linking between membrane transporters and Syts in nonneuronal cells, which bears analogy to the relationship between neurotransmitter-containing synaptic vesicles and Syt1 in neurons, remains to be identified. These observations suggest that there may be different mechanisms for WNK1 to control blood pressure.

As discussed in Chapter 3, there are still many questions remaining to be addressed to understand WNK1-mediated membrane events better. Notable among them, just as WNK can regulate ion homeostasis, ion flux might regulate the function of the WNK

protein kinase by a feedback mechanism. The increase of NaCl or KCl flux may activate WNK1 kinase. Furthermore, hyperkalemic hypertension in PHAII patients is also accompanied by hypercalciuria. This phenotype leads me to speculate that for electrolyte balance, WNK might also regulate one or more subsets of calcium channels (either in the plasma membrane or in the endoplasmic reticulum or both) by controlling their resident time on the membrane. Furthermore, PI3 kinase has been also shown to be involved in trafficking of calcium channels, and WNK1 is downstream of the PI3K signaling pathway (see Chapter 3). Because the functional interactions among WNK1, Syt2, and phospholipids are highly electrostatic and influenced by calcium, calcium ion flux may be at least one regulatory mechanism for WNK1 actions on hypertension. Elaborate physiological, cell biological, and biochemical approaches will likely be required to test this hypothesis as well as other issues described in Chapter 3.

Smad2 and LC8/PIN were identified as additional interactors for WNK from yeast two-hybrid screens. Due to the limited amount of data that I was able to gather on these proteins, the functional relationship between WNK and these distinctive substrates is not clear. Pending tasks will be the identification of sites on these proteins phosphorylated by WNK. As discussed in Chapter 4, WNK1 (and WNK4 for Smad2) may have multiple roles in different aspects of Smad- and LC8/PIN-mediated signaling pathways. Regarding Smad and WNK, WNK may function in early embryonic development through Smad proteins. Animal models will be certainly useful to address these questions. LC8/PIN is a subunit for motor transporters, and is involved in other functions as well. WNK1 may be both a cargo molecule and a motor receptor. The proper localization of WNK1 by transport machinery

may be critical for the actions of WNK1, but at the same time, WNK1 may regulate the transport machinery, thereby regulating the localization of other cargo molecules, by phosphorylating LC8/PIN dynein light chain.

WNKs possess multiple protein interaction modules and motifs. Perhaps this is why a variety of seemingly unrelated proteins have been identified from my yeast-based screening. For example, a bait from the WNK1 C-terminus (residues 1811-1910) interacted with a ubiquitin conjugation enzyme belonging to a ubc4/5 family, suggesting that WNK1 has a functional relation to ubiquitin-mediated degradation pathways. WNK1 may be a signaling center by acting as a docking platform for numerous signal transducers, adaptors, regulators, and other scaffolding proteins. More biochemical and genetic screens may be required for uncovering upstream and downstream targets to better understand WNK functions. WNKs also have numerous putative post-translational modification sites. As an example among many more, rat WNK1 contains at least three putative sumoylation sites; $_{1651}$VKPE, $_{1679}$AKSE, and $_{1716}$IKKE. These post-translational modifications may be critical for the regulation of WNK activities.

References

Alonso, A., Sasin, J., Bottini, N., Friedberg, I., Osterman, A., Godzik, A., Hunter, T., Dixon, J., and Mustelin, T. (2004). Protein tyrosine phosphatases in the human genome. Cell *117*, 699-711.

Anderson, R. G. (1998). The caveolae membrane system. Annu Rev Biochem *67*, 199-225.

Bai, J., and Chapman, E. R. (2004). The C2 domains of synaptotagmin--partners in exocytosis. Trends Biochem Sci *29*, 143-151.

Bai, Y., Yang, C., Hu, K., Elly, C., and Liu, Y. C. (2004). Itch E3 ligase-mediated regulation of TGF-beta signaling by modulating smad2 phosphorylation. Mol Cell *15*, 825-831.

Bershadsky, A. D., Balaban, N. Q., and Geiger, B. (2003). Adhesion-dependent cell mechanosensitivity. Annu Rev Cell Dev Biol *19*, 677-695.

Bossemeyer, D., Engh, R. A., Kinzel, V., Ponstingl, H., and Huber, R. (1993). Phosphotransferase and substrate binding mechanism of the cAMP-dependent protein kinase catalytic subunit from porcine heart as deduced from the 2.0 A structure of the complex with Mn^{2+} adenylyl imidodiphosphate and inhibitor peptide PKI (5-24). Embo J *12*, 849-859.

Bowman, A. B., Kamal, A., Ritchings, B. W., Philp, A. V., McGrail, M., Gindhart, J. G., and Goldstein, L. S. (2000). Kinesin-dependent axonal transport is mediated by the sunday driver (SYD) protein. Cell *103*, 583-594.

Brown, J. D., DiChiara, M. R., Anderson, K. R., Gimbrone, M. A., Jr., and Topper, J. N. (1999). MEKK-1, a component of the stress (stress-activated protein kinase/c-Jun N-terminal kinase) pathway, can selectively activate Smad2-mediated transcriptional activation in endothelial cells. J Biol Chem *274*, 8797-8805.

Caenepeel, S., Charydczak, G., Sudarsanam, S., Hunter, T., and Manning, G. (2004). The mouse kinome: discovery and comparative genomics of all mouse protein kinases. Proc Natl Acad Sci U S A *101*, 11707-11712.

Chang, C. I., Xu, B. E., Akella, R., Cobb, M. H., and Goldsmith, E. J. (2002). Crystal structures of MAP kinase p38 complexed to the docking sites on its nuclear substrate MEF2A and activator MKK3b. Mol Cell *9*, 1241-1249.

Chapman, E. R. (2002). Synaptotagmin: a Ca^{2+} sensor that triggers exocytosis? Nat Rev Mol Cell Biol *3*, 498-508.

Chen, W., Yazicioglu, M., and Cobb, M. H. (2004). Characterization of OSR1, a member of

the mammalian Ste20p/germinal center kinase subfamily. J Biol Chem *279*, 11129-11136.
Chen, X., Weisberg, E., Fridmacher, V., Watanabe, M., Naco, G., and Whitman, M. (1997). Smad4 and FAST-1 in the assembly of activin-responsive factor. Nature *389*, 85-89.

Choate, K. A., Kahle, K. T., Wilson, F. H., Nelson-Williams, C., and Lifton, R. P. (2003). WNK1, a kinase mutated in inherited hypertension with hyperkalemia, localizes to diverse Cl- -transporting epithelia. Proc Natl Acad Sci U S A *100*, 663-668.

Cobb, M. H., and Goldsmith, E. J. (1995). How MAP kinases are regulated. J Biol Chem *270*, 14843-14846.

Cohen, P. (2002). Protein kinases--the major drug targets of the twenty-first century? Nat Rev Drug Discov *1*, 309-315.

Colbran, R. J. (2004). Targeting of calcium/calmodulin-dependent protein kinase II. Biochem J *378*, 1-16.

Collett, M. S., and Erikson, R. L. (1978). Protein kinase activity associated with the avian sarcoma virus src gene product. Proc Natl Acad Sci U S A *75*, 2021-2024.

Conery, A. R., Cao, Y., Thompson, E. A., Townsend, C. M., Jr., Ko, T. C., and Luo, K. (2004). Akt interacts directly with Smad3 to regulate the sensitivity to TGF-beta induced apoptosis. Nat Cell Biol *6*, 366-372.

Conner, S. D., and Schmid, S. L. (2003). Regulated portals of entry into the cell. Nature *422*, 37-44.

Cowan, C. A., and Henkemeyer, M. (2001). The SH2/SH3 adaptor Grb4 transduces B-ephrin reverse signals. Nature *413*, 174-179.
Craxton, M. (2004). Synaptotagmin gene content of the sequenced genomes. BMC Genomics *5*, 43.

Crepieux, P., Kwon, H., Leclerc, N., Spencer, W., Richard, S., Lin, R., and Hiscott, J. (1997). I kappaB alpha physically interacts with a cytoskeleton-associated protein through its signal response domain. Mol Cell Biol *17*, 7375-7385.

Dahan, M., Levi, S., Luccardini, C., Rostaing, P., Riveau, B., and Triller, A. (2003). Diffusion dynamics of glycine receptors revealed by single-quantum dot tracking. Science *302*, 442-445.

Davletov, B., Sontag, J. M., Hata, Y., Petrenko, A. G., Fykse, E. M., Jahn, R., and Sudhof, T. C. (1993). Phosphorylation of synaptotagmin I by casein kinase II. J Biol Chem *268*, 6816-6822.

de Caestecker, M. P., Parks, W. T., Frank, C. J., Castagnino, P., Bottaro, D. P., Roberts, A.

B., and Lechleider, R. J. (1998). Smad2 transduces common signals from receptor serine-threonine and tyrosine kinases. Genes Dev *12*, 1587-1592.

de Caestecker, M. P., Piek, E., and Roberts, A. B. (2000). Role of transforming growth factor-beta signaling in cancer. J Natl Cancer Inst *92*, 1388-1402.

Delaloy, C., Lu, J., Houot, A. M., Disse-Nicodeme, S., Gasc, J. M., Corvol, P., and Jeunemaitre, X. (2003). Multiple promoters in the WNK1 gene: one controls expression of a kidney-specific kinase-defective isoform. Mol Cell Biol *23*, 9208-9221.

Derynck, R., Gelbart, W. M., Harland, R. M., Heldin, C. H., Kern, S. E., Massague, J., Melton, D. A., Mlodzik, M., Padgett, R. W., Roberts, A. B.*, et al.* (1996). Nomenclature: vertebrate mediators of TGFbeta family signals. Cell *87*, 173.

Derynck, R., and Zhang, Y. E. (2003). Smad-dependent and Smad-independent pathways in TGF-beta family signalling. Nature *425*, 577-584.

Di Guglielmo, G. M., Le Roy, C., Goodfellow, A. F., and Wrana, J. L. (2003). Distinct endocytic pathways regulate TGF-beta receptor signalling and turnover. Nat Cell Biol *5*, 410-421.

Dick, T., Ray, K., Salz, H. K., and Chia, W. (1996). Cytoplasmic dynein (ddlc1) mutations cause morphogenetic defects and apoptotic cell death in Drosophila melanogaster. Mol Cell Biol *16*, 1966-1977.

Duesbery, N. S., Webb, C. P., Leppla, S. H., Gordon, V. M., Klimpel, K. R., Copeland, T. D., Ahn, N. G., Oskarsson, M. K., Fukasawa, K., Paull, K. D., and Vande Woude, G. F. (1998). Proteolytic inactivation of MAP-kinase-kinase by anthrax lethal factor. Science *280*, 734-737.

Engel, M. E., McDonnell, M. A., Law, B. K., and Moses, H. L. (1999). Interdependent SMAD and JNK signaling in transforming growth factor-beta-mediated transcription. J Biol Chem *274*, 37413-37420.

Espindola, F. S., Suter, D. M., Partata, L. B., Cao, T., Wolenski, J. S., Cheney, R. E., King, S. M., and Mooseker, M. S. (2000). The light chain composition of chicken brain myosin-Va: calmodulin, myosin-II essential light chains, and 8-kDa dynein light chain/PIN. Cell Motil Cytoskeleton *47*, 269-281.

Fernandez, I., Arac, D., Ubach, J., Gerber, S. H., Shin, O., Gao, Y., Anderson, R. G., Sudhof, T. C., and Rizo, J. (2001). Three-dimensional structure of the synaptotagmin 1 C2B-domain: synaptotagmin 1 as a phospholipid binding machine. Neuron *32*, 1057-1069.

Fire, A., Xu, S., Montgomery, M. K., Kostas, S. A., Driver, S. E., and Mello, C. C. (1998). Potent and specific genetic interference by double-stranded RNA in Caenorhabditis

elegans. Nature *391*, 806-811.

Fuhrmann, J. C., Kins, S., Rostaing, P., El Far, O., Kirsch, J., Sheng, M., Triller, A., Betz, H., and Kneussel, M. (2002). Gephyrin interacts with Dynein light chains 1 and 2, components of motor protein complexes. J Neurosci *22*, 5393-5402.

Fukuda, M., Moreira, J. E., Liu, V., Sugimori, M., Mikoshiba, K., and Llinas, R. R. (2000). Role of the conserved WHXL motif in the C terminus of synaptotagmin in synaptic vesicle docking. Proc Natl Acad Sci U S A *97*, 14715-14719.

Galli, T., Chilcote, T., Mundigl, O., Binz, T., Niemann, H., and De Camilli, P. (1994). Tetanus toxin-mediated cleavage of cellubrevin impairs exocytosis of transferrin receptor-containing vesicles in CHO cells. J Cell Biol *125*, 1015-1024.

Gandhi, S. P., and Stevens, C. F. (2003). Three modes of synaptic vesicular recycling revealed by single-vesicle imaging. Nature *423*, 607-613.

Gao, Z., Reavey-Cantwell, J., Young, R. A., Jegier, P., and Wolf, B. A. (2000). Synaptotagmin III/VII isoforms mediate Ca^{2+}-induced insulin secretion in pancreatic islet beta -cells. J Biol Chem *275*, 36079-36085.

Garcia, R. A., Forde, C. E., and Godwin, H. A. (2000). Calcium triggers an intramolecular association of the C2 domains in synaptotagmin. Proc Natl Acad Sci U S A *97*, 5883-5888.

Geppert, M., Archer, B. T., 3rd, and Sudhof, T. C. (1991). Synaptotagmin II. A novel differentially distributed form of synaptotagmin. J Biol Chem *266*, 13548-13552.

Giangrande, P. H., Hallstrom, T. C., Tunyaplin, C., Calame, K., and Nevins, J. R. (2003). Identification of E-box factor TFE3 as a functional partner for the E2F3 transcription factor. Mol Cell Biol *23*, 3707-3720.

Graff, J. M., Bansal, A., and Melton, D. A. (1996). Xenopus Mad proteins transduce distinct subsets of signals for the TGF beta superfamily. Cell *85*, 479-487.

Han, W., Rhee, J. S., Maximov, A., Lao, Y., Mashimo, T., Rosenmund, C., and Sudhof, T. C. (2004). N-glycosylation is essential for vesicular targeting of synaptotagmin 1. Neuron *41*, 85-99.

Hanahan, D., and Weinberg, R. A. (2000). The hallmarks of cancer. Cell *100*, 57-70.
Hanks, S. K., and Hunter, T. (1995). Protein kinases 6. The eukaryotic protein kinase superfamily: kinase (catalytic) domain structure and classification. Faseb J *9*, 576-596.

Hanks, S. K., Quinn, A. M., and Hunter, T. (1988). The protein kinase family: conserved features and deduced phylogeny of the catalytic domains. Science *241*, 42-52.

Hata, A., Lagna, G., Massague, J., and Hemmati-Brivanlou, A. (1998). Smad6 inhibits BMP/Smad1 signaling by specifically competing with the Smad4 tumor suppressor. Genes Dev *12*, 186-197.

Hata, A., Lo, R. S., Wotton, D., Lagna, G., and Massague, J. (1997). Mutations increasing autoinhibition inactivate tumour suppressors Smad2 and Smad4. Nature *388*, 82-87.

Hata, A., Shi, Y., and Massague, J. (1998). TGF-beta signaling and cancer: structural and functional consequences of mutations in Smads. Mol Med Today *4*, 257-262.

Hemmens, B., Woschitz, S., Pitters, E., Klosch, B., Volker, C., Schmidt, K., and Mayer, B. (1998). The protein inhibitor of neuronal nitric oxide synthase (PIN): characterization of its action on pure nitric oxide synthases. FEBS Lett *430*, 397-400.

Hilfiker, S., Pieribone, V. A., Nordstedt, C., Greengard, P., and Czernik, A. J. (1999). Regulation of synaptotagmin I phosphorylation by multiple protein kinases. J Neurochem *73*, 921-932.

Hirokawa, N. (1998). Kinesin and dynein superfamily proteins and the mechanism of organelle transport. Science *279*, 519-526.

Hudson, A. W., and Birnbaum, M. J. (1995). Identification of a nonneuronal isoform of synaptotagmin. Proc Natl Acad Sci U S A *92*, 5895-5899.

Hunter, T. (2000). Signaling--2000 and beyond. Cell *100*, 113-127.

Huse, M., and Kuriyan, J. (2002). The conformational plasticity of protein kinases. Cell *109*, 275-282.

Ito, M., Shichijo, S., Tsuda, N., Ochi, M., Harashima, N., Saito, N., and Itoh, K. (2001). Molecular basis of T cell-mediated recognition of pancreatic cancer cells. Cancer Res *61*, 2038-2046.

Ito, M., Yoshioka, K., Akechi, M., Yamashita, S., Takamatsu, N., Sugiyama, K., Hibi, M., Nakabeppu, Y., Shiba, T., and Yamamoto, K. I. (1999). JSAP1, a novel jun N-terminal protein kinase (JNK)-binding protein that functions as a Scaffold factor in the JNK signaling pathway. Mol Cell Biol *19*, 7539-7548.

Jacob, Y., Badrane, H., Ceccaldi, P. E., and Tordo, N. (2000). Cytoplasmic dynein LC8 interacts with lyssavirus phosphoprotein. J Virol *74*, 10217-10222.

Jaffrey, S. R., and Snyder, S. H. (1996). PIN: an associated protein inhibitor of neuronal nitric oxide synthase. Science *274*, 774-777.

Johnson, L. N., Noble, M. E., and Owen, D. J. (1996). Active and inactive protein kinases:

structural basis for regulation. Cell *85*, 149-158.

Kahle, K. T., Gimenez, I., Hassan, H., Wilson, F. H., Wong, R. D., Forbush, B., Aronson, P. S., and Lifton, R. P. (2004). WNK4 regulates apical and basolateral Cl- flux in extrarenal epithelia. Proc Natl Acad Sci U S A *101*, 2064-2069.

Kahle, K. T., Macgregor, G. G., Wilson, F. H., Van Hoek, A. N., Brown, D., Ardito, T., Kashgarian, M., Giebisch, G., Hebert, S. C., Boulpaep, E. L., and Lifton, R. P. (2004). Paracellular Cl- permeability is regulated by WNK4 kinase: insight into normal physiology and hypertension. Proc Natl Acad Sci U S A *101*, 14877-14882.

Kahle, K. T., Wilson, F. H., Lalioti, M., Toka, H., Qin, H., and Lifton, R. P. (2004). WNK kinases: molecular regulators of integrated epithelial ion transport. Curr Opin Nephrol Hypertens *13*, 557-562.

Kahle, K. T., Wilson, F. H., Leng, Q., Lalioti, M. D., O'Connell, A. D., Dong, K., Rapson, A. K., MacGregor, G. G., Giebisch, G., Hebert, S. C., and Lifton, R. P. (2003). WNK4 regulates the balance between renal NaCl reabsorption and K+ secretion. Nat Genet *35*, 372-376.

Kang, R., Swayze, R., Lise, M. F., Gerrow, K., Mullard, A., Honer, W. G., and El-Husseini, A. (2004). Presynaptic trafficking of synaptotagmin I is regulated by protein palmitoylation. J Biol Chem.

Karandikar, M., and Cobb, M. H. (1999). Scaffolding and protein interactions in MAP kinase modules. Cell Calcium *26*, 219-226.

Karcher, R. L., Deacon, S. W., and Gelfand, V. I. (2002). Motor-cargo interactions: the key to transport specificity. Trends Cell Biol *12*, 21-27.

Karet, F. E. (2002). Monogenic tubular salt and acid transporter disorders. J Nephrol *15 Suppl 6*, S57-68.

Kelkar, N., Gupta, S., Dickens, M., and Davis, R. J. (2000). Interaction of a mitogen-activated protein kinase signaling module with the neuronal protein JIP3. Mol Cell Biol *20*, 1030-1043.

King, S. J., Bonilla, M., Rodgers, M. E., and Schroer, T. A. (2002). Subunit organization in cytoplasmic dynein subcomplexes. Protein Sci *11*, 1239-1250.

King, S. M., Barbarese, E., Dillman, J. F., III, Patel-King, R. S., Carson, J. H., and Pfister, K. K. (1996). Brain cytoplasmic and flagellar outer arm dyneins share a highly conserved Mr 8,000 light chain. J Biol Chem *271*, 19358-19366.

King, S. M., and Patel-King, R. S. (1995). The M(r) = 8,000 and 11,000 outer arm dynein

light chains from Chlamydomonas flagella have cytoplasmic homologues. J Biol Chem *270*, 11445-11452.

Knighton, D. R., Zheng, J. H., Ten Eyck, L. F., Ashford, V. A., Xuong, N. H., Taylor, S. S., and Sowadski, J. M. (1991). Crystal structure of the catalytic subunit of cyclic adenosine monophosphate-dependent protein kinase. Science *253*, 407-414.

Kohn, K. W. (1999). Molecular interaction map of the mammalian cell cycle control and DNA repair systems. Mol Biol Cell *10*, 2703-2734.

Kohn, K. W., Riss, J., Aprelikova, O., Weinstein, J. N., Pommier, Y., and Barrett, J. C. (2004). Properties of switch-like bioregulatory networks studied by simulation of the hypoxia response control system. Mol Biol Cell *15*, 3042-3052.

Kranz, J. E., Satterberg, B., and Elion, E. A. (1994). The MAP kinase Fus3 associates with and phosphorylates the upstream signaling component Ste5. Genes Dev *8*, 313-327.

Krebs, E. G., and Fischer, E. H. (1989). The phosphorylase b to a converting enzyme of rabbit skeletal muscle. 1956. Biochim Biophys Acta *1000*, 302-309.

Kretzschmar, M., Doody, J., and Massague, J. (1997). Opposing BMP and EGF signalling pathways converge on the TGF-beta family mediator Smad1. Nature *389*, 618-622.

Kretzschmar, M., Doody, J., Timokhina, I., and Massague, J. (1999). A mechanism of repression of TGFbeta/ Smad signaling by oncogenic Ras. Genes Dev *13*, 804-816.

Krupa, A., Preethi, G., and Srinivasan, N. (2004). Structural modes of stabilization of permissive phosphorylation sites in protein kinases: distinct strategies in Ser/Thr and Tyr kinases. J Mol Biol *339*, 1025-1039.

Kuratomi, G., Komuro, A., Goto, K., Shinozaki, M., Miyazawa, K., Miyazono, K., and Imamura, T. (2004). Neural precursor cell expressed, developmentally down-regulated 4-2 (NEDD4-2) negatively regulates transforming growth factor-beta (TGF-beta) signaling by inducing ubiquitin-mediated degradation of Smad2 and TGF-beta type I receptor. Biochem J.

Lang, J., Fukuda, M., Zhang, H., Mikoshiba, K., and Wollheim, C. B. (1997). The first C2 domain of synaptotagmin is required for exocytosis of insulin from pancreatic beta-cells: action of synaptotagmin at low micromolar calcium. Embo J *16*, 5837-5846.

Lee, B. H., Min, X., Heise, C. J., Xu, B. E., Chen, S., Shu, H., Luby-Phelps, K., Goldsmith, E. J., and Cobb, M. H. (2004). WNK1 phosphorylates synaptotagmin 2 and modulates its membrane binding. Mol Cell *15*, 741-751.

Levinson, A. D., Oppermann, H., Levintow, L., Varmus, H. E., and Bishop, J. M. (1978).

Evidence that the transforming gene of avian sarcoma virus encodes a protein kinase associated with a phosphoprotein. Cell *15*, 561-572.

Lhuillier, L., and Dryer, S. E. (2002). Developmental regulation of neuronal K(Ca) channels by TGFbeta1: an essential role for PI3 kinase signaling and membrane insertion. J Neurophysiol *88*, 954-964.

Li, C., Ullrich, B., Zhang, J. Z., Anderson, R. G., Brose, N., and Sudhof, T. C. (1995). $Ca(^{2+})$-dependent and -independent activities of neural and non-neural synaptotagmins. Nature *375*, 594-599.

Li, J., Lee, G. I., Van Doren, S. R., and Walker, J. C. (2000). The FHA domain mediates phosphoprotein interactions. J Cell Sci *113 Pt 23*, 4143-4149.

Liang, J., Jaffrey, S. R., Guo, W., Snyder, S. H., and Clardy, J. (1999). Structure of the PIN/LC8 dimer with a bound peptide. Nat Struct Biol *6*, 735-740.

Lifton, R. P., Gharavi, A. G., and Geller, D. S. (2001). Molecular mechanisms of human hypertension. Cell *104*, 545-556.

Lu, Z., Xu, S., Joazeiro, C., Cobb, M. H., and Hunter, T. (2002). The PHD domain of MEKK1 acts as an E3 ubiquitin ligase and mediates ubiquitination and degradation of ERK1/2. Mol Cell *9*, 945-956.

Manning, G., Whyte, D. B., Martinez, R., Hunter, T., and Sudarsanam, S. (2002). The protein kinase complement of the human genome. Science *298*, 1912-1934.

Marcus, S., Polverino, A., Barr, M., and Wigler, M. (1994). Complexes between STE5 and components of the pheromone-responsive mitogen-activated protein kinase module. Proc Natl Acad Sci U S A *91*, 7762-7766.

Mark, G. E., and Rapp, U. R. (1984). Primary structure of v-raf: relatedness to the src family of oncogenes. Science *224*, 285-289.

Martin, T. F. (2003). Tuning exocytosis for speed: fast and slow modes. Biochim Biophys Acta *1641*, 157-165.

Massague, J. (1998). TGF-beta signal transduction. Annu Rev Biochem *67*, 753-791.

Massague, J., and Wotton, D. (2000). Transcriptional control by the TGF-beta/Smad signaling system. Embo J *19*, 1745-1754.

McMahon, H. T., Ushkaryov, Y. A., Edelmann, L., Link, E., Binz, T., Niemann, H., Jahn, R., and Sudhof, T. C. (1993). Cellubrevin is a ubiquitous tetanus-toxin substrate homologous to a putative synaptic vesicle fusion protein. Nature *364*, 346-349.

Min, X., Lee, B. H., Cobb, M. H., and Goldsmith, E. J. (2004). Crystal structure of the kinase domain of WNK1, a kinase that causes a hereditary form of hypertension. Structure (Camb) *12*, 1303-1311.

Moore, T. M., Garg, R., Johnson, C., Coptcoat, M. J., Ridley, A. J., and Morris, J. D. (2000). PSK, a novel STE20-like kinase derived from prostatic carcinoma that activates the c-Jun N-terminal kinase mitogen-activated protein kinase pathway and regulates actin cytoskeletal organization. J Biol Chem *275*, 4311-4322.

Morrison, D. K., and Davis, R. J. (2003). Regulation of MAP kinase signaling modules by scaffold proteins in mammals. Annu Rev Cell Dev Biol *19*, 91-118.

Moustakas, A., Souchelnytskyi, S., and Heldin, C. H. (2001). Smad regulation in TGF-beta signal transduction. J Cell Sci *114*, 4359-4369.

Murakami-Kojima, M., Nakamichi, N., Yamashino, T., and Mizuno, T. (2002). The APRR3 component of the clock-associated APRR1/TOC1 quintet is phosphorylated by a novel protein kinase belonging to the WNK family, the gene for which is also transcribed rhythmically in Arabidopsis thaliana. Plant Cell Physiol *43*, 675-683.

Murray, D., and Honig, B. (2002). Electrostatic control of the membrane targeting of C2 domains. Mol Cell *9*, 145-154.

Naisbitt, S., Valtschanoff, J., Allison, D. W., Sala, C., Kim, E., Craig, A. M., Weinberg, R. J., and Sheng, M. (2000). Interaction of the postsynaptic density-95/guanylate kinase domain-associated protein complex with a light chain of myosin-V and dynein. J Neurosci *20*, 4524-4534.

Nakamichi, N., Murakami-Kojima, M., Sato, E., Kishi, Y., Yamashino, T., and Mizuno, T. (2002). Compilation and characterization of a novel WNK family of protein kinases in Arabiodpsis thaliana with reference to circadian rhythms. Biosci Biotechnol Biochem *66*, 2429-2436.

Noble, M. E., Endicott, J. A., and Johnson, L. N. (2004). Protein kinase inhibitors: insights into drug design from structure. Science *303*, 1800-1805.

Nolen, B., Taylor, S., and Ghosh, G. (2004). Regulation of protein kinases; controlling activity through activation segment conformation. Mol Cell *15*, 661-675.

Oancea, E., and Meyer, T. (1998). Protein kinase C as a molecular machine for decoding calcium and diacylglycerol signals. Cell *95*, 307-318.

O'Reilly, M., Marshall, E., Speirs, H. J., and Brown, R. W. (2003). WNK1, a gene within a novel blood pressure control pathway, tissue-specifically generates radically different

isoforms with and without a kinase domain. J Am Soc Nephrol *14*, 2447-2456.

Pawson, T. (1995). Protein modules and signalling networks. Nature *373*, 573-580.
Phillis, R., Statton, D., Caruccio, P., and Murphey, R. K. (1996). Mutations in the 8 kDa dynein light chain gene disrupt sensory axon projections in the Drosophila imaginal CNS. Development *122*, 2955-2963.

Popoli, M. (1993). Synaptotagmin is endogenously phosphorylated by Ca^{2+}/calmodulin protein kinase II in synaptic vesicles. FEBS Lett *317*, 85-88.

Poskanzer, K. E., Marek, K. W., Sweeney, S. T., and Davis, G. W. (2003). Synaptotagmin I is necessary for compensatory synaptic vesicle endocytosis in vivo. Nature *426*, 559-563.

Pulaski, L., Landstrom, M., Heldin, C. H., and Souchelnytskyi, S. (2001). Phosphorylation of Smad7 at Ser-249 does not interfere with its inhibitory role in transforming growth factor-beta-dependent signaling but affects Smad7-dependent transcriptional activation. J Biol Chem *276*, 14344-14349.

Puthalakath, H., Huang, D. C., O'Reilly, L. A., King, S. M., and Strasser, A. (1999). The proapoptotic activity of the Bcl-2 family member Bim is regulated by interaction with the dynein motor complex. Mol Cell *3*, 287-296.

Raux, H., Flamand, A., and Blondel, D. (2000). Interaction of the rabies virus P protein with the LC8 dynein light chain. J Virol *74*, 10212-10216.

Remy, I., Montmarquette, A., and Michnick, S. W. (2004). PKB/Akt modulates TGF-beta signalling through a direct interaction with Smad3. Nat Cell Biol *6*, 358-365.

Rodriguez-Crespo, I., Straub, W., Gavilanes, F., and Ortiz de Montellano, P. R. (1998). Binding of dynein light chain (PIN) to neuronal nitric oxide synthase in the absence of inhibition. Arch Biochem Biophys *359*, 297-304.

Rodriguez-Crespo, I., Yelamos, B., Roncal, F., Albar, J. P., Ortiz de Montellano, P. R., and Gavilanes, F. (2001). Identification of novel cellular proteins that bind to the LC8 dynein light chain using a pepscan technique. FEBS Lett *503*, 135-141.

Rossier, B. C. (2003) Negative regulators of sodium transport in the kidney: key factors in understanding salt-sensitive hypertension? J Clin Invest*111*, 947-950

Sakai, N., Sasaki, K., Ikegaki, N., Shirai, Y., Ono, Y., and Saito, N. (1997). Direct visualization of the translocation of the gamma-subspecies of protein kinase C in living cells using fusion proteins with green fluorescent protein. J Cell Biol *139*, 1465-1476.

Sanjay, A., Horne, W. C., and Baron, R. (2001). The Cbl family: ubiquitin ligases regulating signaling by tyrosine kinases. Sci STKE *2001*, PE40.

Schnorrer, F., Bohmann, K., and Nusslein-Volhard, C. (2000). The molecular motor dynein is involved in targeting swallow and bicoid RNA to the anterior pole of Drosophila oocytes. Nat Cell Biol *2*, 185-190.

Shao, X., Fernandez, I., Sudhof, T. C., and Rizo, J. (1998). Solution structures of the Ca^{2+}-free and Ca^{2+}-bound C2A domain of synaptotagmin I: does Ca^{2+} induce a conformational change? Biochemistry *37*, 16106-16115.

Shao, X., Li, C., Fernandez, I., Zhang, X., Sudhof, T. C., and Rizo, J. (1997). Synaptotagmin-syntaxin interaction: the C2 domain as a Ca^{2+}-dependent electrostatic switch. Neuron *18*, 133-142.

Shi, Y., and Massague, J. (2003). Mechanisms of TGF-beta signaling from cell membrane to the nucleus. Cell *113*, 685-700.

Snyder, P. M. (2000). Liddle's syndrome mutations disrupt cAMP-mediated translocation of the epithelial Na(+) channel to the cell surface. J Clin Invest *105*, 45-53.

Sobko, A., Ma, H., and Firtel, R. A. (2002). Regulated SUMOylation and ubiquitination of DdMEK1 is required for proper chemotaxis. Dev Cell *2*, 745-756.

Souchelnytskyi, S., Tamaki, K., Engstrom, U., Wernstedt, C., ten Dijke, P., and Heldin, C. H. (1997). Phosphorylation of Ser465 and Ser467 in the C terminus of Smad2 mediates interaction with Smad4 and is required for transforming growth factor-beta signaling. J Biol Chem *272*, 28107-28115.

Staub, O., Dho, S., Henry, P., Correa, J., Ishikawa, T., McGlade, J., and Rotin, D. (1996). WW domains of Nedd4 bind to the proline-rich PY motifs in the epithelial Na+ channel deleted in Liddle's syndrome. Embo J *15*, 2371-2380.

Stevens, C. F., and Williams, J. H. (2000). "Kiss and run" exocytosis at hippocampal synapses. Proc Natl Acad Sci U S A *97*, 12828-12833.

Sudhof, T. C. (2002). Synaptotagmins: why so many? J Biol Chem *277*, 7629-7632.

Tanoue, T., Maeda, R., Adachi, M., and Nishida, E. (2001). Identification of a docking groove on ERK and p38 MAP kinases that regulates the specificity of docking interactions. Embo J *20*, 466-479.

ten Dijke, P., and Hill, C. S. (2004). New insights into TGF-beta-Smad signalling. Trends Biochem Sci *29*, 265-273.

ten Dijke, P., Miyazono, K., and Heldin, C. H. (2000). Signaling inputs converge on nuclear effectors in TGF-beta signaling. Trends Biochem Sci *25*, 64-70.

Tochio, H., Ohki, S., Zhang, Q., Li, M., and Zhang, M. (1998). Solution structure of a protein inhibitor of neuronal nitric oxide synthase. Nat Struct Biol *5*, 965-969.

Trivier, E., De Cesare, D., Jacquot, S., Pannetier, S., Zackai, E., Young, I., Mandel, J. L., Sassone-Corsi, P., and Hanauer, A. (1996). Mutations in the kinase Rsk-2 associated with Coffin-Lowry syndrome. Nature *384*, 567-570.

Tsukazaki, T., Chiang, T. A., Davison, A. F., Attisano, L., and Wrana, J. L. (1998). SARA, a FYVE domain protein that recruits Smad2 to the TGFbeta receptor. Cell *95*, 779-791.
Tsukita, S., Furuse, M., and Itoh, M. (2001). Multifunctional strands in tight junctions. Nat Rev Mol Cell Biol *2*, 285-293.

Tucker, W. C., and Chapman, E. R. (2002). Role of synaptotagmin in Ca^{2+}-triggered exocytosis. Biochem J *366*, 1-13.

Tucker, W. C., Weber, T., and Chapman, E. R. (2004). Reconstitution of Ca^{2+}-regulated membrane fusion by synaptotagmin and SNAREs. Science *304*, 435-438.

Ullrich, B., Li, C., Zhang, J. Z., McMahon, H., Anderson, R. G., Geppert, M., and Sudhof, T. C. (1994). Functional properties of multiple synaptotagmins in brain. Neuron *13*, 1281-1291.

Vadlamudi, R. K., Bagheri-Yarmand, R., Yang, Z., Balasenthil, S., Nguyen, D., Sahin, A. A., den Hollander, P., and Kumar, R. (2004). Dynein light chain 1, a p21-activated kinase 1-interacting substrate, promotes cancerous phenotypes. Cancer Cell *5*, 575-585.

Vale, R. D. (2003). The molecular motor toolbox for intracellular transport. Cell *112*, 467-480.

Verhey, K. J., Meyer, D., Deehan, R., Blenis, J., Schnapp, B. J., Rapoport, T. A., and Margolis, B. (2001). Cargo of kinesin identified as JIP scaffolding proteins and associated signaling molecules. J Cell Biol *152*, 959-970.

Verissimo, F., and Jordan, P. (2001). WNK kinases, a novel protein kinase subfamily in multi-cellular organisms. Oncogene *20*, 5562-5569.

Viard, P., Butcher, A. J., Halet, G., Davies, A., Nurnberg, B., Heblich, F., and Dolphin, A. C. (2004). PI3K promotes voltage-dependent calcium channel trafficking to the plasma membrane. Nat Neurosci *7*, 939-946.

Vitari, A. C., Deak, M., Collins, B. J., Morrice, N., Prescott, A. R., Phelan, A., Humphreys, S., and Alessi, D. R. (2004). WNK1, the kinase mutated in an inherited high-blood-pressure syndrome, is a novel PKB (protein kinase B)/Akt substrate. Biochem J *378*, 257-268.

Vojtek, A. B., and Hollenberg, S. M. (1995). Ras-Raf interaction: two-hybrid analysis.

Methods Enzymol *255*, 331-342.

von Poser, C., Ichtchenko, K., Shao, X., Rizo, J., and Sudhof, T. C. (1997). The evolutionary pressure to inactivate. A subclass of synaptotagmins with an amino acid substitution that abolishes Ca^{2+} binding. J Biol Chem *272*, 14314-14319.

Wang, C. T., Lu, J. C., Bai, J., Chang, P. Y., Martin, T. F., Chapman, E. R., and Jackson, M. B. (2003). Different domains of synaptotagmin control the choice between kiss-and-run and full fusion. Nature *424*, 943-947.

Wang, Z., Yang, C. L., and Ellison, D. H. (2004). Comparison of WNK4 and WNK1 kinase and inhibiting activities. Biochem Biophys Res Commun *317*, 939-944.

Weinstein, M., Yang, X., and Deng, C. (2000). Functions of mammalian Smad genes as revealed by targeted gene disruption in mice. Cytokine Growth Factor Rev *11*, 49-58.

Wetzker, R., and Bohmer, F. D. (2003). Transactivation joins multiple tracks to the ERK/MAPK cascade. Nat Rev Mol Cell Biol *4*, 651-657.

Wicks, S. J., Lui, S., Abdel-Wahab, N., Mason, R. M., and Chantry, A. (2000). Inactivation of smad-transforming growth factor beta signaling by $Ca(^{2+})$-calmodulin-dependent protein kinase II. Mol Cell Biol *20*, 8103-8111.

Wilson, F. H., Disse-Nicodeme, S., Choate, K. A., Ishikawa, K., Nelson-Williams, C., Desitter, I., Gunel, M., Milford, D. V., Lipkin, G. W., Achard, J. M.*, et al.* (2001). Human hypertension caused by mutations in WNK kinases. Science *293*, 1107-1112.

Wilson, F. H., Kahle, K. T., Sabath, E., Lalioti, M. D., Rapson, A. K., Hoover, R. S., Hebert, S. C., Gamba, G., and Lifton, R. P. (2003). Molecular pathogenesis of inherited hypertension with hyperkalemia: the Na-Cl cotransporter is inhibited by wild-type but not mutant WNK4. Proc Natl Acad Sci U S A *100*, 680-684.

Wrana, J. L. (2000). Regulation of Smad activity. Cell *100*, 189-192.
Wu, G., Chen, Y. G., Ozdamar, B., Gyuricza, C. A., Chong, P. A., Wrana, J. L., Massague, J., and Shi, Y. (2000). Structural basis of Smad2 recognition by the Smad anchor for receptor activation. Science *287*, 92-97.

Xu, B., English, J. M., Wilsbacher, J. L., Stippec, S., Goldsmith, E. J., and Cobb, M. H. (2000). WNK1, a novel mammalian serine/threonine protein kinase lacking the catalytic lysine in subdomain II. J Biol Chem *275*, 16795-16801.

Xu, B. E., Min, X., Stippec, S., Lee, B. H., Goldsmith, E. J., and Cobb, M. H. (2002). Regulation of WNK1 by an autoinhibitory domain and autophosphorylation. J Biol Chem *277*, 48456-48462.

Xu, B. E., Stippec, S., Lenertz, L., Lee, B. H., Zhang, W., Lee, Y. K., and Cobb, M. H. (2004). WNK1 activates ERK5 by an MEKK2/3-dependent mechanism. J Biol Chem *279*, 7826-7831.

Xu, Q., Modrek, B., and Lee, C. (2002). Genome-wide detection of tissue-specific alternative splicing in the human transcriptome. Nucleic Acids Res *30*, 3754-3766.
Yaffe, M. B., and Cantley, L. C. (1999). Signal transduction. Grabbing phosphoproteins. Nature *402*, 30-31.

Yakymovych, I., Ten Dijke, P., Heldin, C. H., and Souchelnytskyi, S. (2001). Regulation of Smad signaling by protein kinase C. Faseb J *15*, 553-555.

Yamauchi, K., Rai, T., Kobayashi, K., Sohara, E., Suzuki, T., Itoh, T., Suda, S., Hayama, A., Sasaki, S., and Uchida, S. (2004). Disease-causing mutant WNK4 increases paracellular chloride permeability and phosphorylates claudins. Proc Natl Acad Sci U S A *101*, 4690-4694.

Yang, C. L., Angell, J., Mitchell, R., and Ellison, D. H. (2003). WNK kinases regulate thiazide-sensitive Na-Cl cotransport. J Clin Invest *111*, 1039-1045.

Yang, Z., Vadlamudi, R. K., and Kumar, R. (2004). Dynein light chain 1 phosphorylation controls macropinocytosis. J Biol Chem.

Yoo, D., Kim, B. Y., Campo, C., Nance, L., King, A., Maouyo, D., and Welling, P. A. (2003). Cell surface expression of the ROMK (Kir 1.1) channel is regulated by the aldosterone-induced kinase, SGK-1, and protein kinase A. J Biol Chem *278*, 23066-23075.

Yoshihara, M., Adolfsen, B., and Littleton, J. T. (2003). Is synaptotagmin the calcium sensor? Curr Opin Neurobiol *13*, 315-323.

Zambrowicz, B. P., Abuin, A., Ramirez-Solis, R., Richter, L. J., Piggott, J., BeltrandelRio, H., Buxton, E. C., Edwards, J., Finch, R. A., Friddle, C. J.*, et al.* (2003). Wnk1 kinase deficiency lowers blood pressure in mice: a gene-trap screen to identify potential targets for therapeutic intervention. Proc Natl Acad Sci U S A *100*, 14109-14114.

Zhang, J. Z., Davletov, B. A., Sudhof, T. C., and Anderson, R. G. (1994). Synaptotagmin I is a high affinity receptor for clathrin AP-2: implications for membrane recycling. Cell *78*, 751-760.

Zhang, X., Rizo, J., and Sudhof, T. C. (1998). Mechanism of phospholipid binding by the C2A-domain of synaptotagmin I. Biochemistry *37*, 12395-12403.

Zheng, J., Knighton, D. R., ten Eyck, L. F., Karlsson, R., Xuong, N., Taylor, S. S., and Sowadski, J. M. (1993). Crystal structure of the catalytic subunit of cAMP-dependent protein kinase complexed with MgATP and peptide inhibitor. Biochemistry *32*, 2154-2161.

Zolnierowicz, S., and Bollen, M. (2000). Protein phosphorylation and protein phosphatases. De Panne, Belgium, September 19-24, 1999. Embo J *19*, 483-488.

Vita

Byung-Hoon Lee was born on January 25, 1971 as the eldest son of Wan-Soo Lee and Yeon-Oak Kim in Seoul, Korea. After entering the Department of Microbiology in Seoul National University in 1990, he did his military service from 1992 – 1994. He resumed and completed his B.A. in 1996, and started his M.S. research in the laboratory of Biophysics in the Department of Microbiology supervised by Dr. Sa-Ouk Kang. In 1998, he graduated with an M.S. degree and worked for the Department of Toxicology in the National Institute of Health in Korea until 1999. In the fall of 1999, he was admitted into the Graduate School of Biomedical Sciences at the University of Texas Southwestern Medical Center at Dallas. He joined the research laboratory of Dr. Melanie H. Cobb in 2000 for his dissertation research. He received his Ph.D. in the Program of Genetics and Development in December, 2004.

Permanent Address: 610-466 Sillim 3-Dong Guanank-Gu

Seoul 151-032, Republic of Korea

This dissertation was typed by the author.